IDENTIFICATION AND MOLECULAR INTERACTING NETWORK OF THE CONSERVED OLIGOMERIC GOLGI (COG) TETHERING COMPLEX

EVA LOH

B.Sc. (Hons.)

A THESIS SUBMITTED

FOR THE DEGREE OF DOCTOR OF PHILOSOPHY

INSTITUTE OF MOLECULAR AND CELL BIOLOGY

NATIONAL UNIVERSITY OF SINGAPORE

2004

Acknowledgements

I would like to express my heartfelt gratitude to Professor Hong Wanjin for his supervision, guidance and constant support, and to Dr. Nathan Subramaniam for imparting his knowledge and skills in the numerous molecular and cell biological techniques. Much appreciation is also due to past members of my supervisory committee Prof. William Chia, Dr. Anthony Ting and present members, Dr. Walter Hunziker and Dr. Li Baojie for their encouragement, advice and invaluable discussions on my work. I would also like to thank past and present members of the Membrane Biology Laboratory (IMCB) for making it a great place to work, in addition to all the help, advice and support given, especially to Dr. Tang Bor Luen and Dr. Seet Li Fong for their helpful comments to this thesis. I am also grateful to Dr. Frank Peter for his help with the *in vitro* ER-Golgi transport assays on Bet3 and to Dr. Heinz Horstmann for his contribution to EM studies done on Syntaxin 8.

Special thanks to my family for their constant care and concern, and especially to hubby Weng for his patience, understanding and encouragement and finally to baby Ethan, who gives a whole new meaning to life.

Eva Loh

May 2004

TABLE OF CONTENTS

List of Publications

This thesis is written based on the four first author papers listed below (1-4).

1) Loh, E. and Hong, W.
The binary interacting network of the conserved oligomeric Golgi (COG) tethering complex.
J. Biol. Chem. (2004) Jun 4;279(23):24640-8. Epub 2004 Mar.

2) Loh, E. and Hong, W.
Sec34 is implicated in traffic from the endoplasmic reticulum to the Golgi and exists in a complex with GTC-90 and ldlBp.
J. Biol. Chem. (2002) Jun 14;277(24):21955-61. Epub 2002 Apr.

3) Subramaniam, V.N.*, Loh, E.*, Horstmann, H., Habermann, A., Xu, Y., Coe, J., Griffiths, G., and Hong, W. (*co-first author)
Preferential association of syntaxin 8 with the early endosome.
J. Cell Sci. (2000) Mar;113 (Pt 6):997-1008.

4) Loh, E., Peter, F., Subramaniam, V.N. and Hong, W.
Mammalian Bet3 functions as a cytosolic factor participating in transport from the endoplasmic reticulum to the Golgi apparatus
Manuscript in preparation

5) Subramaniam, V.N., Loh, E., and Hong, W.
N-Ethylmaleimide-sensitive factor (NSF) and alpha-soluble NSF attachment proteins (SNAP) mediate dissociation of GS28-syntaxin 5 Golgi SNAP receptors (SNARE) complex.
J. Biol. Chem. (1997) Oct 10;272(41):25441-4.

List of figures

Abbreviation

α-SNAP	alpha-soluble NSF attachment protein
ARF	ADP-ribosylation factor
ATP	Adenosine 5'-triphosphate
COG	Conserved oligomeric Golgi
COP	coat protein
DMEM	Dulbecco's Modified Eagle medium
DTT	1,4-dithiothreitol
EDTA	ethylenediaminetetraacetic acid
Endo H	Endoglycosidase H
ER	endoplasmic reticulum
ERES	ER exit site
ERGIC	ER-Golgi intermediate compartment
EST	expressed sequence tag
FBS	fetal bovine serum
FITC	fluorescein isothiocyanate
GST	glutathione-S-transferase
GTC	Golgi transport complex
GTP	guanosine 5'-triphosphate
Hepes	N-2-hydroxyethyl piperazine-N'-2-ethanesulphonic acid
IC	intermediate compartment
Ig	immunoglobulin
IPTG	isopropyl-b-D-thiogalactopyranoside
LDL	low density lipoprotein
NP-40	nonidet P-40

NRK	normal rat kidney cells
NSF	N-ethylmaleimide-sensitive factor
PBS	phosphate buffered saline
PCR	polymerase chain reaction
PMSF	Phenylmethylsulfony fluoride
SDS-PAGE	Sodium dodecyl sulfate-polyacrylamide gel electrophoresis
SNAP	Soluble NSF attachment protein
SNARE	SNAP Receptor
TGN	Trans-Golgi network
TRAPP	transport protein particle
Tris	2-amino-2(hydroxymethyl)-1-3-propanediol
TX-100	Tritox X-100
VAMP	vesicle-associated membrane protein
VSVG	Vesicular stomatitis virus (VSV) glycoprotein G

Notes on nomenclature

Sec34 is the mammalian homologue to yeast sec34p. Chapter 3 is dedicated to the work done on the molecule named Sec34 ("**Sec34** is implicated in traffic from the endoplasmic reticulum to the Golgi and exists in a complex with GTC-90 and ldlBp", Loh and Hong 2002). Since then, most researchers in this field have agreed on a 'common' naming system. The sec34-containing complex is re-named the conserved oligomeric Golgi (COG) complex. All the subunits are named Cog1-8 and Sec34 is designated Cog3. The term Sec34 shall be used throughout the writings in Chapter 3. Thereafter, the COG complex subunits takes on the new naming system, as in Chapter 4 and the corresponding publication ("The binary interacting network of the conserved oligomeric Golgi (COG) tethering complex", Loh and Hong 2004). COG and Cog are used interchangeably in the text.

Summary

The mechanisms underlying intracellular membrane trafficking has been intensively studied. Eukaryotic cells have many biochemically distinct intracellular compartments and trafficking among these compartments is largely mediated by vesicular membrane carriers. There is a huge array of proteins functioning in the budding, target selection, tethering and fusion of these carriers. These molecules contribute to membrane targeting specificity. Amongst this complex array of molecules, SNAREs have been shown to be key components of the vesicle-target membrane fusion machinery.

Not many mammalian SNAREs were identified or characterized when my project begun. We took advantage of the bioinformatic tools developed in conjunction with the expanding human genome databases, which led to the identification and characterization of a novel SNARE: syntaxin 8. Members of the syntaxin family play a fundamental role in vesicle docking and fusion of diverse membrane transport events. Syntaxin 8 transcript is detected in all rat tissues examined by Northern blot analysis. Syntaxin 8 specific antibodies recognize a 27 kDa protein enriched in membrane fractions containing Golgi and endosomal/lysosomal membranes. We showed that syntaxin 8 is indeed a SNAP receptor (SNARE) and that it coprecipitates with another SNARE, vti1-rp1. Indirect immunofluorescence microscopy reveals that the majority of syntaxin 8 is localized to the early endosome compartment marked by Rab5. Taken together, these results suggest that syntaxin 8 may be associated with endosomal SNARE complexes.

Before membrane fusion, vesicle tethering is important for initial target membrane association before fusion occurs. Two broad classes of molecules have been proposed to play a role in tethering: a group of long rigid coiled-coil proteins and several large

multisubunit complexes. We have studied two mammalian tethering proteins, namely Bet3 and Sec34/Cog3, these belong to large tethering complexes TRAPP and COG complex, respectively. Specific antibodies were generated and used for morphological and functional studies of Sec34/Cog3. Sec34/Cog3 antibodies are inhibitory in an ER-Golgi transport assay and co-immunoprecipitated Cog1, Cog2, Cog4, Cog5, Cog6 and Cog8. Our collective results suggest that Sec34, GTC-90, and ldlBp/ldlCp are part of the same protein complex(es) that regulates diverse aspects of Golgi function, including transport from the ER to the Golgi apparatus. This complex first described in yeast, was subsequently renamed the conserved oligomeric Golgi (COG) complex. It consists of 8 subunits, including several novel proteins as well as known Golgi proteins that were previously identified by independent approaches. The cloning of the last subunit Cog7, enabled us to establish the existence of a network of inter-molecular interactions of the COG complex, revealed by *in vitro* translation and co-immunoprecipitation approaches. Our results suggest that COG4 serves as a core component of the complex by interacting directly with COG1, COG2, COG5 and COG7. COG3 is incorporated into the complex by its direct interaction with COG1 and COG2, while COG6 and COG8 are incorporated via interaction with several subunits. Since COG4 is among the four essential genes of the COG complex in yeast, this molecular network highlights a crucial role of COG4 in the assembly/function of the complex. A model for the cellular assembly of the COG complex is presented.

The yeast TRAPP complex had been shown to regulate vesicular transport in the early secretory pathway. Although some components of the TRAPP complex are structurally conserved in mammalian cells, the function of their mammalian counterparts has not been examined. We describe biochemical and functional analysis of mammalian

Bet3, whose mRNA is ubiquitously expressed in all tissues. Anti-Bet3 antibodies recognize specifically a protein 22 kDa in size. In contrast to yeast Bet3p, the majority of Bet3 is present in the cytosol with a lesser amount being associated with the membrane. We further established the involvement of Bet3 in ER-Golgi transport and showed that it acts in a step after COPII-mediated vesicle budding but before the Rab1, α-SNAP and the EGTA-sensitive stages. Gel filtration analysis demonstrates that Bet3 exists in two distinct pools in the cytosol. A high molecular weight pool may correspond to the mammalian TRAPP complex, while the other most likely represents monomeric Bet3. The results presented in this thesis added mechanistic insights into two membrane fusion processes along the mammalian exocytic pathway, particularly that of ER-Golgi transport.

CHAPTER 1

Introduction

1.1 Intracellular membrane transport pathways

The secretory/exocytic pathway plays a fundamental role in many biological processes of the living cell. The bulk of extracellular proteins such as growth factors, antibodies, neurotransmitters, peptide hormones, extracellular matrix proteins and other secreted proteins are delivered to the extracellular space via this pathway. Proper functioning of the secretory pathway is important for all stages of development and for maintaining the normal physiology of a mature organism. The general scheme of the exocytic pathway is shown in Figure 1. It includes numerous functionally distinct, membrane-bound compartments such as the endoplasmic reticulum (ER), the Golgi apparatus, the endosome, the secretory granules in cells that possess the regulated secretory pathway, the plasma membrane, and various types of vesicular and/or tubular intermediates that mediate the dynamic connections between these membrane compartments (Farquhar and Palade, 1981; Rothman and Orci, 1992; Mellman and Simons, 1992).

Protein transport in the exocytic and endocytic pathways via vesicles is a highly regulated process. Vesicular transport is primarily mediated via various types of transport vesicles that bud from a donor compartment and fuse with a target compartment (Hong, 1996; Palade, 1975; Pryer et al., 1992; Rothman, 1994; Rothman and Wieland, 1996; Schekman and Orci, 1996). Tight regulation of vesicular transport is important for maintaining the integrity of the composition in various specialized cellular compartments, which in turn is crucial for the different and highly demanding roles required of each organelle of the cell.

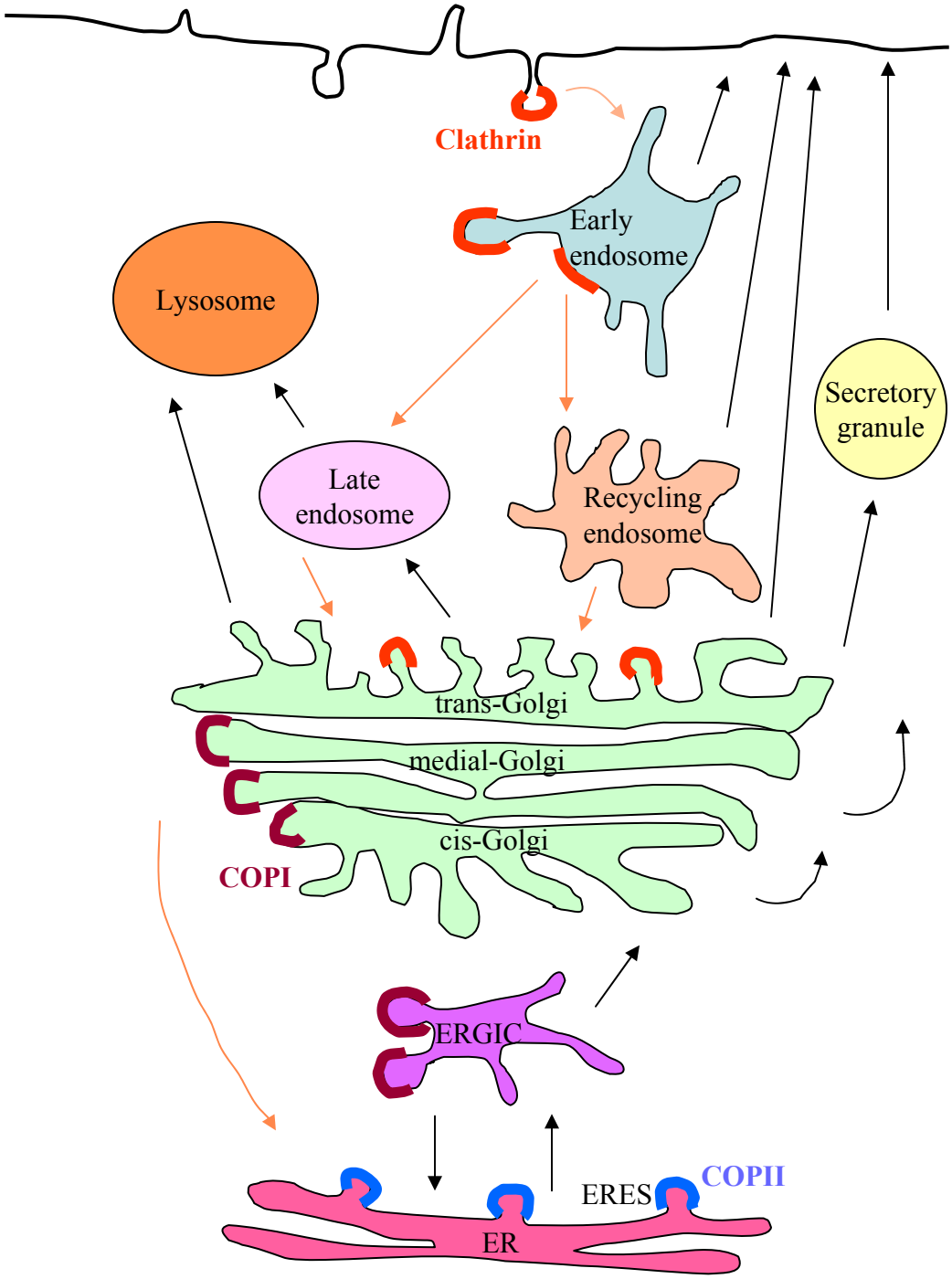

Figure 1. Organization of the intracellular transport pathways.
The compartments of the secretory, lysosomal and endocytic pathways are depicted. The major organelles consists of the endoplasmic reticulum (ER), various compartments of the Golgi apparatus, the early endosome, late endosome, recycling endosome and the lysosomes which make up the endosomal/lysosomal system, and also the plasma membrane and the membranous intermediates that mediate trafficking among these membrane structures.

1.2 Molecular mechanism of vesicular transport

The composition of membranous organelles along the exocytic/endocytic pathway is maintained by the precise targeting of different classes of vesicles to their correct destination. Targeting of the vesicle involves recognition of the vesicles by the target membrane which is then followed by 2 different types of membrane associated processes – the specific tethering of vesicles to the target site, followed by the assembly of the fusion machinery. Both are important for targeting specificity and involve distinct sets of proteins. However, vesicular transport is firstly initiated by the formation of buds on the donor membrane, a process mediated by cytosolic coat components. Buds pinch off by a fission step to generate coated vesicles. The coat components then dissociate from the coated vesicles, resulting in uncoated vesicles. These uncoated vesicles then dock onto the acceptor membrane, thereby leading to fusion of the docked vesicles with the target membrane (Figure 2).

1.3 Vesicle Budding and Cargo Selection

The regulation of cargo sorting and vesicle budding mediated by protein coats is crucial to the specificity of membrane trafficking (Kirchhausen, 2000; Bonifacino and Lippincott-Schwartz, 2003). These coats are supramolecular assemblies of proteins which are recruited from the cytosol to the nascent vesicles. The coats deform flat membrane patches into round buds, thereby leading to the release of coated transport vesicles. The coats participate in cargo selection by recognizing sorting signals present in the cytosolic domains of transmembrane cargo proteins. Vesicle budding and cargo selection at different stages of the secretory and endocytic pathways are mediated by different coats and sorting signals.

There are two well characterized types of protein coats: Clathrin coats and

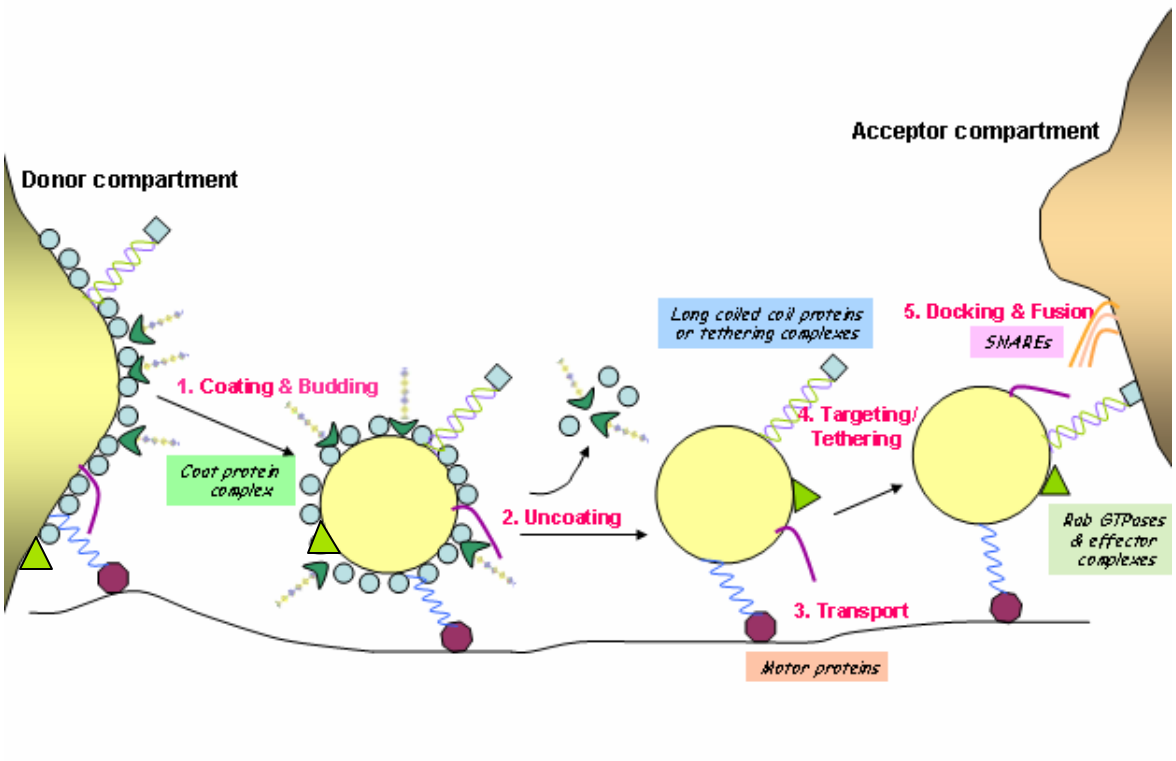

Figure 2. Mechanism of vesicular transport

1. **Initiation of coat assembly and budding-** Coat components are recruited to the donor membrane by binding to a membrane associated GTPase. Cargo becomes concentrated, followed by membrane curvature and generation of transport vesicle.
2. **Uncoating** – Vesicle loses its coat due to various events such as activation of small GTPase, phosphoinositide hydrolysis and the action of uncoating enzymes. Cytosolic coat proteins are then recycled for additional rounds of vesicle budding.
3. **Transport** – Guided by cytoskeletal tracks driven by motor proteins till vesicle arrives at target membrane.
4. **Tethering** – Molecules recruited earlier on, makes first contact with target membrane. Usually either long coiled-coil proteins (shown in diagram) or multisubunit complexes. GTP bound Rabs are also involved (depicted as green triangles).
5. **Docking and fusion** – v- and t-SNAREs assemble into four-helix bundle, promotes fusion of vesicle and acceptor lipid bilayers. Cargo is transferred to acceptor compartment, and SNAREs are recycled. (SNAREs are depicted as purple and orange curved lines).

nonclathrin coats. Clathrin coats comprise of clathrin and several adaptor proteins (APs). Non-clathrin coats mediate vesicular transport in the early secretory pathway (Waters et al., 1991; Barlowe et al., 1994). One of these coats, COPII is now known to mediate export from the ER to either the ER-Golgi intermediate compartment (ERGIC) or the Golgi complex (Barlowe et al., 1994) while another coat, COPI, is implicated in intra-Golgi transport and retrograde transport from the Golgi to the ER (Letourneur et al., 1994).

Large-scale purification of COPI vesicles has helped in the molecular characterization of the coat complex called coatomer, which consists of 7 polypeptides: α (160 kDa), β (110 kDa) (β-COP), β' (102 kDa), γ (98 kDa), δ (61 kDa), ε (31 kDa) and ζ (20 kDa). COPI vesicles also contain in abundance a 20 kDa GTP-binding protein, the ADP-ribosylation factor (ARF) (Serafini et al., 1991). Coatomer binding to membranes is preceded by ARF, the membrane association of which is in turn regulated by a BFA-sensitive GDP/GTP nucleotide dissociation factor on Golgi membranes (Donaldson et al., 1991; Donaldson et al., 1992; Palmer et al., 1993). A considerable amount of data favors a retrograde transport role for COPI in the secretory pathway, but COPI appears to be also required for anterograde transport. Recent findings that both anterograde and retrograde directed cargo proteins are present in Golgi-derived vesicles, both *in vitro* and *in vivo*, argue for a bi-directional transport mechanism within the Golgi mediated by COPI vesicles (Orci et al., 1997).

The identification and characterization of COPII genes came about by genetic studies in yeast and were initially defined as genes mutated in the SEC mutants (Novick and Schekman, 1979; Novick et al., 1980). The core COPII components are the small Ras-like GTPase Sar1p, the Sec23p/Sec24p subcomplex, and the Sec13p/Sec31p subcomplex (Barlowe et al., 1994). Additional regulatory proteins

participating in the assembly of COPII include Sec16p, a putative scaffold protein (Espenshade et al, 1995) and Sec12p, a guanine nucleotide exchange factor (GEF) for Sar1p (Barlowe and Schekman, 1993). Sed4p, a Sec12p homolog that may function as an inhibitor of GTP hydrolysis by Sar1p (Gimeno et al., 1995; Saito-Nakano and Nakano, 2000) is most likely specific to *S. cerevisiae*. There are two additional paralogs of Sec24p in *S. cerevisiae* (Lst1p and Lss1p) and two or more paralogs of Sar1p, Sec23p, Sec24p and Sec31p in humans (Bonifacino and Glick, 2004). This diversification of COPII subunits in higher eukaryotes most likely endows the coat with the ability to sort different cargo proteins and to be differentially regulated (Roberg et al., 1999; Shimoni et al., 2000).

Clathrin is a trimeric scaffold protein, which organizes itself into cagelike lattices (Kirchhausen T, 1993). Clathrin takes the shape of a triskelion, where each one of the 3 legs is made of a heavy and a light chain. The major proteins that drive clathrin coat formation are the 'clathrin AP complexes' or 'clathrin adaptors'. These are heterotetramers that couple coated pit assembly to the entrapment of cargo in the form of membrane receptors.

The adaptor complex consists of four subunits: a β chain, a μ chain, a σ chain and a more divergent chain. Adaptors have been demonstrated to perform two roles. The first is a role in coat assembly. Although clathrin triskelions are able to self assemble into cages in the absence of the adaptor complex, the addition of adaptors enhances the efficiency of coat assembly *in vitro* (Zaremba and Keen, 1983). Secondly, the adaptor complex also plays an important role in cargo binding and sorting signal recognition (Glickman et al., 1989; Sorkin and Carpenter, 1993).

Four adaptor complexes have been characterized: AP-1, AP-2, AP-3 and AP-4. Endocytic coated pits and coated vesicles contain the AP-2 complex while coated buds

and coated vesicles derived from the TGN contain the related complex AP-1. AP-3, found to be enriched in the perinuclear region of the cell, is known to be important for targeting of selected transmembrane proteins to the lysosome and is also involved in the biogenesis of specialized organelles such as pigment granules and synaptic vesicles (Ooi et al., 1997, Le Borgne et al., 1998; Jackson et al., 1998, Faundez et al., 1998). AP-4 has been found to be associated with a perinuclear compartment, possibly the TGN or adjacent structures, but its function is still not clear.

1.4 Docking and fusion - SNAREs

There is an extensive array of proteins involved in the budding, target selection, and fusion of transport carriers. Central to the theme of membrane fusion are the members of the SNARE (soluble N-ethylmaleimide-sensitive-factor attachment protein receptor) protein superfamily. The SNARE hypothesis maintains that soluble NSF (N-ethylmaleimide-sensitive factor) attachment protein (SNAP) receptors on a vesicle membrane (v-SNAREs) bind to their cognate SNAP receptor proteins on the target membrane (t-SNAREs) in the process of vesicle docking and fusion (Rothman, 1994). Fusion of the docked vesicle with the target membrane is promoted by binding of the soluble proteins α-SNAP and NSF to this SNARE complex and is driven by the ATPase activity of NSF, forming a SNARE complex with a sedimentation coefficient of 20S (Sollner et al., 1993; Subramaniam et al., 1996).

Members of the SNARE protein superfamily act not only in neurotransmitter release at the synapse, but also in most other intracellular trafficking pathway (Chen and Scheller, 2001; Jahn et al., 2003; Kavalali, 2001; Pelham, 2001; Rizo and Sudhof, 2002). In general, SNARE proteins are characterized by the presence of a SNARE motif which is a 60-70 residues long coiled-coil region (Weimbs et al., 1997) located

adjacent to the C-terminal transmembrane anchor. The best characterized SNAREs are those required for the fusion of synaptic vesicles with the presynaptic plasma membrane. This SNARE complex consists of a synaptic vesicle v-SNARE called VAMP, and two presynaptic plasma membrane t-SNAREs named syntaxin 1 and SNAP-25. High resolution X-ray crystallography studies suggested that SNAREs assemble via their SNARE motifs into a parallel four α-helix bundle, with syntaxin 1 and VAMP contributing one α-helix and SNAP-25 contributing two α-helixes (Poirier et al., 1998; Sutton et al., 1998). This structure also revealed a central polar layer in which a highly hydrophilic side chain from each SNARE motif is unexpectedly embedded within the otherwise hydrophobic core of the bundle. An arginine (R) and three glutamine (Q) residues compose this polar layer, forming a hydrogen-bonded network sequestered from solvent. The polar layer residues gave rise to the R/Q nomenclature of SNAREs (Fasshauer et al., 1998). This nomenclature categorizes SNAREs in terms of a single residue, R-SNAREs or Q-SNAREs. Both naming schemes- one functional, the other structural- are still commonly used. Most, if not all, intracellular membrane fusion reactions involve one R-SNARE and three Q-SNAREs (Bock et al., 2001, McNew et al., 2000). In many cases, the R-SNARE is contributed by the vesicle, and three Q-SNAREs are contributed by the target organelle.

SNARE proteins are not the sole determinants of targeting specificity. This is shown by some SNAREs which can function at several transport steps *in vivo* (von Mollard et al., 1997). Some SNAREs can be found in multiple SNARE complexes by co-immunoprecipitation (Holthuis et al., 1998; Lupashin et al., 1997) and others that faithfully function at different transport steps *in vivo* have been shown to interact promiscuously *in vitro* (Yang et al., 1999). SNARE proteins can mostly be assigned to the three protein families — the syntaxins, the VAMPs and the SNAP-25 family. The

hallmark of all SNARE proteins is the presence of multiple coiled-coil domains.

Syntaxins are the prototype family of t-SNARE proteins. The syntaxin family consists of 15 genes in mammals and 7 in yeast (Teng et al., 2001). All mammalian syntaxins, except syntaxin 11, are transmembrane proteins anchored by their carboxy-terminal tails with a type II orientation. The SNARE motif of a syntaxin mediates its interaction with the SNARE motifs of other t-SNARE proteins from the syntaxin or SNAP-25 families, forming t-SNARE complexes at target membranes. The t-SNARE complexes hence interact with SNARE motifs of the v-SNAREs found on specific vesicle membranes to form the core fusion complex (Chen & Scheller, 2001).

While SNARE proteins are essential for membrane fusion, they are not likely to provide the sole layer of specificity in the vesicle docking step. Specificity in vesicle traffic is generally accepted to be generated by the interaction of several factors in such a way that no individual component plays a dominant role.

1.5 Rabs

Rabs function as key regulatory factors of vesicular traffic, and have a multitude of effectors. Rabs organize distinct protein scaffolds within a single organelle and act in a combinatorial manner with their effectors to regulate all stages of membrane traffic. Rabs are members of the small GTP-binding family of proteins which activate downstream effector proteins when in their GTP-bound state. Activation and deactivation of Rabs is regulated by GTP exchange factors and GTPase activating proteins (Figure 3). In their active state, Rabs can bind to a variety of effector proteins, which include components of motor complexes involved in vesicle movement (Hammer & Wu, 2002), vesicle cargo proteins (van Ijzendoorn et al., 2002) and even GTP exchange factors for other Rab proteins (Ortiz et al., 2002; Wang &

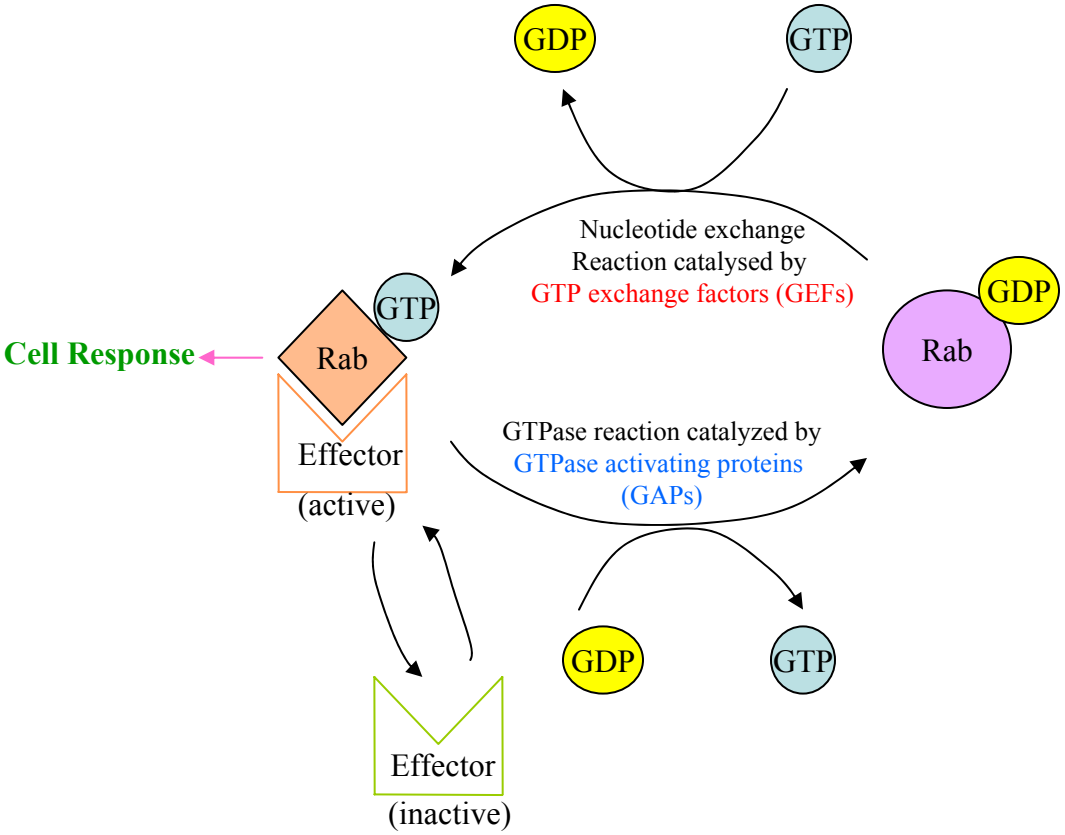

Figure 3. Activation and deactivation of Rab proteins. Rab proteins are activated to their GTP bound form by GTP exchange factors (GEFs) and deactivated to GDP bound form by GTPase activating proteins (GAPs).

Ferro-Novick, 2002).

Several early reports suggest that Rab proteins interact directly with either v- or t-SNAREs and activate them for trans-SNARE complex assembly (Lian et al., 1994; Lupashin & Waters, 1997). Rabs have also been demonstrated to regulate SNARE assembly and function indirectly through interactions with effector proteins such as tethering factors (Pfeffer, 1999; Waters & Hughson, 2000; Whyte and Munro, 2002; Zerial & McBride, 2001). Rabs were ruled out as determinants of targeting specificity when it was found that a single chimeric Rab protein could function at two transport steps (Brennwald and Novick, 1993; Dunn et al., 1993).

1.6 Targeting/Tethering

Tethering factors are not sole determinants of specificity as they are soluble or peripheral membrane proteins and hence must interact with integral membrane components with distinct localization patterns. These factors mediate the initial interactions between two membranes that are destined to fuse (Guo et al., 2000; Pfeffer, 1999; Waters & Hughson, 2000; Whyte & Munro, 2002). Tethering factors are usually either long coiled-coil proteins such as the Golgi protein p115/Uso1p (Nakajima et al., 1991; Waters et al., 1992) and the endosomal EEA1 (Simonsen et al., 1998) which form elongated dimers, or they come in the form of large hetero-oligomeric complexes such as the conserved oligomeric Golgi (COG) complex and several other tethering complexes which have been identified and are involved in the tethering event at distinct intracellular compartments. The exocyst (Sec6/Sec8) complex is the best studied tethering complex, originally identified in yeast, known to be important for polarized vesicle transport to the growing bud during cell cycle. The exocyst complex is involved in the tethering processes on defined regions of the

plasma membrane in mammalian cells and is the effector of several small GTPases including Cdc42, RalA and ARF6 (Prigent et al., 2003; Lipschutz and Mostov, 2002; Sugihara et al., 2002; Zhang et al., 2001). In addition, a protein (VFT for Vps fifty-three or GARP for Golgi-associated retrograde protein) complex consisting of Vps52, Vps53 and Vps54 participates in the tethering process on the late Golgi for incoming traffic from endosomes (Conibear and Stevens, 2000) and Vps51 acts to link the tethering complex to the SNARE complex (Siniossoglou and Pelham, 2002; Conibear et al., 2003). Mammalian homologues of the VFT/GARP complex were identified and could function similarly as tethering proteins in the trans-Golgi network (TGN) (Panic et al., 2003). TRAPPI and II are two related tethering complex that function in ER-Golgi and intra-Golgi transport and act together with Ypt1/Rab1 (Sacher et al., 2001), while the HOPS complex (or Class C VPS complex) consisting of Vps11, Vps16, Vps18, Vps33, Vps39, and Vps41 act together with Ypt7 and SNAREs in mediating tether and fusion at the vacuole in yeast (Seals et al., 2000). The HOPS complex has been shown to function in multiple transport steps in addition to fusion at the vacuolar membrane (Peterson and Emr, 2001; Preston et al., 1991). In addition, the Dsl1p complex has been shown to be essential for Golgi-to-endoplasmic reticulum (ER) retrograde traffic in yeast (Reilly et al., 2001).

Many tethering factors interact with SNAREs. Subunits of the yeast COG complex were demonstrated to interact genetically and/or physically with five intra-Golgi SNARE proteins: Bet1p, Sec33p, Ykt6p, Gos1p and Sed5p (Ram et al., 2002; Suvorova et al., 2002; VanRheenen et al., 1998, VanRheenen et al., 1999). Since tethering factors can facilitate SNARE assembly (McBride et al., 1999; Sato et al., 2000; Seals et al., 2000; Shorter et al., 2002), they can potentially orchestrate a sequential process, triggered by one or more activated Rab proteins, starting with

initial membrane tethering culminating with the assembly of trans-SNARE complexes. The capability of tethering factors to functionally interact with SNAREs, Rabs, and vesicle coat proteins is strongly indicative of a central role in membrane trafficking. Two proteins known to have implicated roles in tethering are initially identified in yeast, and are discussed in some detail below:

1.6.1 Sec34/Cog3 and the COG complex

Yeast		Mammals	
New name	**Previous names**	**New name**	**Previous names**
Cog1p	**Cod3p Sec36p Tfi1p**	**Cog1**	**ldlBp**
Cog2p	**Sec35p**	**Cog2**	**ldlCp**
Cog3p	**Sec34p Grd20p**	**Cog3**	**Sec34/hSec34**
Cog4p	**Cod1p Sgf1p Sec38p Tfi3p**	**Cog4**	**Cod1/hCod1**
Cog5p	**Cod4p**	**Cog5**	**GTC-90**
Cog6p	**Cod2p Sec37p Tfi2p**	**Cog6**	**Cod2/hCod2**
Cog7p	**Cod5p**	**Cog7**	**-**
Cog8p	**Dor1p**	**Cog8**	**Dor1/hDor1**

Table 1. Revised nomenclature for the COG complex

A screen for mutants of *Saccharomyces cerevisiae* secretory pathway components yielded *Sec34/Cog3p*, a mutant that accumulates numerous vesicles and fails to transport proteins from the ER to the Golgi complex at the restrictive temperature (Wuestehube et al., 1996). Thereafter, two groups showed that Sec34p/Cog3p and Sec35p/Cog2p are part of a large complex. VanRheenen et al., (1999) found that *Sec34* encodes a novel protein of 93kD, peripherally associated with membranes. Semi-intact cells made from *sec34-2* strain were able to bud vesicles from the endoplasmic reticulum, but these vesicles failed to efficiently tether to the Golgi complex at the restrictive temperature, indicating that Sec34p/Cog3p is required for tethering of ER-derived vesicles to the cis-Golgi complex. The temperature-sensitive phenotype of *sec34-2* is suppressed by the Rab GTPase Ypt1p that functions early in the secretory pathway, or by the dominant form of ER to Golgi complex

target-SNARE associated protein Sly1p, *Sly1-20p*. This trait is shared with all previously characterized ER to Golgi complex tethering factors (Sapperstein et al., 1996; Cao et al., 1998; VanRheenen et al., 1998). Weaker suppression is seen with overexpression of genes encoding Uso1p or the v-SNAREs. Kim et al., (1999) showed that Sec34p/Cog3p specifically suppresses *sec35-1* and that Sec34p/Cog3p and Sec35p/Cog2p stably associate with each other to form part of a large multiprotein complex.

Whyte and Munro, (2001) identified the other six components of the complex through the study of Dor1p/Cog8p, which is involved in vesicle targeting to the yeast Golgi apparatus. Identification of all 8 components revealed that they fall into two complementation groups with four subunits - (Dor1p/Cog8p, Cod2p/Cog6p, Cod4p/Cog5p and Cod5p/Cog7p) showing no growth defect when deleted and no severe defect in Golgi glycosylation. Deletion of the other 4 subunits causes slow growth and glycoslation defects. Sec34p/Cog3p, Sec35p/Cog2p, Cod1p/Cog4p and Cod3p/Cog1p are therefore required for a transport step necessary for normal growth and glycosylation, and recycling of vesicles containing Golgi enzymes back to early Golgi. It was suggested that the complex tethers two distinct classes of vesicles to the early Golgi: vesicles recycling within the Golgi and vesicles recycling to the Golgi from later endosomal compartments.

Defects in retrograde transport could lead indirectly to failure in ER-to-Golgi transport. It has been proposed that the compromised biosynthetic trafficking seen in some yeast Sec34/35 (COG) complex mutants (Wuestehube et al., 1996; Kim et al., 2001) may be a consequence of secondary anterograde trafficking defects arising from primary retrograde trafficking defects (Gaynor and Emr, 1997; Reilly et al., 2001). Spelbrink and Nothwehr, (1999) reported the identification of Sec34p/Cog3p (as

Grd20) involved in protein sorting in the TGN/endosomal system of *Saccharomyces cerevisiae*. Grd20/Cog3p is important in localization of a resident TGN endoprotease Kex2p. It is important also in carbohydrate processing machinery in the Golgi apparatus as a loss of Grd20p function results in missorting of a soluble vacuolar hydrolase carboxypeptidase Y (CPY). Cog4p was identified as Sgf1p by Kim et al., (2001). These authors showed that reduced levels of Sgf1p led to accumulation of a variety of membranes and also a kinetic block in ER to Golgi traffic. *sec34-2* and *sec35-1* mutations were demonstrated to cause a pleitropic block in the secretion of all proteins into the growth medium.

Cog1p was first identified as Sec36p by Ram et al., (2002). The authors demonstrated the binding of Sec36p/Cog1p to Sec34p/Cog3p and Sec35p/Cog2p. Missense mutations of Sec36p/Cog1p are lethal with mutations in COPI subunits, suggesting a functional connection between Sec34p/Sec35p (COG) complex and COPI vesicle coat. Sec37p/Cog6p and Sec38p/Cog4p were also discovered through affinity purification of proteins that bind to Sec35p/Cog2p-myc. Mutations in Sec34p/Cog3p, Sec35p/Cog2p, Sec36p/Cog1p and Sec38p/Cog4p are either lethal or greatly compromise cell growth. In addition, they also result in a pronounced defect in transport of CPY and they disrupt the integrity of the Sec34p/Sec35p (COG) complex. Hence, Sec34p/Cog3p, Sec35p/Cog2p, Sec36p/Cog1p and Sec38p/Cog4p seem to form the essential core of the complex to which Sec37p/Cog6p, Cod4p/Cog5p, Cod5p/Cog7p and Dor1p/Cog8p appear to be peripherally attached. This is similar to the assignment of the 8 subunits into two lobes of four subunits each by other labs as discussed later.

Interactions of the COG complex that support a recycling role was suggested by the work of Suvorova et al., (2002). The Sec34/35 (COG) complex interacts

genetically and physically with the Rab protein Ypt1p, intra-Golgi SNARE molecules and with the Golgi vesicle coat complex COPI, but not with a component of ER-to-Golgi COPII coat. Mutants show defects in basic Golgi functions including glycosylation of secretory proteins, sorting and retention of Golgi resident proteins. A function for the Sec34/35 (COG) complex in vesicle tethering is favored based on three observations (a) both *sec34-2* and *sec35-1* mutant cells accumulate numerous undocked 50nm transport vesicles (Wuestehube et al., 1996); (b) structural relationships between Sec34/35 (COG) complex and other yeast tethering complexes have been recently uncovered (Pfeffer, 2001; Whyte and Munro, 2001) and (c) like other tethering factors, the sec34/35p (COG) complex intimately interacts with the activated, GTP-bound form of the cis-Golgi localized Rab protein Ypt1p. Thus the proposal that the Sec34/35 (COG) protein complex acts as a tether that connects cis-Golgi membranes and COPI-coated, retrogradely targeted intra-Golgi vesicles. Mutation of Sec36p/Cog1p showed no defect when tested in the *in vitro* assay for the ER-to-Golgi transport at restrictive temperature (Ram et al., 2002). Hence, the ER-to-Golgi tethering defect may therefore be an indirect effect.

Morsomme and Riezman, (2002) demonstrated the ER-to-Golgi tethering defect in a different *in vitro* assay that measures tethering of ER-derived vesicles, whether homotypic or to another membrane. Rab GTPase Ypt1p and the Sec34/35 (COG) tethering complex, but not Bet3p, a member of the TRAPP complex, are also involved in sorting of GPI-anchored proteins from other secretory proteins upon ER exit (Morsomme and Riezman, 2002). Therefore, the Ypt1p tethering complex couples protein sorting in the ER to vesicle targeting to the Golgi apparatus. Heterotypic tethering function of Ypt1p, Uso1p, Sec35p/Cog2p, Sec34p/Cog3p and TRAPP were established using different assays (Barrowman et al., 2000; Cao et al.,

1998, VanRheenen et al., 1998, 1999). The first of these assays measured tethering by examining loss of diffusible ER-derived vesicles generated using purified COPII components. In another assay, budding was performed in the presence of radiolabeled membranes prepared from the Gap1p strain and unlabeled membranes prepared from the Gap1pHA strain. If labeled vesicles tether to the unlabeled membranes, then immunoisolation with anti-HA antibodies will indirectly precipitate these vesicles. The radioactive signal detected in the pellet after a medium speed centrifugation step will reflect tethering of ER-derived vesicles. 28% of the tethering signal was observed at 24ºC after Bet3p depletion, indicating only a partial defect of tethering in the absence of the TRAPP component.

Rab mediated recruitment of tethering factors to membranes may be a general mechanism to couple protein sorting and packaging into vesicles for targeting, docking and fusion. The tethering factors Uso1p and Sec34/35p (COG) along with the Rab GTPase, Ypt1p, are involved in sorting as well as in tethering of ER-derived vesicles. Sorting and tethering are not interdependent functions. Data suggests that these factors are required on the donor membrane for the correct sorting process upon vesicle budding (Morsomme and Riezman, 2002). Coupling of sorting to vesicle targeting via Rab GTPases and tethering factors could constitute a general mechanism whereby specificity throughout the secretory pathway is ensured. In the first step of the secretory pathway, Ypt1p could recruit Uso1p and the Sec34/35 (COG) complex at the ER, where sorting, packaging and budding occurs. These factors would be transported with the vesicles targeting them to the cis-Golgi compartment, where heterotypic tethering, docking and fusion can occur. The target on the cis-Golgi might be the TRAPP I complex that was shown to be statically localized to this compartment (Barrowman et al., 2000) and to be the specific target of COPII-coated vesicles.

The eight yeast components of the COG complex display homology to several, characterized and uncharacterized mammalian proteins (Whyte and Munro, 2001). This led to the prediction that the mammalian Sec34p-containing (COG) complex (Suvorova et al., 2001) is the same as the Golgi Transport Complex (GTC) (Walter et al., 1998). Human Sec34/Cog3 cDNA was first identified by Suvorova et al., (2001), and its predicted amino acid sequence showed 41% similarity to yeast Sec34p/Cog3p with homology throughout the entire coding region. Affinity purified antibodies recognized a cellular protein of 94kDa in both soluble and membrane fractions. Similar to yeast Sec34p/Cog3p, cytosolic hSec34/Cog3 migrates at a molecular mass of 300 kDa on a glycerol velocity gradient, suggesting that it is part of a protein complex. hSec34/Cog3 is localized to the Golgi compartment in cells of all species examined. Green fluorescent protein (GFP)-tagged hSec34/Cog3 expressed in HeLa cells was restricted to the Golgi cisternae, and its membrane association was sensitive to brefeldin A treatment. Taken together, these findings indicate that hSec34/Cog3 is part of a peripheral membrane protein complex localized on *cis*/medial Golgi cisternae where it may participate in tethering intra-Golgi transport vesicles.

GTC-90/Cog5 was originally discovered by Walter et al., (1998) as one of the subunits of Golgi transport complex (now known as the COG complex) which has transport stimulating activity in an *in vitro* intra-Golgi transport assay that reconstitutes vesicle trafficking between cis and medial Golgi cisternae. The Golgi transport complex is about 800kDa in size and GTC-90/Cog5 is a 90KDa subunit of the complex. Anti-GTC-90/Cog5 antibodies are inhibitory in an *in vitro* Golgi transport assay. Subcellular fractionation indicates that GTC-90 exists in both membrane and cytosolic pools with the cytosolic pool associated exclusively with the GTC complex while the membrane associated pool of GTC-90 is localized to the Golgi. The GTC

was also suspected to be identical to the ldlC complex, a Golgi associated complex thought to contain ldlBp/Cog1 and ldlCp/Cog2, two proteins that complement mutant cultured cell lines having a range of Golgi defects. Chatterton et al., (1999) demonstrated that the Chinese hamster ovary (CHO) cell mutants ldlC/Cog2 and ldlB/Cog1, exhibited almost identical phenotypes. In these mutants, the synthesis of virtually all N- and O- linked glycoproteins and of the major lipid-linked oligosaccharides is abnormal. The abnormal glycosylation of LDL receptors in ldlB/Cog1 and ldlC/Cog2 cells results in their reduced stability and therefore very low LDL receptor activity (Podos et al., 1994). These 2 genes are required for multiple steps in the normal medial and trans Golgi-associated processing of glycoconjugates. In wild-type cell cytosols, ldlCp/Cog2 is a component of an 950 kDa 'ldlCp complex'. Normal assembly of this complex is ldlBp/Cog1-dependent and may be required for Golgi association of ldlCp/Cog2 and for normal activities of multiple luminal Golgi processes.

Ungar et al., (2002) and ourselves (Loh and Hong, 2002) have shown that the mammalian Sec34/35, the GTC and the ldlCp complexes are one and the same. Henceforth, this complex has been named the conserved oligomeric Golgi (COG) complex (Krieger et al., 1981; Kingsley et al., 1986; Podos et al., 1994; Wuestehube et al., 1996; VanRheenen et al., 1998, 1999; Walter et al., 1998; Chatterton et al., 1999; Spelbrink and Nothwehr, 1999; Kim et al., 1999, 2001 Whyte and Munro, 2001; Ram et al., 2002; Ungar et al., 2002; Suvorova et al., 2002; Loh and Hong 2002; and Farkas et al., 2003). The COG complex comprises four previously characterized proteins (Cog1/ldlBp, Cog2/ldlCp, Cog3/Sec34, and Cog5/GTC-90), three homologues of yeast Sec34/35 complex subunits (Cog4/Cod1, Cog6/Cod2 and Cog8/Dor1) and a previously unidentified Golgi-associated protein (Cog7). "Deep etch" electron microscopy of

purified COG revealed a 37nm long structure comprising 2 similarly sized globular domains connected by smaller extensions. Consideration of biochemical and genetic data for mammalian COG and its yeast homologue suggests a model for the subunit distribution within this complex, which plays critical roles in Golgi structure and function. It is suggested by Ungar et al. that the subunits of the COG complex be divided into two approximately equal-sized subcomplexes, each having four subunits. This is in functional agreement with the classification by Whyte and Munro, (2001) of the yeast Sec34/35 (COG) complex's subunits into two groups of four, based on the severity of their mutant phenotypes. The first group, characterized by more severe phenotypes, contains Sec34p/Cog3p, Sec35p/Cog2p, Cod1p/Cog4p, and Cod3p/Cog1p, whereas the other group, distinguished from the first by weaker phenotypes, comprises Dor1p/Cog8p, Cod2p/Cog6p, Cod4p/Cog5p, and Cod5p/Cog7p (Whyte and Munro, 2001).

The COG complex may be directly involved in vesicular membrane transport processes (e.g., vesicle budding, targeting, or fusion reactions). Alternatively, the COG complex may indirectly influence vesicular trafficking as a consequence of a direct influence on the structure or activity of one or more compartments of the Golgi apparatus (e.g., potential scaffolding activity).

Analysis of the components of the COG complex has revealed some sequence similarity to components of the exocyst and the GARP complex. Many of the subunits of all three complexes seem to have a common domain of two short stretches of potential coiled coil or amphipathic helix at the amino termini (Whyte and Munro, 2001). This similarity between some of the tethering complexes may suggest that they have similar modes of action (Whyte and Munro, 2002).

Recently, Oka et al., (2004) identified a set of COG-sensitive, integral

membrane Golgi proteins called GEARs (mannosidase II, GOS-28, GS15, GPP130, CASP, giantin and golgin-84). The abundance of these proteins were decreased in the mutant cells and, in some cases, augmented in COG-overexpressing cells. Some GEARs were abnormally localized in the ER and were degraded by proteasomes in the mutants. The distribution of the GEARs were altered by siRNA depletion of ε-COP in wild-type cells in conditions where COG-insensitive proteins were unaffected. In addition, synthetic phenotypes arose in mutants deficient in both ε-COP and either Cog1 or Cog2. COG and COPI may therefore work in concert for the proper retention or retrieval of a subset of proteins in the Golgi, and COG helps prevent the ER accumulation and degradation of some GEARs.

1.6.2 BET3 and the TRAPP complex

BET3 was initially discovered as a new member of a group of interacting genes whose products were implicated in the targeting and fusion of ER to Golgi transport vesicles. A temperature-sensitive mutant, *bet3-1*, was isolated in a synthetic lethal screen used to identify new genes whose products may interact with BET1, a SNARE protein that is required for ER to Golgi transport. At 37ºC, *bet3-1* fails to transport invertase, alpha-factor, and CPY from the ER to the Golgi complex. Therefore, this mutant exhibits dilated ER and accumulates small vesicles. The SNARE complex fails to form in this mutant. BET3 encodes an essential 22-kDa hydrophilic protein that is conserved in evolution, and is not a component of the SNARE complex. These findings support the hypothesis that Bet3p may act before the assembly of the SNARE complex (Rossi et al., 1995). Bet3p has subsequently been shown to be one of the subunits of the TRAPP (transport protein particle) complex, which was first described as a large protein complex functioning in the later stages of ER-to-Golgi traffic in yeast (Sacher et al., 2000, Sacher et al., 1998). TRAPP was shown to represent two

distinct subcomplexes- TRAPP I contains 7 subunits (Bet5, Trs20, Bet3, Trs23, Trs33, Trs31 and Trs85) and is about 300kDa in size while TRAPP II is about 1000kDa and has an additional three subunits Trs65, Trs120 and Trs130 (Sacher et al., 2001). TRAPP I and TRAPP II both cofractionate with an early Golgi marker and are present in a cytosolic pool. The Golgi association is stable, since Bet3p does not relocate to the ER when anterograde ER-to-Golgi traffic is blocked and the complex remains assembled under these conditions (Barrowman et al., 2000). TRAPP I, but not TRAPP II, is required for an ER-to-Golgi *in vitro* transport assay (Sacher et al., 2001). TRAPP I binds to COPII vesicles formed *in vitro* from permeabilized yeast cells, independent of other factors, and even when the COPII vesicles are formed from purified coat components in the absence of cytosol and Golgi. In addition, when Bet3p is depleted from both vesicles and Golgi, no tethering occurs, showing that other factors are not sufficient to tether vesicles in the absence of TRAPP I (Barrowman et al., 2000). On the other hand, TRAPP II might be required for a later transport step. A temperature-sensitive mutant of a TRAPP II-specific subunit accumulates Golgi forms of invertase and CPY, as well as aberrant Golgi structures. Its subunits also show synthetic interactions with mutants of *ARF1* and components of COPI but not COPII (Sacher et al., 2001). Bet3p genetically interacts with SNAREs and Ypt1p (Rossi et al., 1995; Wang et al., 2000; Jones et al., 2000).

Tethering proteins have been shown to be linked with SNARE complex assembly. p115, a tethering protein associated with the Golgi, promotes SNARE complex assembly (Shorter et al., 2002). The assembly of certain Golgi-SNARE complexes is mediated by direct p115-SNARE interactions, as p115 directly and independently binds syntaxin 5 and GOS 28 and promotes their association. This suggests that the p115-SNARE interaction is probably essential for the activation of

the downstream fusion machinery. Many combinations of interactions between the various determinants namely the SNAREs, tethers, coat proteins, and Rabs contribute to the targeting specificity and are fundamental to the mechanism of vesicular transport.

1.7 Rationale of current work

In recent years, our understanding of the mechanism of membrane transport has been greatly enhanced owing to the discovery of a wealth of novel protein molecules and lipids that play fundamental roles in membrane targeting and fusion. In addition to the variety of SNARE molecules, individual transport events use unique multisubunit tethering complexes and distinct Rab GTPases. This extra level of complexity helps to ensure the selectivity, spatial and temporal regulation of membrane targeting in eukaryotic cells.

Numerous studies of membrane vesicle docking and fusion components were done on yeast, while much less is known about these processes in mammalian cells. Hence, we were eager to embark on unraveling the role of the mammalian counterparts and their contribution to various stages of protein transport. The mammalian system represents a more complex intracellular architecture and comprises multiple differentiated and specialized tissues, thereby making the identification and characterization of components of the transport machinery highly challenging. In this regard, we have focused on the components and mechanisms regulating tethers and SNAREs.

Sec34p/Grd20p (Cog3p) has been implicated in endoplasmic reticulum (ER)-to-Golgi transport and/or post-Golgi trafficking events and exists in a protein complex in yeast. Although the mammalian counterpart (Sec34/Cog3) of Sec34p has been

molecularly identified, its role in membrane traffic in mammalian cells and its interacting partners remain to be established. The importance of the tethering process in ensuring faithful docking and fusion of transport intermediates with the target compartment is becoming more recognized. While our work on Sec34/Cog3 was in progress, other labs have also established that Sec34/Cog3 exists in a multi-subunit complex and have renamed the complex as the conserved oligomeric Golgi (COG) complex. We were interested in the structural and molecular basis underlying the assembly and function of the COG complex and thus undertook to systematically investigate the inter-molecular interactions between the various subunits. The results obtained enabled us to present a model for the assembly of the complex, as detailed in chapter 4.

Besides the COG complex, we investigated the role of mammalian Bet3 in ER-Golgi transport in mammalian cells. Studies on Bet3 are described in chapter 5. Results obtained from the studies on these 2 tethering proteins will add to the growing knowledge on the theme of multisubunit complexes in the tethering process and its role in intracellular protein trafficking.

In addition to the tethering process, docking and fusion play a very essential role to ensure the specificity of membrane trafficking. Our knowledge of the regulation and organization of membrane compartments in mammalian cells is far from complete. It is therefore useful to identify and characterize novel SNARE members. To this end, syntaxin 8, a novel member of the syntaxin family was identified through EST database search using the sequence of known SNARE proteins. This is described in chapter 6.

CHAPTER 2

Materials and Methods

2.1 Materials

2.1.1 Antibodies

No.	Antigen	Species	Source	Reference
1	TGN38	Mouse	G. Banting	Luzio et al., 1990
2	Rab5	Mouse	A. Wandinger-Ness	Qiu et al., 1994
3	Rabaptin5	Mouse	Transduction Lab. (USA).	Stenmark et al., 1995
4	GS28 (HFD9)	Mouse	This lab	Subramaniam et al., 1995, 1996
5	Asialoglycoprotein receptor subunit R2 and R3	Rabbit	This lab	Wong et al., 1998
6	Syntaxin 7	Rabbit	This lab	Wong et al., 1998
7	α-SNAP	Rabbit	This lab	Subramaniam et al., 1997
8	NSF	Rabbit	This lab	
9	Mannosidase II	Mouse	Babco	Moremen and Robbins, 1991
10	Lamp2	Mouse	This lab	Sandoval and Bakke, 1994

Table 2. List of common antibodies used

2.1.2 Cell lines and EST clones

All cell lines were obtained from the American Type Culture Collection (Manassas, VA). Expressed sequence tag (EST) clones were generated by the Washington University-Merck expressed sequence tag project and obtained from the I.M.A.G.E. consortium via Research Genetics Inc. (Huntsville, Alabama).

2.1.3 Other materials

Fluorescein isothiocyanate-conjugated goat anti-rabbit immunoglobulin (IgG) and Texas Red-conjugated goat anti-mouse IgG were from Jackson ImmunoResearch. Supersignal substrate and peroxidase-conjugated goat anti-mouse and anti-rabbit antibodies were products of Pierce (Rockford, IL). Freund's adjuvants (complete and incomplete) were from Invitrogen. Synthetic oligonucleotides were either obtained

from Oligos Etc. (Wilsonville, OR) or Research Biolabs (Singapore). The rat multiple tissue northern blot filter was purchased from Clontech (Palo Alto, CA). *Pyrococcus furiosus* polymerase and the rat brain cDNA library in λZAP were obtained from Stratagene (La Jolla, CA). Hybond C+ nitrocellulose and *Taq* DNA polymerase were purchased from Amersham (Little Chalford, Buckinghamshire, UK). *Pfu* DNA polymerase was a product of Stratagene (La Jolla, CA).

Anti-myc and anti-HA antibodies (rabbit polyclonal IgG) were obtained from Upstate Biotechnology. Anti-Flag antibodies were from Sigma. The TNT T7 Quick Master Mix were obtained from Promega. Protein A-horseradish peroxidase (HRPO) was used as secondary antibody detection for Western blotting (BD Transduction Laboratories). Restriction enzymes were all purchased from Roche Molecular Biochemicals and New England Biolabs. Human Universal QUICK –Clone II (cDNA template) were purchased from BD Biosciences Clontech. Gluthathione-Sepharose 4B was a product of Pharmacia (Upsala, Sweden). pQE-60 HisX6 vector, M15 (pREP4) bacterial strain and Ni^{2+}-NTA beads were from Qiagen (Hilden, Germany). Local New Zealand White rabbits were purchased from the Sembawang Laboratory Animals Centre (Singapore). Monoclonal anti-β-COP antibodies (ascites maD) were purchased from Sigma, Singapore.

2.2 Methods

2.2.1 Data-base searches and sequence alignment

Data base searches were done with several BLAST programs available at the National Centre for Biotechnology Information (NCBI) World Wide Web server (http://www.ncbi.nim.nih.gov/BLAST/) (Altschul et al., 1990; 1997). Sequence alignments were performed using the MegAlign program (DNAStar Inc.)

2.2.2 cDNA cloning, library screening and sequencing

Among the known syntaxins, syntaxin 8 is most homologous to syntaxin 6. The TBLASTN program (Altschul et al., 1997) was used to search the EST database with the amino acid sequence of syntaxin 6 (Bock et al., 1996). Several EST clones (GenBank accession nos AA000586, W41301, W63907 and W83363) were identified whose sequences could encode protein fragments homologous to syntaxin 6. Oligonucleotides 1 (5'-GAACTCCCAACCCTT) and 2 (5'-ACTTTCTGTCCACCA) were used to obtain a fragment of about 280 bp from the EST clone no. W83363 by polymerase chain reaction (PCR) which was ^{32}P-labeled and used to screen a rat brain λZAP cDNA library (Promega).

Library screening was performed as described previously (Lowe et al., 1996). In summary, about 100,000 pfu was plated on 20cm x 20cm plates and plaques were allowed to form overnight. Duplicate lifts were made using Hybond N nylon filters (Amersham). The filters were marked and soaked for 3 minutes on Whatman paper wetted with denaturing buffer (1.5M NaCl, 0.5M NaOH), transferred to a paper wetted with neutralizing buffer (1.5M NaCl, 0.5M Tris pH8.0), followed by a rinse in 6 x SSC solution (1.5M NaCl and 0.3M sodium citrate). The filters were left to air dry for 5 minutes and then subjected to cross-linking by ultraviolet light. The filters were then washed twice, 1 h each at 42°C, in washing buffer which contains 50mM Tris, pH8.0, 1 M NaCl, 1 mM EDTA and 0.1% SDS. The washed filters were prehybridized in a prehybridization solution containing 6 x SSC, 0.1% SDS, 5 x Denhardts solution, 100 μg/ml denatured salmon sperm DNA and 0.05% sodium pyrophosphate for 2 h or more. cDNA probes were labeled by random priming using a kit from Pharmacia. Fifty to a hundred ng of template was heat denatured and incubated with a reagent mix (containing dNTP and Klenow polymerase buffer), 100 μCi [α^{32}P]dCTP (specific

activity ~ 3000Ci/mmol) and Klenow polymerase according to the manufacturer's protocol. The reaction was allowed to proceed for 2 h at 37°C. Labeled DNA was separated from the free labels using a Pharmacia NAP-5 desalting column. Hybridization was carried out at 50°C for at least 16 h in the prehybridization solution. Filters were washed with progressive increase in stringency by either decreasing the content of SSC in the washing buffer or increasing the washing temperature. Washed filters were subjected to autoradiography. Positive clones from the primary screenings were re-plated for the secondary and tertiary screenings until single plaques could be isolated. Four positive clones were obtained. One clone with an insert size of 1 kb was sequenced completely. This was the procedure adopted to screen for syntaxin 8.

2.2.3 Construction of recombinant fusion proteins

	Species	Genbank Acc. #	Source of clone
COG1	*Homo sapiens*	AB037802 (Kiaa1381)	Kazusa DNA Research Institute
COG2	*Homo sapiens*	AI492237	IMAGE consortium
COG3	*Homo sapiens* *Homo sapiens*	AK026305 AA429818	NEDO human cDNA sequencing project Wash-U Merck (EST) Project
COG4	*Homo sapiens*	AI634312 (SCOD1M4)	Sean Munro
COG5	*Homo sapiens*	NP_859422	Human Universal QUICK-Clone II (cDNA template)
COG6	*Homo sapiens*	AB032960 (Kiaa1134)	Kazusa DNA Research Institute
COG7	*Homo sapiens*	BE261220	IMAGE consortium
COG8	*Homo sapiens*	NP_115758	Human Universal QUICK-Clone II (cDNA template)

Table 3. Human cDNA clones used for the study of the COG proteins

cDNA Cloning of Human Sec34/Cog3—Full-length human Cog3 cDNA was assembled by first obtaining a 1.8-kb fragment from cDNA clone AK026305 by digestion with *Xho*I and *Nsi*I. This fragment, which contains the 5' coding region of Cog3, was ligated to an ~3.6-kb fragment obtained from cDNA clone AA429818 by digestion with *Xho*I and *Nsi*I, which also includes the vector pT7T3D-Pac. An additional 1.8-kb fragment was obtained from cDNA clone AA429818 by digestion with *Nsi*I alone. These fragments were ligated to construct an overall 4.3-kb Cog3 cDNA in pT7T3D-Pac vector.

Expression Constructs for myc Epitope-tagged ldlBp/Cog1, ldlCp/Cog2, Sec34/Cog3, Cod1/Cog4, GTC-90/Cog5, Cod2/Cog6, Cog7 and Dor1/Cog8

The cDNA clones for COG1, COG2, COG3, COG4, COG5, COG6, COG7 and COG8 are all of human origin and the detailed information about the clones are listed in table 3.

For Myc-Cog1, oligonucleotides 3 and 4 were used to amplify an ~1-kb fragment from KIAA1381, and the resulting PCR fragment was digested with *Xho*I and *Bam*HI. This was ligated to a fragment retrieved from KIAA1381 by digestion with *Bam*HI and *Not*I, together with pDMyc-neo vector (Seet and Hong, 2001) pre-cut with *Xho*I and *Not*I.

For Myc-Cog2, oligonucleotides 5 and 6 were used to amplify the entire coding sequence of ldlCp/Cog2 from IMAGE clone AI492237 by PCR, and the resulting product was digested with *Xho*I and *Xba*I and ligated into the corresponding sites of pDMyc-neo vector.

For Myc-Cog3, Cog3 cDNA in pT7T3D-Pac vector was digested with *Xho*I and *Not*I, and the resulting fragments were digested with *Bgl*I to obtain an ~2.5-kb fragment that contains the entire coding region of Cog3. This fragment was blunt-ended and ligated to pDMyc-neo vector pre-cut with *Xba*I and blunt-ended.

For myc-COG4, oligonucleotides 7 and 8 were used to amplify an ~700bp fragment from plasmid SCOD1M4 (generously provided by Dr. Sean Munro) (Whyte and Munro, 2001) and the resulting PCR fragment was digested with *XhoI* and *BglII*. This fragment was ligated to a fragment retrieved from SCOD1M4 by digestion with *BglII* and *XbaI*, together with pDMyc-neo vector pre-cut with *XhoI* and *XbaI*.

For myc-COG5, oligonucleotides 9 and 10 were used to amplify an ~1500bp fragment from Universal QUICK-Clone II cDNA template and the resulting PCR fragment was

digested with *XbaI* and *ClaI*. This fragment was ligated to another PCR fragment which was generated using the same template with oligonucleotides 11 and 12, digested with *ClaI* and *NotI*, together with pDMycneo vector pre-cut with *XbaI* and *NotI*.

For Myc-Cog6, oligonucleotides 13 and 14 were used to amplify a 450-bp fragment from the KIAA1134 clone, and the resulting PCR product was digested with *Xho*I and *Sac*I. This fragment was ligated to another fragment retrieved by digesting KIAA1134 with *Sac*I and *Not*I, together with the pDMyc-neo vector pre-cut with *Xho*I and *Not*I.

For myc-COG7, oligonucleotides 15 and 16 were used to amplify the entire coding sequence of COG7 from IMAGE clone BE261220 by PCR, and the resulting product was digested with *EcoRI* and *XbaI* and ligated into the corresponding sites of pDMyc-neo vector.

For myc-COG8, oligonucleotides 17 and 18 were used to amplify the entire coding sequence of COG8 from Human Universal QUICK-Clone II cDNA template by PCR, and the resulting product was digested with *XhoI* and *NotI* and ligated into the corresponding sites of pDMyc-neo vector.

All the above 8 subunits of the COG complex which were constructed in pDMyc-neo vector, were also digested using its corresponding restriction enzyme sites out of the vector and ligated to the corresponding sites of pDHA-neo and pFlag-neo vector to construct HA-tagged and Flag-tagged versions of COG1-8.

For production of recombinant GST fusion proteins of Cog3, oligonucleotides 19 and 20 were used to amplify the coding sequence for residues 1–276 of Cog3. This PCR product was digested with *Bam*HI and *Xho*I. Oligonucleotides 21 and 22 were used to retrieve the region coding for residues 277–552 of Cog3. The PCR product was digested with *Sma*I and *Xho*I. Oligonucleotides 23 and 24 were used to amplify the

sequence coding for residues 553–828 of Cog3. This PCR product was digested with *Bam*HI and *Xho*I. The bacterial expression vector pGEX-4T-1 (Amersham Biosciences) was digested accordingly and ligated with these PCR fragments. The ligated plasmids were transformed into DH5α cells, and ampicillin-resistant colonies expressing the GST fusion proteins were screened.

The oligonucleotides from 3 to 30 are listed below:

3: 5' GAGCTCGAGCGGGTGGGCGAACGGTAC 3'

4: 5' TACACATGTGGATCCATTTCTGCAGC 3'

5: 5' GGCCTCGAGCGGGAGAAAAGTAGG 3'

6: 5' GGTCTAGACGAGAGGCTGCTCTGCTGT-TGC 3'

7: 5' GAGCTCGAGCGCGCGGACCTTGATTCG 3'

8: 5' CAGTGGGAAGATCTTGAAGAAG 3'

9: 5' GACCGTGCCCGTCTAGAGATGGGCTGGGTGGGCGGGCGGCGCCGG 3'

10: 5' GTACCTGCGGCCGCATCAATCGATTTCATCAGAGGAAGGAGGATTA-CGACCACC 3'

11: 5' GACCGTGCCCGTCTAGAGATCGATGGTATTATTAAAACTATAGCAA-GTGAACTA 3'

12: 5' GTACCTGCGGCCGCATTACTGAAGAGCAGACATAGCCTTTTGAAG 3'

13: 5' GAGCTCGAGCGGGCAGAGGGCAGCGGGGAAGTG 3'

14: 5' GGCATCTGCAACTTGAGCTCTTATCTCTAATTT 3'

15: 5' AAGAATTCAGACTTCTCCAAGTTC 3'

16: 5' GCTCTAGACGACGTAATTCACACT 3'

17: 5' GAGCTCGAGCGCGCGACCGCGGCGACTATCCCA 3'

18: 5' ATAGCGGCCGCAAATCTAGGGCCCCACGCTGGGCGGTTC 3'

19: 5' ATTGGATCCATTATGGCGGAGGCGGCG 3'

20: 5’ CGGCTCGAGCGGACTTGTGAGGGTCTGTAGTGTGTT 3’

21: 5’ CTCCCGGGTCATCAGTTACTGAAAAGGGATCCT 3’

22: 5’ CGGCTCGAGCGGTCCATGAAGATCTGC 3’

23: 5’ CCCGGATCCCCCATGTGGTATCCTACGGTTCGAAGA 3’

24: 5’CGGCTCGAGCGGTTTAGAAACTGACAGCAGAAG 3’

25: 5’ TTTAAAGCCATGGCCCCAGACCCC 3’

26: 5’ GTGGATCCCTTTCTGTCCACCAG 3’

27: 5’ GCCATGGAAATGTCGAGGCAGGCG 3’

28: 5’ CGCGGATCCCTCTTCTCCAGCTGG 3’

29: 5’ CGCGGATCCATGTCGAGGCAGGCG 3’

30: 5’ CCCAAGCTTCTCTTCTCCAGCTGG 3’

Construction of recombinant syntaxin 8 fusion proteins **--** Oligonucleotides 25 and 26 were used to amplify the coding sequence for the cytoplasmic domain (residues 1-210) of syntaxin 8 by PCR to express C-terminally HisX6-tagged syntaxin 8 (HisX6-syntaxin 8). This PCR product was digested with *Nco*I and *Bam*HI, ligated into the corresponding sites of pQE60 vector and then transformed into the *Escherichia coli* host, M15(pRep4). The recombinant protein was affinity purified on Ni^{2+}-NTA beads (Qiagen).

Construction of recombinant Bet3 fusion proteins **--** Oligonucleotides 27 and 28 were used to amplify the coding region of mouse Bet3 by polymerase chain reaction (PCR). The PCR product was digested with *NcoI* and *BamHI* and ligated into the corresponding sites of pQE60 vector. The ligation reaction was transformed into competent M15(pRep4) bacterial cells. Cells harbouring properly inserted Bet3 coding region was identified and used for the purification of HisX6-tagged Bet3 (His-Bet3). To prepare recombinant glutathione sulphotransferase (GST) fused Bet3 (GST-Bet3),

oligonucleotides 29 and 30 were used to amplify the Bet3 coding sequence by PCR. The resulting product was digested with *BamHI* and *HindIII*, ligated into the corresponding sites of pGEX-KG vector (Guan and Dixon, 1991) and transformed into competent BL21 cells. Cells harbouring the recombinant plasmid were identified and used for the purification of GST-Bet3.

2.2.4 Protein purification

The purification of GST-fusion protein was performed as described previously (Lowe et al., 1996). 1 litre of bacterial cultures was grown to an OD_{600} of 0.8 before overnight induction with IPTG to a final concentration of 0.5 mM at room temperature. Cells were pelleted and resuspended in 50 ml lysis buffer (phosphate buffered-saline [PBS] containing 50 mM Tris pH 8.0, 1 mg/ml lysozyme, 1 mM DTT, 1mM PMSF, 0.5 mM $MgCl_2$ and 0.1% Triton X-100). Lysis was performed by incubation on ice for half an hour followed by sonication at 4 ºC for 3 minutes (1 minute x 3). The lysates were clarified by centrifugation and applied to glutathione Sepharose 4B column (Pharmacia). After washing with PBS, the GST fusion proteins were eluted with 10mM reduced glutathione in GST buffer (PBS containing 50 mM Tris pH8.0, 0.5 mM $MgCl_2$) and stored in aliquots at -20ºC.

For the purification of HisX6-tagged proteins, a similar procedure was used. Bacterial cultures were grown in 2xTY broth containing 100 µg/ml carbenicillin and 25 µg /ml kanamycin at 37°C until an OD_{600} of 0.8 was reached. Expression of the recombinant protein was induced by the addition of IPTG to 0.5 mM, after which cells were grown at room temperature for a further 12 hours. Bacterial cultures were pelleted and the pellet was resuspended in cracking buffer (100 mM Hepes-KOH pH 7.3, 500 mM KCl, 5 mM MgCl2, 2 mM β-mercaptoethanol, 1 mM PMSF and 0.1% Triton X-100) by sonication for 3 min. The lysate was centrifuged for 20 min at

10,000rpm in a refrigerated SS-34 rotor (Sorvall). The supernatant was passed twice through a column of Ni^{2+}-NTA resin (Qiagen) pre-equilibrated with buffer A (20 mM Hepes-KOH pH 7.3, 100 mM KCl, 2 mM β-mercaptoethanol, 10% glycerol) containing 25 mM imidazole. The beads were washed with 50 volumes of buffer A containing 25 mM imidazole. Bound protein was eluted in buffer A containing 250 mM imidazole. 1 ml fractions were collected and analyzed by SDS-PAGE. Fractions containing His6-Bet3 were pooled and dialyzed against PBS (phosphate-buffered saline).

2.2.5 Preparation of polyclonal antibodies

400 μg of GST-fusion protein was emulsified with Freund's complete adjuvant and injected subcutaneously into two local New Zealand White rabbits. Booster injections with the same amount of antigen in Freund's incomplete adjuvant were administered every 2 weeks. The rabbits were bled 10 days after the second and subsequent boosters. For affinity purification, the antiserum was first diluted with an equal volume of PBS and then incubated for 2 h at 4 °C with GST coupled to cyanogen bromide activated Sepharose 4B beads (Amersham Biosciences) to remove antibodies against GST. The flow-through was then incubated overnight at 4°C with beads coupled with the respective GST-fusion protein. The beads were washed extensively with PBS, buffer A (50mM Tris-HCl, pH 7.4, 500 mM NaCl), buffer B (50mM Tris pH 7.4, 1% Triton X-100), buffer C (50mM Tris pH 7.4, 500 mM NaCl, 1% Triton X-100) and PBS again. Specific antibodies were eluted with Immunopure IgG elution buffer (Pierce Chemical Co.). Collected fractions were analyzed by SDS-PAGE to determine the concentration of the antibodies. Positive fractions containing the specific antibodies were pooled and dialyzed against PBS or 25/125 buffer (25 mM Hepes-KOH, pH 7.3, 125 mM KOAC).

2.2.6 Indirect immunofluorescence microscopy

Cells were grown on coverslips overnight to 50–80% confluence, rinsed twice with phosphate-buffered saline with 1 mM $CaCl_2$ and 1 mM $MgCl_2$ (PBSCM). and processed as described previously (Subramaniam et al, 1995; Lowe et al, 1996). Cells were fixed in 3% paraformaldehyde in PBSCM for 30 minutes at room temperature. Thereafter, the cells were sequentially washed with PBSCM, PBSCM containing 50 mM NH_4Cl and then with PBSCM again, followed by a further permeabilization step in PBSCMS (PBSCM containing 0.1% saponin) for 15 minutes at room temperature. After permeabilization, the cells were incubated with the primary antibodies in fluorescence dilution buffer (PBSCM with 5% normal goat serum, 5% fetal bovine serum, and 2% bovine serum albumin, pH 7.6) at RT for 1 h followed by washing with PBSCMS and then incubation with fluorescent-labeled secondary antibodies. After further washing with PBSCMS, the cells were mounted with Vectashield (Vector Lab) and then viewed. Conventional fluorescence microscopy was done with a Carl Zeiss axiophot microscope equipped with epifluorescence optics. Confocal microscopy was performed using a Biorad MRC600 or MRC 1024 confocal scanning system connected to a Carl Zeiss Axiophot microscope with epifluorescence optics. For blocking experiments, 0.5 μg of antigen was used to neutralize the antibodies for 30 minutes on ice before the antibodies were applied to the cells.

2.2.7 Preparation of membrane fractions

Membranes were prepared as described (Subramaniam et al., 1992), with some minor modifications. Livers obtained from Sprague-Dawley rats which had been fasted overnight were rinsed once in ice cold PBS, then in homogenization buffer (0.25 M sucrose, 25 mM Hepes, pH 7.4, 5 mM MgCl2, 1 mM PMSF) and weighed. Livers were homogenized in 3 volumes (ml/g) of homogenization buffer using a Teflon pestle

and homogenizer at 3000 rpm. The homogenate was centrifuged at 3000 rpm in a GSA rotor for 10 minutes to remove nuclei, mitochondria and any unbroken cells. The postnuclear supernatant was then spun at 40000 rpm in a TY45 (Beckman) rotor for 1 hour to pellet the total membrane fraction (TM). The supernatant (cytosol) was also saved. The TM fraction was resuspended in a minimal volume of the homogenization buffer. A sufficient volume of 2.0 M Sucrose, 5 mM $MgCl_2$, 1 mM PMSF, buffered with 25 mM Hepes pH 7.3 was added to obtain a final concentration of 1.25 M sucrose. This membrane homogenate was overlaid with step gradients of 1.1 M, 1.0 M, 0.8 M and 0.25 M sucrose containing 5 mM $MgCl_2$, 1 mM PMSF, buffered with 25 mM Hepes pH 7.3. The samples were centrifuged at 28,000 rpm for 3 h in a Beckman SW28 rotor. Four major fractions were isolated: Golgi enriched fractions G1 (1.1/1.0 M interphase), G2 (1.0/0.8 M interphase), endosome-enriched membrane fraction EM (0.8/0.25 M sucrose interphase) and the microsomal pellet (M). The G1, G2 and EM membranes were diluted fourfold with 25 mM Hepes, 5mM $MgCl_2$ and 1 mM PMSF and pelleted by a 100,000 *g* centrifugation step in a TY45 rotor as above. Membranes were resuspended in homogenization buffer and flash-frozen in aliquots. For some experiments, the gradients were prepared by overlaying the 1.25 M total membrane suspension with step gradients of 1.1 M and 0.5 M sucrose. The interphase between the 0.5 M and 1.1 M steps (GEM) which comprises Golgi, endosomes and lysosomes was pelleted, and resuspended in the appropriate buffer.

2.2.8 Preparation of rat liver cytosol

Livers from two rats starved overnight were rinsed once in ice cold PBS, and then with ice cold 25/125 buffer. Homogenization was carried out in 3 volumes (ml/g) of 25/125 buffer using a manual Teflon homogenizer. The homogenate was centrifuged at 3000 rpm in a GSA rotor for 10 minutes. The supernatants were filtered

through cheese cloths and further centrifuged at 40 k rpm in a SW41 rotor (Beckman) for 2 h. The top lipid layer was discarded and the cytosol was flash frozen in liquid nitrogen.

2.2.9 *In Vitro* ER-to-Golgi Transport Using Semi-intact Cells

The biochemical assay to measure the transport of VSV-G protein from the ER to the cis-Golgi was performed as previously described (Beckers *et al*., 1987; Beckers and Balch, 1989; Davidson and Balch, 1993; Zhang and Hong 2001). Briefly, normal rat kidney cells were grown on 10-cm petri dishes to form a confluent monolayer and infected with a temperature sensitive strain of the vesicular stomatitis virus, VSVts045 at 32ºC for 1 h. The cells were pulse labeled with [^{35}S]-methionine at the restrictive temperature (40ºC) and then subjected to perforation on ice by hypotonic swelling and scraping. (Beckers *et al*., 1987; Beckers and Balch, 1989; Davidson and Balch, 1993). These semi-intact cells were then incubated in a complete assay cocktail of 40 μl containing (in final concentrations) 25 mM Hepes-KOH, pH 7.2, 90 mM KOAc, 2.5 mM $Mg(OAc)_2$, 5 mM EGTA, 1.8 mM $CaCl_2$, 1 mM ATP, 5 mM creatine phosphate, 0.2 IU of rabbit muscle creatine phosphokinase, 25 μg rat liver cytosol (Davidson and Balch, 1993) and 5 μl (25-30 μg of protein;. 1-2 x 10^5 cells) of semi-intact cells. Additional reagents were added as indicated in the Results. Samples were incubated for 90 min at 32^{o}C and transport terminated by transfer to ice. The membranes were collected by a brief spin in a microfuge, solubilized in 20 μl of 0.2% SDS, 50 mM sodium citrate (pH 5.5). After boiling for 5 min, the samples were digested overnight with 2.5 units of endoglycosidase H (Endo H). Subsequently, 6 x SDS sample buffer was added and the samples were separated on 7.5% SDS polyacrylamide gels. Transport was quantified using a Phosphor Imager (Molecular Dynamics, Sunnyvale, CA).

This method was used for analysis of the role of Bet3 in ER-to-Golgi transport. A similar modified assay was used for the analysis of Cog3. No radioactive methionine was used. Instead, the confluent monolayer was transferred from 32ºC to 40ºC with the addition of more media without [^{35}S]-methionine and incubated for a further 2 h. The rest of the procedure is identical except that the samples after being separated on the polyacrylamide gels, would be transferred to a nitrocellulose filter and processed by immunoblot analysis with anti-vesicular stomatitis virus antibodies (Roche Molecular Biochemicals). For antibody inhibition of transport assay, specific antibodies were added into the complete assay mixture and incubated on ice for 60 min to allow diffusion of antibodies into the semi-intact cells.

2.2.10 Large-scale Immunoprecipitation

300 µl of protein A-Sepharose CL-4B (Amersham Biosciences) was washed in PBS and incubated with 500 µg of rabbit anti-goat IgG (Pierce) or 500 µg of anti-Sec34/Cog3 antibodies separately for 2 h at 4 °C. The antibodies were cross-linked to the beads with 50 mM dimethyl pimelidate in 0.2 M sodium borate, pH 9, overnight at 4 °C and then washed in 0.2 M sodium borate, pH 9, and incubated with 0.2 M ethanolamine, pH 8, for 2 h at room temperature. The beads were washed with PBS and finally in 0.5% TX-100 in gradient buffer (20 mM Hepes, pH 7.3, 100 mM KCl, and 2 mM EDTA). Fifty mg of rat liver cytosol was first incubated with the beads bound with control rabbit IgG in gradient buffer with 0.5% TX-100 for 2 h at 4 °C. The supernatant was then incubated with the beads bound to Sec34 antibodies overnight at 4 °C. The beads were then washed three times with gradient buffer containing 0.5% TX-100 and then finally with gradient buffer without TX-100.

2.2.11 Transfection and Analytical Immunoprecipitation

293T cells were grown on 60-mm dishes to 40–60% confluence. 1 µg of myc-

tagged ldlBp/Cog1, ldlCp/Cog2, Dor1/Cog8, Cod1/Cog4, and Cod2/Cog6 DNA was used for transfection with Effectene Transfection Reagent, according to the manufacturer's instructions (Qiagen). The Effectene procedure has two steps: DNA is first mixed with Enhancer and a buffer that provides optimal salt conditions for efficient DNA condensation. This step requires 2–5 minutes. Effectene Reagent is then added and the mixture is incubated for 5–10 minutes to allow Effectene–DNA complexes to form. The complexes are mixed with growth medium (which contains serum and antibiotics), and added directly to the cells. The next day, the cells were washed twice with PBSCM. 150 μl of PBS containing 1% TX-100 and complete EDTA-free protease inhibitor mixture (Roche Diagnostics) was added, and the cells were then scraped with a cell scraper. The cells were rotated at 4 °C for 15 min and then spun down at 4000 rpm for 10 min. Sec34/Cog3 antibodies (5 μg) were added to the supernatant and incubated at 4 °C for 2 h. Next, protein A-Sepharose CL-4B beads were added and left to bind overnight at 4 °C. The beads were then washed three times with PBS containing 1% TX-100, with PBS containing 0.2% TX-100, and finally washed with PBS and analyzed by SDS-PAGE. Immunoblot analysis was performed with anti-myc monoclonal antibodies.

2.2.12 Immunoblot Analysis

Proteins were separated by SDS-PAGE and electrotransferred onto Hybond C+ nitrocellulose. The blots were then incubated for 1 h at 37 °C in blocking buffer (5% skim milk and 5% fetal bovine serum in PBS containing 0.05% Tween 20). The blots were incubated in blocking buffer containing primary antibodies for 1 h at room temperature, followed by three washes (5 min each) with PBS containing 0.05% Tween 20. The blots were then incubated with either goat anti-rabbit or anti-mouse antibody conjugated to horseradish peroxidase (Jackson ImmunoResearch). For

experiments done with COG proteins, the blots were incubated with Protein A-horse radish peroxidase. After three washes in PBS containing 0.05% Tween 20, SuperSignal West Pico Chemiluminescence Substrate (Pierce) was added, and the blots were processed according to the manufacturer's protocol. For the blocking experiment shown in Fig 5, 50 μg of proteins extracted from Golgi-enriched membranes or cytosol was electrophoresed and transferred to a filter. After blocking, the filter was immunoblotted with 2 μg of affinity-purified Sec34/Cog3 antibodies or with 2 μg of Sec34/Cog3 antibodies preincubated with 20 μg of recombinant GST-Sec34/F1, GST-Sec34/F2, or GST-Sec34/F3.

2.2.13 *In Vitro* Translation and Binding Experiments

The TNT T7 Quick Coupled Transcription/Translation System (Promega) was used for *in vitro* translation according to manufacturer's protocol. This system for eukaryotic *in vitro* translation uses rabbit reticulocyte lysate in combination with RNA polymerase, nucleotides, salts and recombinant RNasin ribonuclease inhibitor to form a single TNT Quick Master Mix. Circular plasmid DNA containing a T7 promoter is added to an aliquot of the TNT Quick Master Mix and incubated at 30°C. The synthesized proteins are then analyzed by SDS-polyacrylamide gel electrophoresis (SDS-PAGE) and detected.

The first experiment was carried out accordingly with radioactive methionine: **(A)** In a 100μl reaction, myc-tagged Sec34/Cog3 and each of the myc-tagged ldlBp/Cog1, ldlCp/Cog2, and Cod2/Cog6 were co-translated for 2 h at 30 °C. 20 μl of each reaction was used for co-immunoprecipitation with 10 μg of anti-myc antibodies (rabbit polyclonal IgG) (Upstate Biotechnology) or 10 μg of anti-Cog3 antibodies bound to protein A-Sepharose beads in gradient buffer with 0.1% TX-100. After 1 h at room temperature, the beads were washed five times with gradient buffer with 0.1%

TX-100 and analyzed by SDS-PAGE and autoradiography together with 2 μg of *in vitro*-translated product (10% starting material). This method was used in chapter 3, figure 10. In chapter 4, similar procedures were employed with the use of non-radioactive methionine:

(B) For binary interactions experiments described in Figures 11, 12, and 14B, 25μl of each translation reactions of the two stated epitope-tagged subunits were mixed and co-translated for 2 hr at 30°C. The reaction volume was then spilt and used for co-immunoprecipitation with 8μg of each antibodies (as stated in the figures) bound to protein A-Sepharose beads in 500 μl of gradient buffer (20mM Hepes, pH 7.3, 100mM KCl, and 2mM EDTA) with 0.1% TX-100. For multiple-subunit interactions described in Figures 13, 15 and 16, all other subunits added into the reaction mixture are myc epitope-tagged, while the subunit of interest (COG6 or COG8) are Flag epitope-tagged. 25μl of each translation reactions of the indicated subunits (as shown in the tables) were mixed and co-translated for 2 hr at 30°C. The reaction volume was then split and used for co-immunoprecipitation with 10μg of anti-myc antibodies (rabbit polyclonal IgG) or 10μg of anti-Flag antibodies (rabbit polyclonal IgG) bound to protein A-Sepharose beads in gradient buffer with 0.1% TX-100. After 1 hr at room temperature, the beads were washed five times with gradient buffer with 0.1% TX-100 and analyzed by SDS-PAGE, followed by immunoblot analysis.

2.2.14 Northern blot analysis

For the analysis of Bet3, a cDNA fragment of about 540bp obtained by the BamHI and HindIII digestion of mouse EST clone (accession number AA255291) was radiolabelled with ^{32}P and hybridized to a mouse multiple tissue Northern blot containing 2 μg of poly(A)$^+$ mRNA from the indicated tissues (Clontech), using the hybridization and washing conditions as described for the screening procedure. The

blot was then exposed to an X-ray film. As for syntaxin 8, the same procedure was performed on a fragment of about 600 bp retrieved by *Cla*I and *Eco*RI digestion of the rat cDNA was ^{32}P-labeled and used as a probe on a rat multiple tissues blot of poly(A)$^+$ mRNA.

2.2.15 Immunogold labeling

NRK cells were allowed to internalize 15 nm BSA-gold for 1 hour in DMEM followed by an overnight chase to label the late endocytotic structures. Cells were then allowed to internalize 5 nm BSA-gold for 6 minutes and were immediately fixed with 8% paraformaldehyde in 200 mM Hepes, pH 7.4. Cryosections were prepared and labeled with antibodies against syntaxin 8 as described (Griffiths, 1993) except that the new method of Liou et al. (1997) was used to pick up frozen sections. The sections were then detected with 10 nm gold-Protein A. The labeling was quantified using systematic sampling and intersection counts as described (Griffiths, 1993). For each structure 20 micrographs were quantified.

For double labeling of syntaxin 8 and Rab5, PC12 cells were rapidly frozen and then processed for freeze-substitution and embeding in Lowicry HM-20 (Steyer et al., 1997; Neuhaus et al., 1998). Ultra-thin sections were double-labeled with syntaxin 8 and Rab5 antibodies and detected with 4 nm gold-Protein A and 9 nm gold-Protein A, respectively.

2.2.16 Differential extraction of membrane fraction

Golgi enriched membrane (GEM) fraction (25 μg) was extracted in a total volume of 200 μl with PBS, 1 M KCl, 2 M urea, 150 mM Na_2CO_3 (pH 11.5), 1% Nonidet P-40 and 1% sodium deoxycholate (DOC) for 1 hour at 4°C. The suspension was centrifuged at 55,000 rpm in a TLA100 rotor (Beckman) for 60 minutes. The resulting supernatants and pellets were resuspended in SDS sample buffer,

electrophoresed and immunoblotted to detect Bet3 and GS28 in chapter 5 and syntaxin 8 in chapter 6.

2.2.17 20S SNARE complex formation

Formation of the 20S SNARE complex was performed as described (Subramaniam et al., 1996). GEM fraction was extracted with assembly buffer (20 mM Hepes, pH 7.3, 100 mM KCl, 2 mM EDTA, 2 mM DTT, 0.5 mM ATP) containing 1% Triton X-100 for 45 minutes at 4°C. The extract was centrifuged for 45 minutes in a TLA100.2 rotor (100,000 ***g***). 15 μg of recombinant α-SNAP and 60 μg of recombinant NSF were incubated with 300 μg of membrane extract in the absence (assembly buffer) or presence (disassembly buffer) of 8 mM $MgCl_2$ in a final volume of 500 μl. The complex was allowed to form for 30 minutes on ice and then loaded onto a cushion of 15-40% glycerol in assembly or disassembly buffer. After centrifugation for 18 hours at 40,000 rpm in a SW41 rotor (Beckman), 0.8 ml fractions were collected from the bottom. Samples were electrophoresed on 12% SDS-PAGE and immunoblotted.

2.2.18 Cellular fractionation

NRK cells were trypsinized, washed with media containing 10% FCS, and resuspended in 300 μl of buffer containing 20 mM Hepes (pH 7.4), 100 mM KCl and 2 mM EDTA. The cells were sonicated twice (15 seconds each) and centrifuged at 600xg to remove unbroken cells and nuclei. The resulting postnuclear supernatant was centrifuged at 55000 rpm for one hour using the TLA 100 rotor (Beckman). The pellet was resuspended in the same volume as the supernatant. 15 μl of the pellet fraction (total membranes, TM) and 15 μl of the supernatant (cytosol) were analyzed and immunoblotted to detect Bet3, RhoGDI1 and GS28.

2.2.19 Immunodepletion of Bet3 from rat liver cytosol

CNBR-activated Sepharose 4B (Pharmacia) was prepared according to the manufacturer's protocol. Saturating amounts of affinity purified Bet3 antibodies were bound to the beads at 4^{o}C overnight and the beads subsequently blocked with glycine. After extensive washing, the beads were equilibrated with PBS to make a 50% suspension. 100 μl of suspension was incubated with 100 μl (about 2.5 mg) of rat liver cytosol (rlc) for 2 hours at 4^{o}C, and the beads removed by centrifugation. The depletion was checked by Western blotting to detect Bet3. The depleted cytosol was flash frozen in liquid nitrogen. As control depletion (mock), the identical procedure was performed using an antibody against hemagglutinin (HA).

2.2.20 Gel filtration analysis

Samples were run in 200μl aliquots on a FPLC Superdex 75 column (Pharmacia) equilibrated with PBS containing 1% deoxycholate at 4 C. Flow rate was 0.5 ml/min and fractions of 0.7 ml each were collected. The fractions were precipitated with trichloroacetic acid (TCA), separated on SDS-PAGE, transferred to nitrocellulose and blotted with the indicated antibodies.

CHAPTER 3

Sec34/Cog3 is implicated in Traffic from the Endoplasmic Reticulum to the Golgi and Exists in a complex with GTC-90/Cog5 and ldlBp/Cog1

3.1 Introduction

Many proteins originally identified in yeast have now been shown to participate in ER-to-Golgi transport in mammalian cells (Hong, 1998; Zhang and Hong, 2001), and more proteins regulating ER-to-Golgi transport in mammalian cells are expected to exist. *SEC34* and *SEC35* were identified as genes whose products are necessary for protein transport from the ER to the Golgi in yeast *Saccharomyces cerevisiae* (Wuestehube et al., 1996). More detailed studies of Sec34p/Cog3p and Sec35p/Cog2p have suggested that they function as components of a protein complex that acts as a tethering factor to ensure the proper docking and fusion of transport intermediates with the Golgi apparatus (Kim et al., 1999, 2001; Van Rheenen et al., 1998, 1999). In addition, the TRAPP protein complex (Sacher et al., 1998) and Uso1p (Cao et al., 1998; Nakajima et al., 1991; Sapperstein et al., 1996) have similarly been shown to function in tethering for the same transport event. Although the spatial, temporal, and mechanistic relationships among the Sec34/Sec35p (COG) complex, the TRAPP complex, and Uso1p have yet to be fully characterized, the importance of the tethering process in ensuring faithful docking and fusion of transport intermediates with the target compartment is becoming more recognized in several trafficking events (Guo et al., 2000; Pfeffer, 1999; Waters and Pfeffer, 1999). GTC-90 /Cog5 was purified as a component of a novel protein complex in mammalian cells that is required for intra-Golgi transport *in vitro* (Walter et al., 1998). Although the GTC-90 protein complex is known to include several other different subunits, their identities were unknown, and the functional aspects of the GTC-90 complex in other transport events remain to be

examined.

Low density lipoprotein receptor is responsible for the clearance of serum low density lipoprotein particles, and diverse mutations in its gene are associated with familial hypercholesterolemia (Hobbs et al., 1992). Due to its importance, understanding the pathway and mechanism underlying low density lipoprotein receptor trafficking has been an active area of cell biology. Genetic approaches have been used to create and identify several mutant lines of Chinese hamster ovary cells, including ldlA-ldlI (Hobbie et al., 1994; Kingsley et al., 1986; Malmstrom and Krieger, 1991). The genes mutated in some of these mutants (such as ldlA, ldlB, ldlC, ldlD, and ldlF) have been identified (Kozarsky et al., 1986; Guo et al., 1994; Chatterton et al., 1999; Kingsley et al., 1986; Podos et al., 1994). Biochemical and cell biological characterizations of ldlBp/Cog1 and ldlCp/Cog2 have revealed that they are components of the same protein complex (Chatterton, 1999; Podos et al., 1994). Both ldlBp/Cog1 and ldlCp/Cog2 are necessary for maintaining normal structure and function of the Golgi apparatus, although the precise function remains to be investigated.

Using antibodies against the recombinant Sec34 N-terminal fragment, evidence is presented to support a role for Cog3 in ER-to-Golgi transport in mammalian cells. Significantly, the observation that antibodies against Cog3 could co-immunoprecipitate GTC-90/Cog5, ldlBp/Cog1, and others, suggests that Sec34/Cog3, GTC-90/Cog5, ldlBp/Cog1, and ldlCp/Cog2 are part of the same protein complex(es) that may regulate diverse aspects of the Golgi functions, including ER-to-Golgi transport.

3.2 Results

3.2.1 *Characterization of Antibodies against Cog3*

Due to the established role of Sec34p/Cog3p in ER-to-Golgi transport in yeast

and our general interest in ER-to-Golgi transport in mammalian cells, we used the amino acid sequence of Sec34p/Cog3p to search for its putative mammalian counterpart by BLAST searches (Altschul et al., 1990). Several cDNA sequences encoding polypeptides homologous to various regions of Sec34p/Cog3p were uncovered. The complete coding region of human Cog3 was assembled from various cDNAs and confirmed by DNA sequencing (GenBank™ accession no. AF332595).

During the course of our work, the molecular identification of human Sec34/Cog3 was independently reported (Suvorova et al., 2001). Examination of the deduced 828 amino acid sequences suggests that Sec34/Cog3 could be roughly divided into two regions (Fig. 4*A*). The N-terminal one-third is highly homologous to counterparts from other species such as yeast, fly, and worm and has the potential (particularly residues 126–211) to form coiled-coil structures. The C-terminal two-thirds is homologous to EEA1 (Fig. 4*B*), a well-established tethering factor that regulates endosome fusion (Christoforidis et al., 1999; Zerial and McBride, 2001). The structural relatedness of Cog3 to a well-defined tethering protein provides some structural evidence for Cog3 to function as a tethering factor. To define the functional and biochemical aspects of Cog3, we expressed recombinant Cog3 in three separate fragments (residues 1–276, Sec34/F1; residues 277–552, Sec34/F2; and residues 553–828, Sec34/F3) fused to GST (Fig. 4*A*). GST-Sec34/F1 was used to raise antibodies against Sec34/Cog3. As shown in Fig. 5, affinity purified Sec34/Cog3 antibodies recognized a polypeptide of about 93 kDa in both membrane (*lane 1*) and cytosol (*lane 5*) fractions derived from rat liver. Detection of this polypeptide by the antibodies was abolished by preincubation of the antibodies with GST- Sec34/F1 (Fig. 5, *lanes 2* and *6*) but not with GST-Sec34/F2 (*lanes 3* and *7*) or GST-Sec34/F3 (*lanes 4* and *8*), suggesting that the antibodies are specific for Cog3 and that Cog3 is present in both

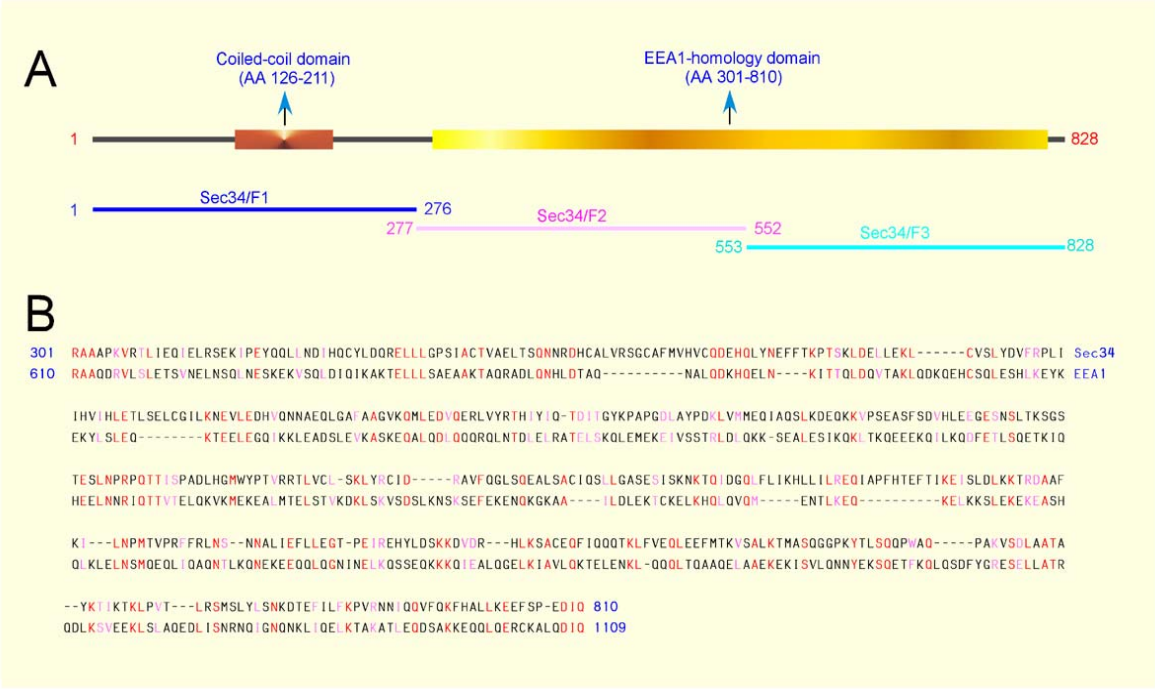

Figure 4. Characterization of Sec34/Cog3 antibodies. (*A)*, domain organization of Sec34/Cog3. The 828-residue Cog3 can be divided into the N-terminal one-third that is conserved among proteins from various species and has the potential to form coiled-coil structures; whereas the C-terminal two-thirds is homologous to EEA1 (Christoforidis et al., 1999). The regions from which various GST fusion proteins were derived are indicated. (*B)*, the C-terminal two-thirds of Cog3 is homologous to EEA1. Residues 301–810 of Cog3 were aligned with residues 610–1109 of EEA1. Identical residues are shown in *red*, whereas conserved residues are shown in *pink*.

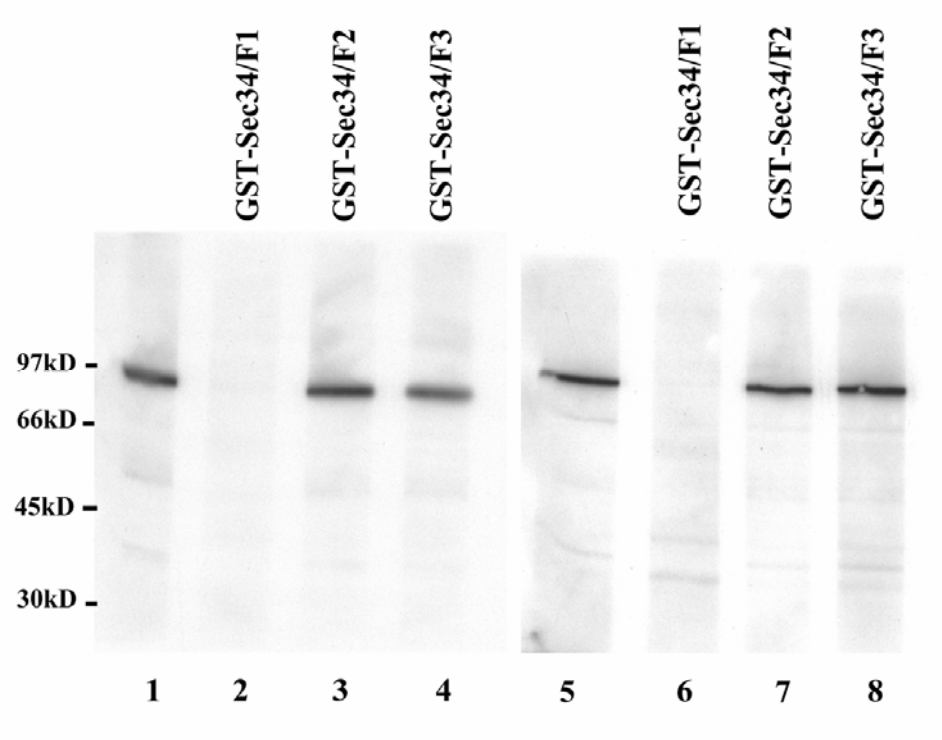

Figure 5. Sec34/Cog3 antibodies are specific. Antibodies raised against GST-Sec34/F1 specifically recognize a 93-kDa protein. The 50 μg of Golgi-enriched membrane fractions (*lanes 1–4*) and 50 μg of total cytosol (*lanes 5–8*) derived from rat liver were resolved by SDS-PAGE and transferred to filters. The filters were incubated with either Sec34 antibodies alone (*lanes 1* and *5*) or in the presence of GST-Sec34/F1 (*lanes 2* and *6*), GST-Sec34/F2 (*lanes 3* and *7*), or GST-Sec34/F3 (*lanes 4* and *8*).

cytosolic and membrane fractions.

Using these antibodies in immunofluorescence microscopy, Cog3 was seen to be enriched in the Golgi apparatus (Fig. 6, a) marked by the Golgi SNARE GS28 (Fig. 6, *b*) (Subramaniam et al 1996; Nagahama et al 1996) in HeLa cells. Furthermore, the Golgi labeling of Cog3 (Fig. 6, *d*) but not GS28 (Fig. 6, *e*) was abolished by preincubation of the antibodies with GST-Sec34/F1, further confirming the specificity of the antibodies. These results are similar to those reported previously (Suvorova et al., 2001) and suggest that our antibodies are specific for Cog3.

3.2.2 Sec34/Cog3 is necessary for ER-to-Golgi Transport

Because evidence for a functional role for Cog3 in ER-to-Golgi transport in mammalian cells is lacking, we investigated the potential transport function of Cog3 using a modified semi-intact cell assay that reconstitutes protein transport from the ER to the Golgi. NRK cells were infected with a temperature-sensitive mutant vesicular stomatitis virus (VSVts045) at 32 °C for 1 h followed by incubation at 40 °C for 2 h to accumulate its envelope glycoprotein (VSVG) in the ER. Cells were then permeabilized by scraping in hypotonic buffer and used to reconstitute transport of VSVG by supplementing them with exogenous rat liver cytosol and an ATP-regenerating system at 32 °C. Transport of VSVG to the Golgi was measured by monitoring the conversion of its endoglycosidase H-sensitive glycans to endoglycosidase H-resistant forms of the entire population of ER-arrested VSVG molecules as revealed by immunoblot analysis. There are two advantages in this modified assay compared with the original protocol of Zhang and Hong, (2001). The first is that no radioactive materials were used. The other is that instead of measuring a small fraction (the radiolabeled pool) of total VSVG, this assay measures the synchronized transport to the Golgi of almost all VSVG molecules accumulated in the

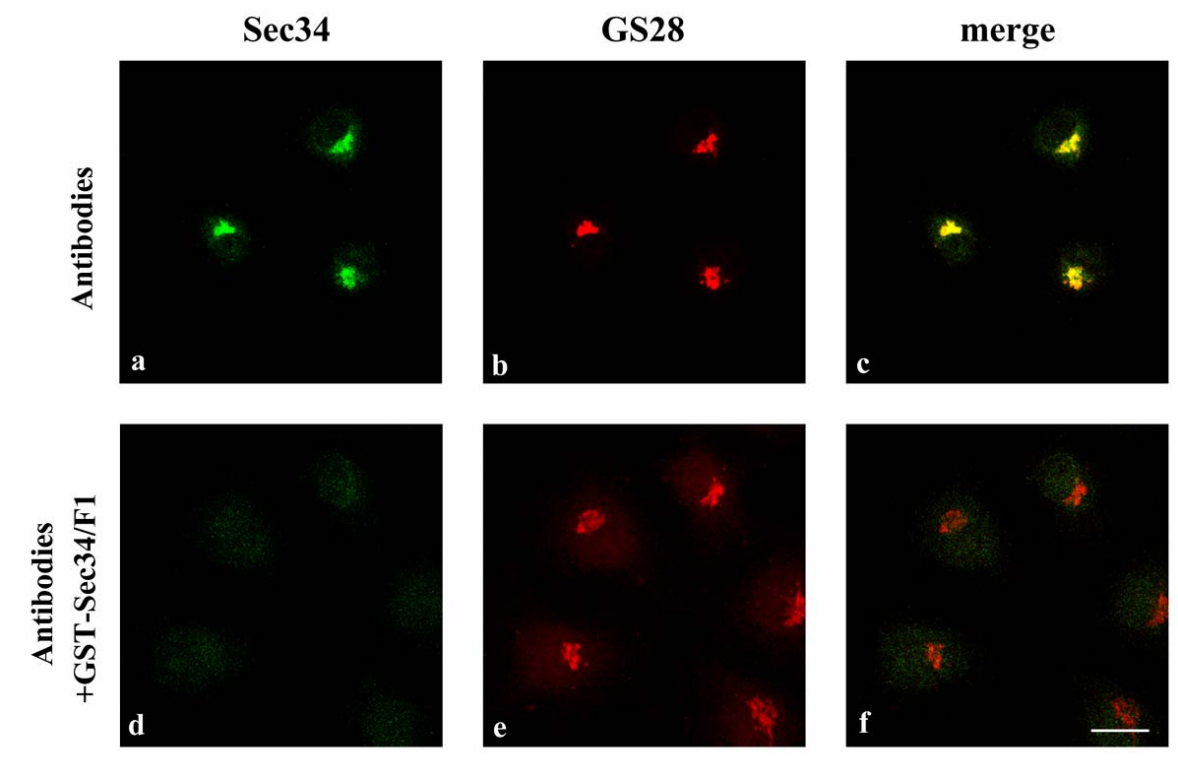

Figure 6. Anti-Sec34/Cog3 antibodies label the Golgi apparatus. HeLa cells were fixed, permeabilized, and double-labeled with Sec34/Cog3 antibodies (*a* and *d*) and monoclonal antibodies against Golgi SNARE GS28 (*b* and *e*). The Golgi labeling of Sec34/Cog3 (*d*) but not GS28 (*e*) was abolished by prior incubation of the antibodies with GST-Sec34/F1. The merged images are shown in *c* and *f*. *Bar*, 10 μm.

ER. As shown in Fig. 7, VSVG remained as the endoglycosidase H-sensitive ER form when the transport reaction was performed on ice (Fig. 7*A*, *lane 1*; Fig. 7*B*, *lane 1*) or in the absence of cytosol (Fig. 7*A*, *lane 2*; Fig. 7*B, lane 2*). Between 60% and 90% of total VSVG was converted into the endoglycosidase H-resistant form when the transport assay was conducted in the presence of complete mixture at 32 °C (Fig. 7*A, lane 3*; Fig. 7*B, lane 3*). Addition of antibodies against GST (Fig. 7*A, lanes 4–6*) did not inhibit this transport, whereas the addition of antibodies against Cog3 (Fig. 7*A, lanes 7–10*) inhibited the transport in a dose-dependent manner. Clear inhibition was observed in the presence of ≥3 μg of anti-Sec34/Cog3 antibodies, and the transport was almost completely inhibited by 7 μg of antibodies (Fig. 7*A*, *lane 10*). The inhibition by Sec34/Cog3 antibodies is specific because it could be neutralized by a noninhibitory amount of GST-Sec34/F1 (Fig. 7*B*, *lanes 5* and *7*), but not by GST (Fig. 7*B*, *lanes 4* and *6*). These results suggest that Sec34/Cog3 is important for ER-to-Golgi transport in mammalian cells.

3.2.3 Co-immunoprecipitation of GTC-90/Cog5, ldlBp/Cog1, Dor1/Cog8, and Cod1/Cog4 from Total Cytosol by Anti-Sec34/Cog3 Antibodies

To define the molecular mechanism underlying the action of Sec34/Cog3, we performed large-scale immunoprecipitations using rat liver cytosol (Fig. 8). Compared with rabbit anti-goat IgG (Fig. 8, *lane 2*), antibodies against Cog3 immunoprecipitated several distinct polypeptides (*lane 3*), as resolved by SDS-PAGE. We have focused our mass spectrometric analyses on polypeptides that are larger than the IgG heavy chain. As shown in Fig. 8, GTC-90/Cog5 (Walter et al., 1998) and ldlBp/Cog1 Chatterton et al., 1999), in addition to Cog3, were identified in the Cog3 immunoprecipitates. The intensities of ldlBp/Cog1 and GTC-90/Cog5, as revealed by Coomassie Blue staining, were stronger than that of Cog3, suggesting that the Cog3

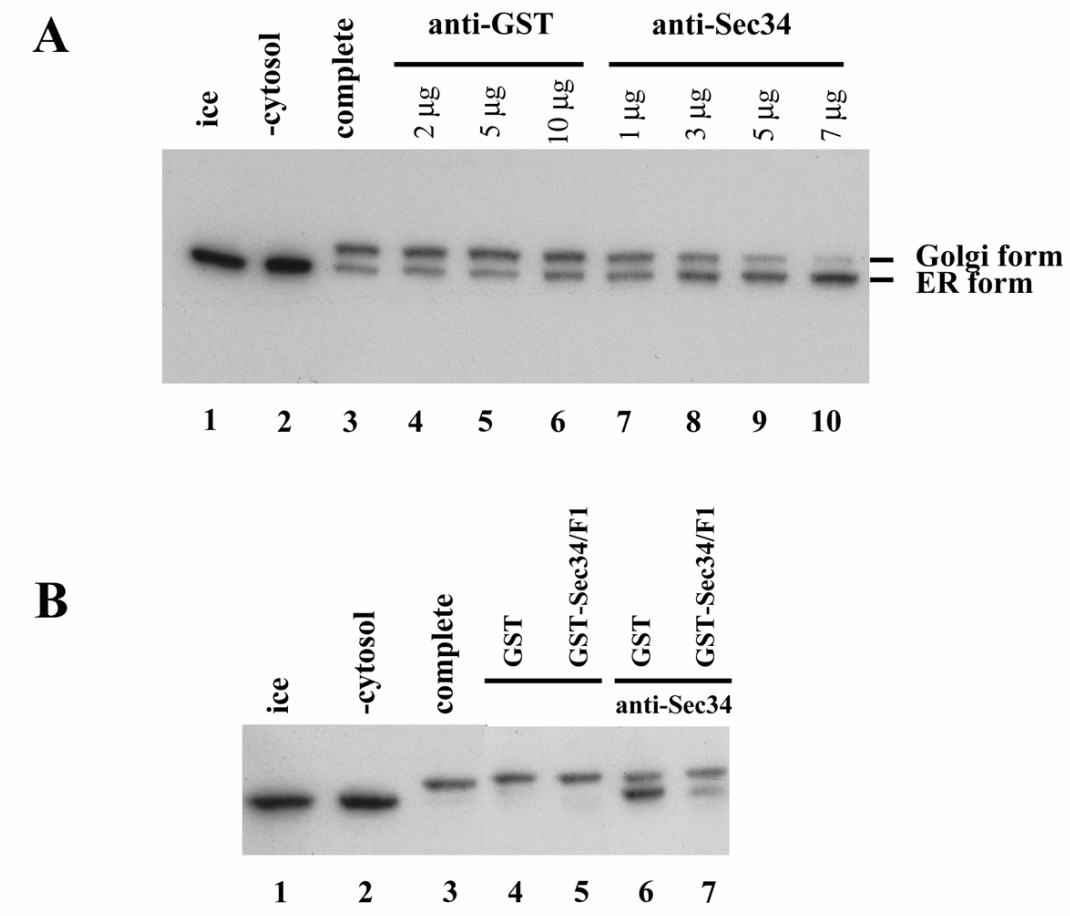

Figure 7. Sec34/Cog3 antibodies specifically inhibit ER-to-Golgi transport *in vitro*. (*A), in vitro* ER-to-Golgi transport assay was performed either on ice (*lane 1*) or at 32 °C (*lanes 2–10*) in the absence (*lane 2*) or presence of rat liver cytosol (*lanes 1* and *3–10*) supplemented with the indicated amounts of GST antibodies (*lanes 4–6*) or Sec34/Cog3 antibodies (*lanes 7–10*). The *upper form* represents VSVG, whose N-linked glycans are resistant to endoglycosidase H digestion, whereas the *lower form* represents the ER form, whose N-linked glycans have been removed by endoglycosidase H. (*B), in vitro* transport was performed either on ice (*lane 1*) or at 32 °C (*lanes 2–7*) in the absence (*lane 2*) or presence of rat liver cytosol (*lanes 1* and *3–7*). The inhibition exhibited by anti-Sec34/Cog3 (7 µg) was neutralized by a noninhibitory amount of GST-Sec34/F1 (3 µg) (*lanes 5* and *7*) but not by GST (3 µg) (*lanes 4* and *6*).

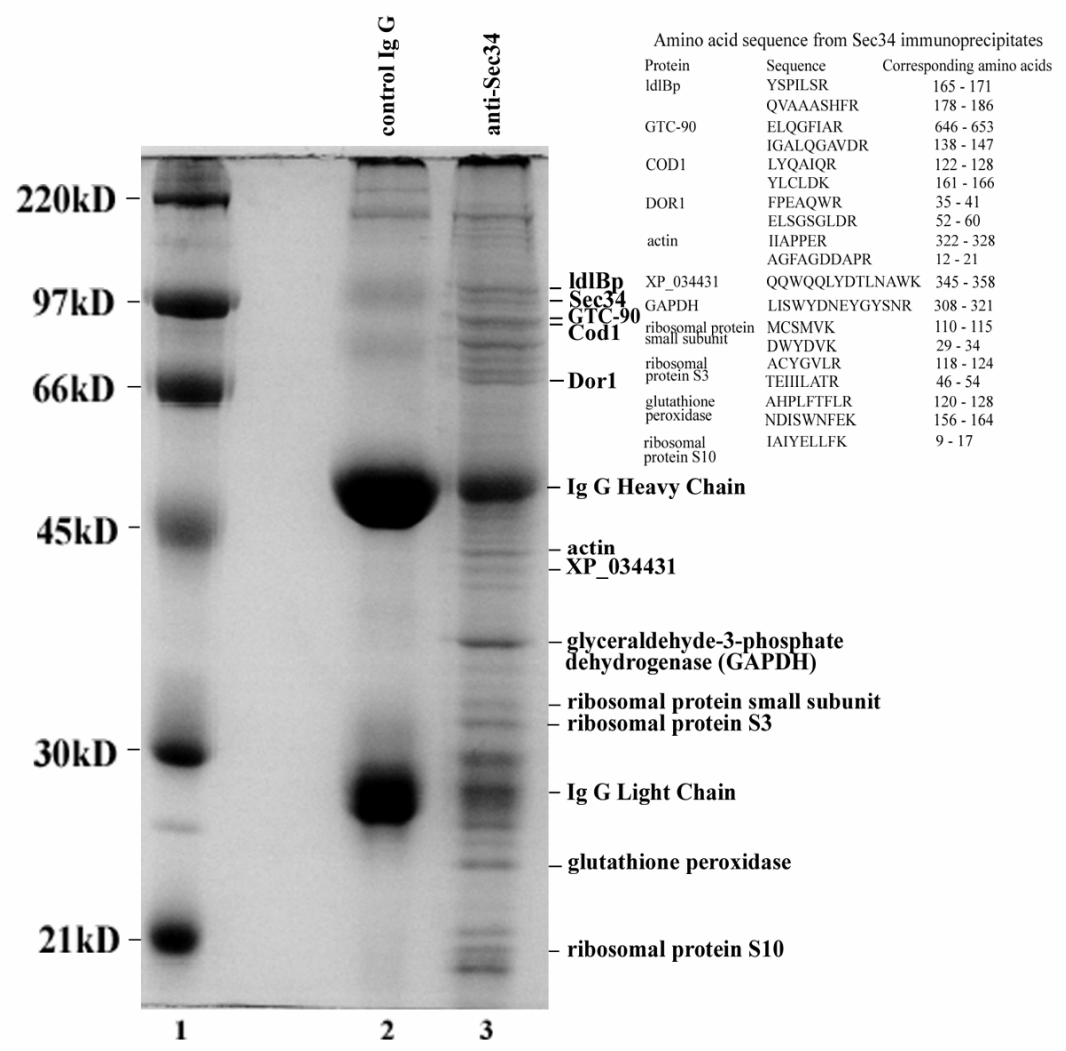

Figure 8. Co-immunoprecipitation of GTC-90 and ldlBp (as well as Dor1 and Cod1) by anti-Sec34/Cog3 antibodies. Rat liver cytosol (50 mg) was immunoprecipitated with 500 μg of Sec34/Cog3 antibodies (*lane 3*) or rabbit anti-goat IgG (*lane 2*) immobilized on protein A-Sepharose beads. The immune complexes collected on the beads were washed extensively. The immunoprecipitated proteins were released by boiling in SDS-PAGE sample buffer and then resolved by 10% SDS-PAGE. Molecular size markers are shown on *lane 1*. Polypeptides larger than the IgG heavy chain were first excised and subjected to mass spectrometric analysis. The amino acid sequences of tryptic peptides of ldlBp, GTC-90, Dor1, and Cod1 are indicated on the *right*. The identity of the Sec34 band was established by immunoblotting analysis. Mass spectrometric analysis of polypeptides smaller than the IgG heavy chain was performed and revealed the presence of abundant cytosolic proteins that could be due to nonspecific interactions

polypeptide might be poorly stained or that other subunits are present at higher abundance in the complex. The quantitative and specific recoveries of ldlBp/Cog1 and GTC-90/Cog5 by anti-Sec34/Cog3 antibodies from total cytosol suggest that Sec34/Cog3, GTC-90/Cog5, and ldlBp/Cog1 are components of the same protein complex(es). Furthermore, two mammalian homologues Dor1/Cog8 and Cod1/Cog4 of the yeast Sec34p-Sec35p (COG) complex (Whyte and Munro, 2001) were also detected in the Cog3 immunoprecipitates (Fig. 8), supporting the hypothesis that they are part of the mammalian complex. To rule out the possibility that some interesting components may have been overlooked, we have also analyzed other polypeptides migrating faster than that of IgG heavy chain. These mainly represented abundant cytosolic proteins such as actin, three ribosomal subunits, glyceraldehyde-3-phosphate dehydrogenase, and glutathione peroxidase. In addition, an uncharacterized protein with GenBank™ accession no. XP_034431 was identified. Although we cannot exclude the possibility that some of these proteins may be involved in Sec34/Cog3 function, the presence of abundant cytosolic proteins such as actin, glyceraldehyde-3-phosphate dehydrogenase, and ribosomal proteins in this low molecular weight region indicates that their presence is likely due to nonspecific interactions.

3.2.4 Co-immunoprecipitation of ldlCp/Cog2 and Cod2/Cog6

While our study was in progress, detail classification of the yeast Sec34p-Sec35p (COG) complex was reported by Whyte and Munro, (2001). It contains eight subunits: Sec34p/Cog3p, Sec35p/Cog2p, Dor1p/Cog8p, Cod1p/Cog4p, Cod2p/Cog6p, Cod3p/Cog1p, Cod4p/Cog5p, and Cod5p/Cog7p. Cod4p corresponds to GTC-90/Cog5 in mammalian cells. Some structural relatedness between Sec35p and ldlCp was noticed, indicating that Sec35p could be a candidate for the functional counterpart of mammalian ldlCp/Cog2 (Whyte and Munro, 2001). Mammalian homologues of

Dor1p/Cog8p, Cod1p/Cog4p, and Cod2p/Cog6p, but not Cod3p or Cod5p, were also identified, and the epitope-tagged mammalian Dor1/Cog8 and Cod1/Cog4 were detected in the Golgi apparatus upon transient transfection (Whyte and Munro, 2001). No apparent structural or functional yeast counterpart of ldlBp was found in the yeast Sec34p/Sec35p (COG) complex. Because GTC-90/Cog5, ldlBp/Cog1, Dor1/Cog8, and Cod1/Cog4 were recovered in the anti-Sec34/Cog3 immunoprecipitates, we examined whether other potential subunits ldlCp/Cog2 and Cod2/Cog6 of the mammalian complex(es) could be immunoprecipitated by anti-Sec34/Cog3 antibodies (Fig. 9). 293T cells were transiently transfected with constructs expressing Myc epitope-tagged ldlBp/Cog1, ldlCp/Cog2, Dor1/Cog8, Cod1/Cog4, or Cod2/Cog6. Cell lysates were immunoprecipitated with anti-Sec34/Cog3 antibodies and analyzed by immunoblot to detect the tagged proteins. As positive controls, cells transiently expressing myc-ldlBp/Cog1, myc-Dor1/Cog8, and myc-Cod1/Cog4 were immunoprecipitated with anti-Sec34/Cog3. About 5% of myc-ldlBp/Cog1 (Fig. 9, *lanes 1* and *2*), myc-Dor1/Cog8 (*lanes 5* and *6*), or myc-Cod1/Cog4 (*lanes 7* and *8*) could be recovered by anti-Sec34/Cog3 antibodies. Under identical conditions, they were not co-immunoprecipitated by other control antibodies (data not shown). These results further support our conclusion that they are specifically co-immunoprecipitated by Cog3 antibodies. Importantly, myc-ldlCp/Cog2 (Fig. 9, *lanes 3*and *4*) and myc-Cod2/Cog6 (*lanes 9* and *10*) were co-immunoprecipitated by anti-Sec34/Cog3 antibodies with efficiencies comparable to that observed for myc-ldlBp/Cog1, myc-Dor1/Cog8, and myc-Cod1/Cog4, supporting the notion that these other proteins are indeed subunits of the same mammalian complex(es).

3.2.5 Direct Interaction of Sec34/Cog3 with ldlBp/Cog1 or ldlCp/Cog2

We next investigated whether Cog3 could interact directly with any of the other

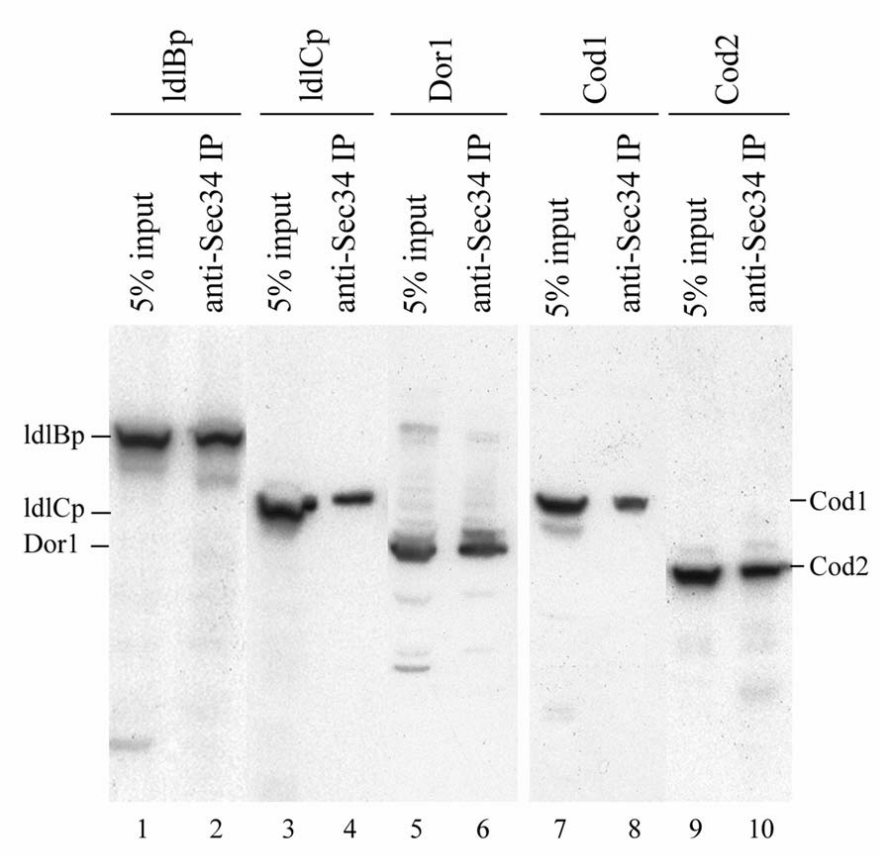

Figure 9. ldlCp/Cog2 and Cod2/Cog6 are present in Sec34/Cog3-containing protein complex. 293T cells were transiently transfected with constructs expressing myc epitope-tagged ldlBp (*lanes 1* and *2*), ldlCp (*lanes 3* and *4*), Dor1 (*lanes 5* and *6*), Cod1 (*lanes 7* and *8*), or Cod2 (*lanes 9* and *10*). Cell lysates were immunoprecipitated with Sec34 antibodies. 5% of each lysate (*odd-numbered lanes*) and the immunoprecipitates (*even-numbered lanes*) were resolved by SDS-PAGE and analyzed by immnoblot with anti-myc antibodies to detect the co-immunoprecipitated proteins. These myc-tagged proteins were not co-immunoprecipitated by control rabbit IgG or antibodies against Bet3 (data not shown).

subunits. Myc-Sec34/Cog3 was co-translated with myc-ldlBp/Cog1, myc-ldlCp/Cog2, or myc-Cod2/Cog6 using an *in vitro* translation system (Promega). The translation reactions were then subjected to immunoprecipitation using Sec34/Cog3 antibodies or anti-myc antibodies. As shown in Fig. 10, myc-Sec34/Cog3 and myc-Cod2/Cog6 were both effectively immunoprecipitated with anti-myc antibodies (*lane 3*). However, myc-Cod2/Cog6 was not co-immunoprecipitated by anti-Sec34/Cog3 under the conditions in which myc-Sec34/Cog3 was efficiently immunoprecipitated (Fig. 10, *lane 2*), suggesting that myc-Cod2/Cog6 and myc-Sec34/Cog3 do not interact directly. Interestingly, both myc-ldlBp/Cog1 and myc-ldlCp/Cog2, upon co-translation with myc-Sec34/Cog3, could be efficiently (30–50% of co-expressed protein) co-immunoprecipitated by anti-Sec34/Cog3 antibodies (Fig. 10, *lanes 5* and *8*, respectively), suggesting that both ldlBp/Cog1 and ldlCp/Cog2 could interact directly with Sec34/Cog3.

3.3 Discussion

3.3.1 Sec34/Cog3, GTC-90/Cog5 and ldlBp/Cog1 are components of the same protein complex

Sec34/Cog3, GTC-90/Cog5, and ldlBp/Cog1 have been independently identified by different approaches. Cog3 was identified based on a genomic approach to search for the mammalian homologue of Sec34p (Suvorova et al., 2001 and this study), which has a well-defined role in ER-to-Golgi transport in yeast (Kim et al., 1999, 2001; Van Rheenen et al., 1998, 1999). GTC-90/Cog5 was previously identified as a component of a novel protein complex that participates in intra-Golgi transport using an *in vitro* biochemical assay (Walter et al., 1998). LdlBp/Cog1 and ldlCp/Cog2 were originally identified by a genetic approach (Hobbs et al., 1992; Hobbie et al.,

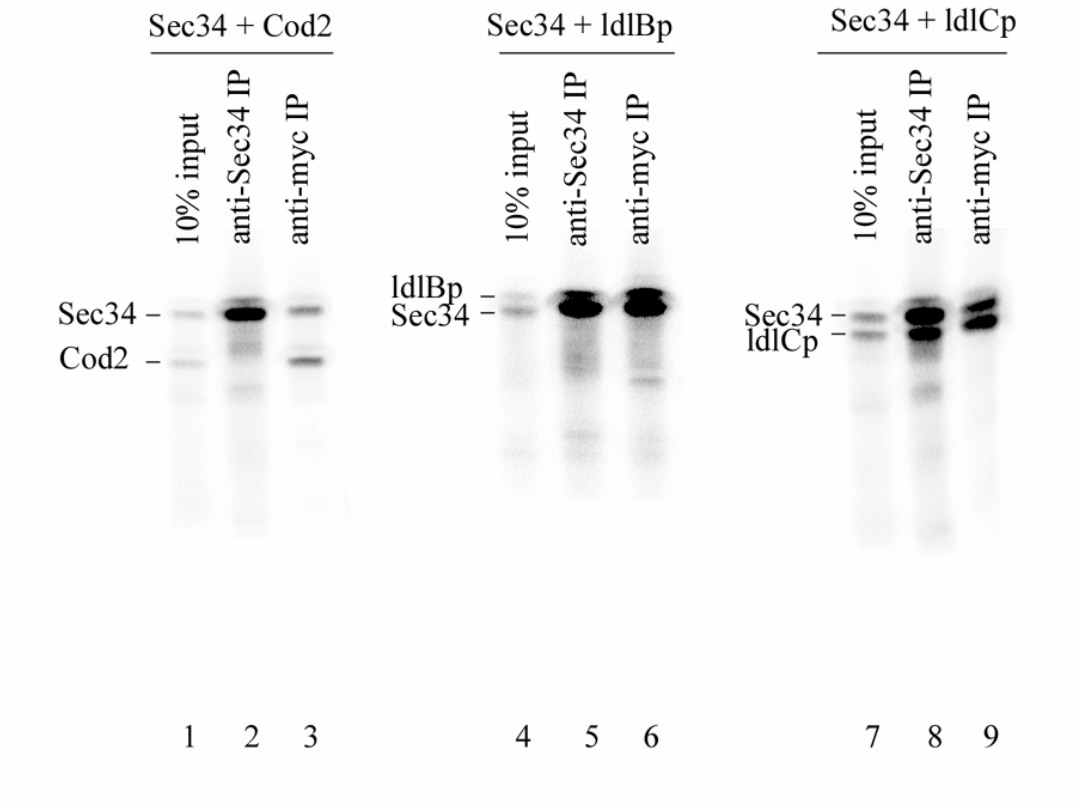

Figure 10. Direct interaction of Sec34/Cog3 with ldlBp/Cog1 and ldlCp/Cog2. Myc-Sec34/Cog3 was co-translated with myc-Cod2 (*lanes 1–3*), myc-ldlBp (*lanes 4–6*), or myc-ldlCp (*lanes 7–9*) by *in vitro* translation reactions in the presence of [^{35}S]methionine. The translation products were immunoprecipitated with either Sec34/Cog3 antibodies (*lanes 2*, *5*, and *8*) or anti-myc antibodies (*lanes 3*, *6*, and *9*). The immunoprecipitates and 10% of the respective translation reactions (*lanes 1*, *4*, and *7*) were analyzed by SDS-PAGE and fluorography.

1994; Kingsley, 1986; Malmstrom and Krieger, 1991) and subsequently shown to exist in the same protein complex that regulates Golgi structure and function (Chatterton et al., 1999; Podos et al., 1994). One of the most important discoveries of the present study is that Sec34, GTC-90, and ldlBp/ldlCp are components of the same protein complex(es) (now re-named the conserved oligomeric Golgi, COG complex). This is based on several lines of observations. Firstly, GTC-90/Cog5 and ldlBp/Cog1 (as well as Dor1/Cog8 and Cod1/Cog4) could be efficiently and specifically co-immunoprecipitated from rat liver cytosol by antibodies against Sec34/Cog3. Secondly, upon expression by transient transfection, myc-tagged ldlBp/Cog1, ldlCp/Cog2, Dor1/Cog8, Cod1/Cog4, and Cod2/Cog6 could be similarly co-immunoprecipitated by anti-Sec34/Cog3 antibodies. Finally, direct interaction of Sec34/Cog3 with ldlBp/Cog1 and ldlCp/Cog2 could be demonstrated in the absence of other subunits using *in vitro*-translated proteins.

Comparing the yeast and mammalian COG complex, no homologue for ldlBp/Cog1 was identified in yeast, suggesting either that there is another subunit that remains to be uncovered in the yeast Sec34p-Sec35p (COG) complex or that ldlBp could be a functional counterpart of either Cod3p or Cod5p. Because myc tagged ldlCp/Cog2 can be co-immunoprecipitated with Sec34/Cog3 upon expression by transient transfection and a direct interaction between Sec34/Cog3 and myc-ldlCp/Cog2 could be observed, ldlCp/Cog2 is indeed a component of the Sec34-GTC-90-ldlBp (COG) complex. Because ldlCp (731 and 738 amino acids for mouse and human protein, respectively) is much larger than Sec35p (275 amino acids), and the observed sequence homology (24% identity over a region of 110 amino acids) is limited, additional evidence is required to resolve whether ldlCp is the structural and/or functional counterpart of yeast Sec35p. The direct interaction of ldlBp/Cog1 or

ldlCp/Cog2 with Sec34/Cog3 suggests that Cog3 harbors structural information for direct interaction with ldlBp/Cog1 and ldlCp/Cog2 in the absence of other subunits.

3.3.2 Six other proteins (ldlBp/Cog1, ldlCp/Cog2, Dor1/Cog8, Cod1/Cog4, Cod2/Cog6 and GTC-90/Cog5) are present in the Sec34/Cog3-containing protein complex

The other potential subunits (Dor1/Cog8, Cod1/Cog4, and Cod2/Cog6) of the mammalian Sec34-GTC-90-ldlBp (COG) complex were similarly confirmed immunologically and/or biochemically as components of the Sec34/Cog3-containing protein complex(es). Both Dor1/Cog8 and Cod1/Cog4 were recovered in Sec34/Cog3 immunoprecipitates. Epitope-tagged versions of Dor1/Cog8, Cod1/Cog4, and Cod2/Cog6, upon expression by transient transfection, could be co-immunoprecipitated by anti-Sec34/Cog3 antibodies at efficiencies comparable to those observed for ldlBp/Cog1 and ldlCp/Cog2 under similar conditions. In summary, six other proteins (ldlBp/Cog1, ldlCp/Cog2, Dor1/Cog8, Cod1/Cog4, Cod2/Cog6, and GTC-90/Cog5) in mammalian cells are shown here to be present in the Sec34/Cog3-containing protein complex(es), with ldlBp/Cog1 and ldlCp/Cog2 having the ability to interact directly with Sec34/Cog3. It remains possible that these proteins, together with others that have yet to be discovered, may form distinct complexes or subcomplexes. Since ldlBp is accepted to be a functional counterpart of Cod3p, then we have uncovered all but one of the components of the mammalian counterparts of the yeast complex in this study.

3.3.3 A role for Cog3 in ER-to-Golgi transport

The function of the Sec34-GTC-90-ldlBp (COG) complex in mammalian cells remains to be explored. In view of all available results, it could be suggested that the COG complex may have a general role in the Golgi apparatus that regulates several

trafficking events, including ER-to-Golgi transport, various steps in intra-Golgi transports, and possibly endosome-to-trans-Golgi network traffic. The role of Sec34p/Cog3p and Sec35p/Cog2p in ER-to-Golgi transport has been well established in yeast (Kim et al., 1999, 2001; Van Rheenen et al., 1998, 1999). Using a modified assay that reconstitutes synchronized transport of almost all ER-arrested VSVG to the Golgi, it was shown that anti-Sec34/Cog3 antibodies could exhibit dose-dependent inhibition. Furthermore, the inhibition could be neutralized by a noninhibitory amount of the antigen. We have thus provided evidence that Sec34/Cog3 plays a similar role in ER-to-Golgi transport in mammalian cells, although the temporal and other mechanistic aspects of its action remain to be explored. Although a role for Sec34p/Cog3p or other subunits in intra-Golgi transport in yeast has yet to be investigated, the purification of GTC-90 complex using an *in vitro* intra-Golgi transport assay suggests that this complex could be intimately involved in intra-Golgi transport (Walter et al., 1998). A role for Sec34p/Cog3 in endosome-to-TGN transport has been reported, and this was the basis for which Sec34p/Cog3p was independently identified as Grd20p (Spelbrink and Nothwehr, 1999). Although it has been suggested that the role of Sec34p/Grd20p (Cog3p) in endosome-to-TGN transport could be due to an indirect effect due to its role in ER-to-Golgi transport (Kim et al., 2001; Van Rheenen et al., 1999), the recent identification of the COG complex and the relatedness of this complex with Ypt6p function indicate that the Sec34p/Grd20p (COG) complex might have a direct role in endosome-to-TGN transport (Whyte and Munro, 2001). Detailed studies of this complex and its individual subunits using genetic, biochemical, and cell biochemical approaches in both yeast and mammalian cells will provide additional understanding of its function and mechanism as well as the general organization and regulation of Golgi structure and function.

CHAPTER 4

The binary interacting network of the conserved oligomeric Golgi (COG) tethering complex

4.1 Introduction

The identification and characterization of one of the subunits of the mammalian COG complex-Cog3 was described in the previous chapter. The COG complex was recently identified in both yeast and mammalian cells and consists of 8 subunits (COG1-8). Some components such as COG3, COG4, COG5, COG6 and COG8 from yeast and mammalian cells are structurally homologous, while mammalian COG1/LdlBp, COG2/LdlCp, and COG7 are not structurally related to the remaining three yeast proteins (COG1/Sec36p/Cod3p, COG2/Sec35p, COG7/Cod5p), although they could represent functional counterparts (Ungar et al., 2002). Amongst the 8 subunits, COG1, COG2, COG3 and COG4 (but not the other 4 proteins) are essential for cell growth in yeast and are therefore essential components of this complex (Ram et al., 2002).

In this chapter, I describe further work on the subunit interaction amongst the 8 subunits of the COG complex. As the COG complex is one of the few major tethering complexes in all eukaryotic cells, understanding its inter-subunit interactions and structure will be of great importance to gain insight into its assembly, function and regulation.

4.2 Results

As little is known about the structural and molecular mechanisms fundamental to the assembly of the complex, we have thus initiated this current systematic study. In our hands after trying several different approaches, it turned out that *in vitro* translation

of subunits of interest using rabbit reticulocyte lysate followed by co-immunoprecipitation provided the most optimal system to assess the protein interaction network of COG complex. Although the reticulocyte lysate-based *in vitro* translation system may contain some endogenous COG proteins and other cytosolic proteins, our results showing specific interactions among selective COG subunits indicate strongly that this system could be used for investigating protein-protein interactions. The high specificity obtained in our comprehensive study suggests that the reticulocyte proteins did not contribute significantly to interactions detected among the tagged COG subunits. The interactions detected are thus an indication of direct interactions that are being examined, despite the caveat that conclusive demonstration of direct interaction will have to await for more stringent assay using purified proteins. Keeping this point in mind, we have used the term "direct interaction" in a relative sense.

4.2.1 Direct interaction of COG4 with COG1, COG2, COG5, and COG7

We initially tested all possible combinations of interaction among any two subunits. Each subunit was tested for possible interaction with the other 7 subunits by co-immunoprecipitation assay of proteins produced by *in-vitro* translation. COG4 was found to be a core interacting protein and it forms binary interactions directly with four other subunits, namely COG1, COG2, COG5 and COG7. The results are presented in a logical way, highlighting the interactions detected. When HA-COG4 was co-translated with myc-COG1, myc-COG2, myc-COG5, or myc-COG7 (Fig 11A), myc-tagged COG1, COG2, COG5 and COG7 (right panels) as well as HA-tagged COG4 (left panels) could be efficiently immunoprecipitated by antibodies against either the myc epitope (lanes 2 and 5) or the HA epitope (lanes 3 and 6). The efficient co-immunoprecipitation of HA-COG4 and myc-tagged COG1, COG2, COG5 or COG7

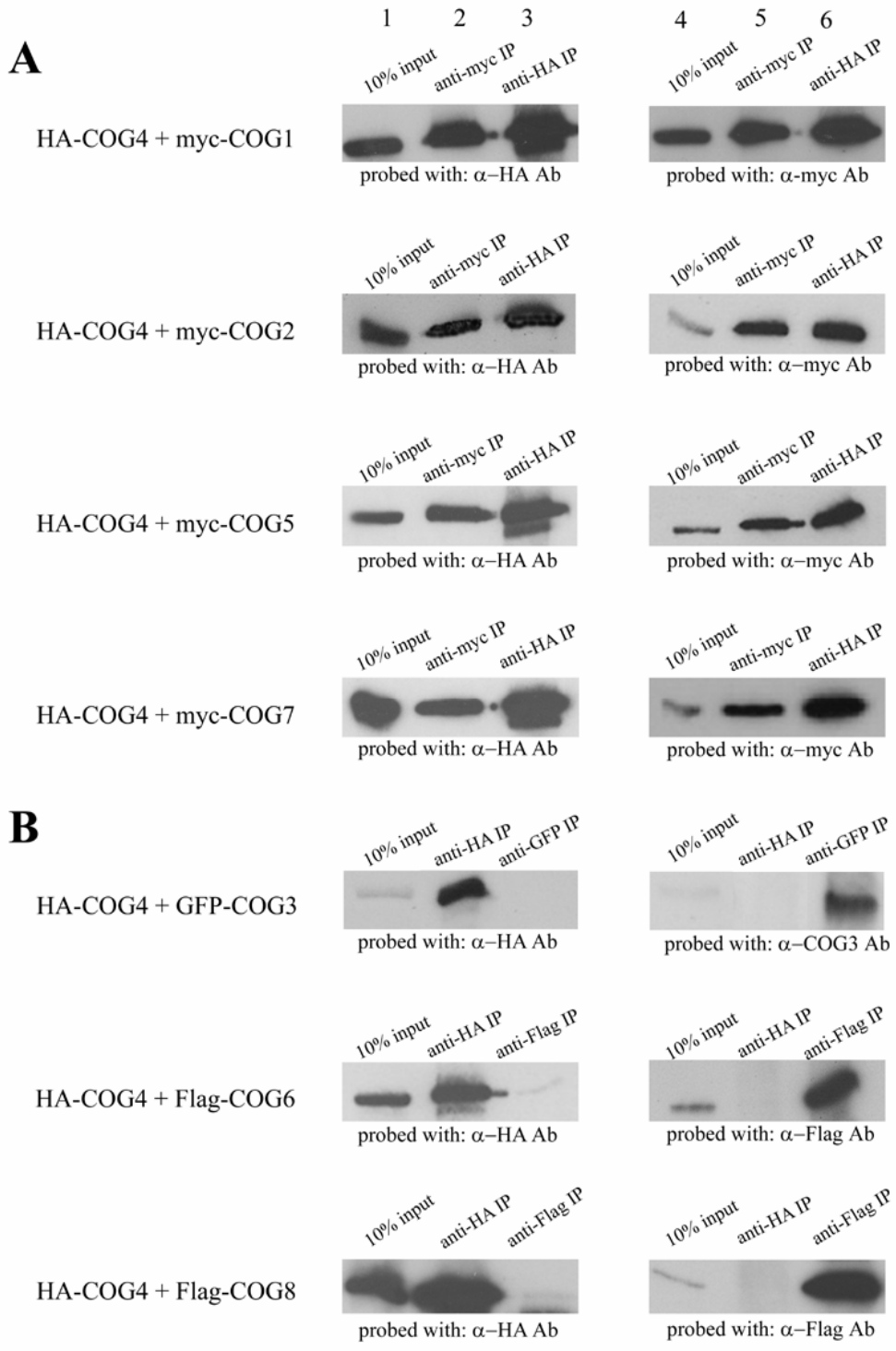

Figure 11. Direct interaction of COG4 with COG1, COG2, COG5 and COG7, but not with COG3, COG6 or COG8. HA-COG4 was co-translated with myc-COG1, myc-COG2, myc-COG5, myc-COG7, GFP-COG3, Flag-COG6 and Flag-COG8 (as indicated) by *in vitro* translation reactions with non-radioactive methionine. The translated products were divided and immunoprecipitated with the antibodies shown with each set of reactions. The immunoprecipitates and 10% of the respective translation reactions (lanes 1 and 4) were analyzed by SDS-PAGE, followed by immunoblot analysis with the respective antibodies (as stated for each reaction).

by either myc or HA antibodies suggest that HA-COG4 and the respective myc-COG interact efficiently.

In marked contrast, when HA-COG4 was co-translated with GFP-COG3, Flag-COG6 and Flag-COG8 (Fig 11B), anti-HA antibodies failed to co-immunoprecipitate GFP-COG3, Flag-COG6 or Flag-COG8 (lane 5), although HA-COG4 was efficiently immunoprecipitated (lane 2). Furthermore, when GFP-COG3, Flag-COG6 and COG8 were efficiently immunoprecipitated by antibodies against GFP/Flag (lane 6), HA-COG4 was not detected in the immunoprecipitates (lane 3). Similar results were obtained when HA-COG4 was co-translated with myc-COG3, myc-COG6 or myc-COG8 (data not shown). These results suggest that COG4 does not interact directly with COG3, COG6 or COG8. Since our previous study has demonstrated a direct interaction of COG3 with COG1 or COG2 (as in chapter 3 and Loh and Hong, 2002), COG3 is likely incorporated into the complex via direct interaction with COG1 and COG2. Similar results were obtained in our comprehensive analysis of all possible binary combinations (Fig 12B).

4.2.2 Binary interaction between COG5 and COG7

Among our systematic binary interaction assays, we have detected a weak interaction between COG5 and COG7 (Fig 12A). When myc-COG5 and HA-COG7 were co-translated, HA-COG7 was efficiently immunoprecipitated by HA antibody (lane 3). However, a small but significant amount of HA-COG7 could be consistently co-immunoprecipiated by myc antibodies (lane 2). Consistent with this observation, a small but significant amount of myc-COG5 was co-immunoprecipitated by HA antibodies (lane 6). Again, myc-COG5 was very efficiently immunoprecipitated by myc antibodies (lane 5). As this weaker but significant co-immunoprecipitation was specifically observed when COG5 and COG7 were co-translated, we believe this

A

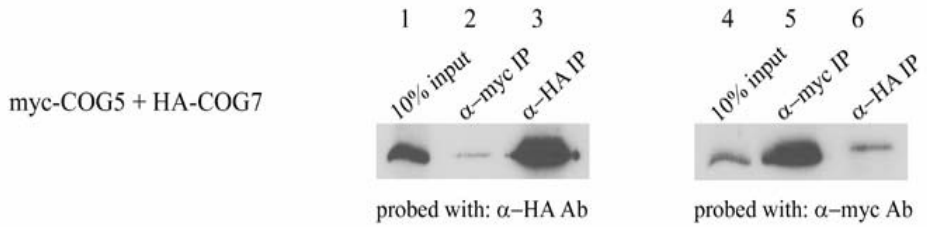

B

	COG1	COG2	COG3	COG4	COG5	COG6	COG7	COG8
COG1		-	+	+	-	-	-	-
COG2			+	+	-	-	-	-
COG3				-	-	-	-	-
COG4					+	-	+	-
COG5						-	+/-	-
COG6							-	-
COG7								-
COG8								

C

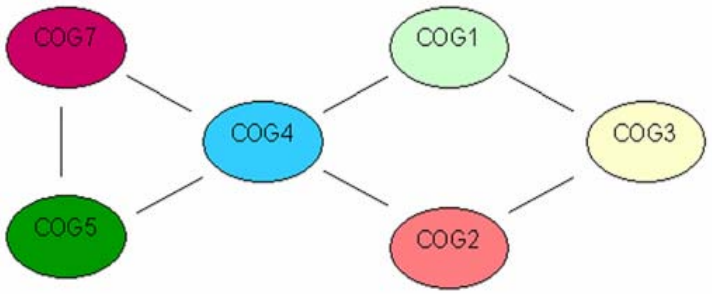

Figure 12. Summary of all binary interactions depicts a sub-complex consisting of COG1, COG2, COG3, COG4, COG5 and COG7. (A), Myc-COG5 was co-translated with HA-COG7 by *in vitro* translation and the products were split and immunoprecipitated with either anti-myc or anti-HA antibodies. The immunoprecipitates and 10% of the translation reactions were resolved by SDS-PAGE and analyzed by immunoblot with anti-myc and anti-HA antibodies respectively. (B), Summary of results of binary interactions revealed by *in vitro* translation of the various combinations of two subunits. Direct interactions of COG3 with COG1 as well as COG3 COG2 were also previously demonstrated (Loh and Hong, 2002). Direct interactions of COG4 with the 4 subunits (COG1, COG2, and COG5 and COG7) were shown in Fig.11, while the direct interaction of COG5 and COG7 was demonstrated in Fig.12A. All the other pairs did not show any direct interaction (data not shown). (C), A schematic diagram depicting all the direct binary interactions.

weaker interaction is specific.

4.2.3 Summary of all binary interactions depicts a sub-complex consisting of COG1, COG2, COG3, COG4, COG5 and COG7

The results of all binary interaction assays (each subunit was tested for possible interactions with the other 7 subunits) are summarized in Fig 12B, +, +/-, and – symbols indicate strong binary interaction (such as COG4 with COG1, COG2, COG5 or COG7), weaker but specific binary interaction (such as COG5 with COG7), and no interaction, respectively. Most significant is the observation that COG6 and COG8 did not show any binary interaction with any individual subunits in the two-subunit assay. The results of the detected interactions were illustrated in a diagrammatic manner in Fig 12C, where direct binary interactions were indicated, assuming that none of the binary interactions are mutually exclusive, which is a point that remains to be established.

4.2.4 Incorporation of COG6 into the COG complex depends on both COG5 and COG7

As COG6 and COG8 did not display any direct interactions with any other subunits, we suspect that their incorporation into the complex is mediated by interacting surfaces that arise from several subunits. In order to identify those subunits that are important for incorporation of COG6 and COG8, we have taken a different strategy in which different subunits (or combination of various subunits) were omitted from an initial co-translation of all 8 subunits. When all 8 of the COG subunits were co-translated by *in vitro* translation (Fig 13A, row 1) (the subunit in question, i.e. COG6, is Flag-tagged, while the other 7 subunits were myc-tagged), Flag-COG6 was efficiently co-immunoprecipitated by antibodies against myc tag (Fig 13B, panel 1, left lane), suggesting that Flag-COG6 has been efficiently incorporated into a complex (or

A

	COG1	COG2	COG3	COG4	COG5	COG7	COG8	Flag-COG6	Detect COG6
1	+	+	+	+	+	+	+	+	+
2	+	+	+	+	+	+		+	+
3	+	+	+		+	+		+	+
4	+	+		+	+	+		+	+

B

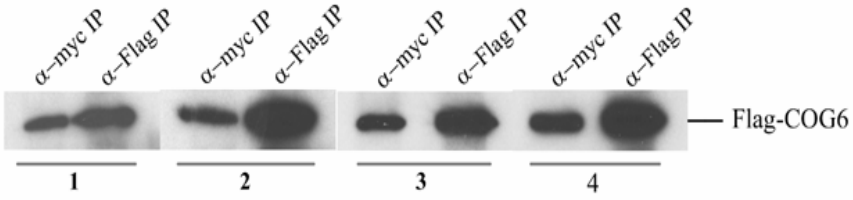

C

	COG1	COG2	COG5	COG7	Flag-COG6	Detect COG6
1	+	+	+	+	+	+
2		+	+	+	+	+
3	+		+	+	+	+
4	+	+		+	+	-
5	+	+	+		+	-

D

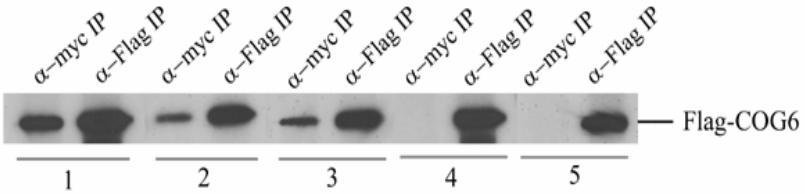

Figure 13. COG5 and COG7 are necessary for incorporation of COG6 into the complex. (A) and (C), Tables showing the various subunits added (shown with symbol +) into the *in vitro* translation reactions for each experiment denoted by the numbers on the extreme left column (COG6 is flag-tagged while all other subunits are myc-tagged). The extreme right column shows the result whether Flag-COG6 was detected in the anti-myc immunoprecipitates. (B) and (D), Immunoblot analysis with anti-Flag antibodies to detect the presence of Flag-COG6 in each of the immunoprecipitation experiments, using either myc (left lane of all panels) or Flag (right lane of all panels) antibodies. The numbers shown below each set of reactions correspond to the numbers in tables 13A or 13C showing which of the subunits was present in each reaction. For each *in vitro* translation reaction, the translated products were divided and co-immunoprecipitated separately with anti-myc or anti-Flag antibodies.

sub-complexes) with the 7 other myc- COGs. The efficiency of co-immunoprecipitation by the myc antibodies (Fig 13B, panel 1, left lane) is close to 70-80% of that achieved by Flag antibody (right lane), suggesting that the majority of Flag-COG6 has been incorporated into the complex. Omission of myc-COG8 from the translation reaction had no effect on incorporation of Flag-COG6 into the complex formed with the other 6 myc-COG subunits (Fig 13A, row 2; Fig 3B, panel 2). Similarly, omission of both myc-COG4 and COG8 had no effect on the interaction of Flag-COG6 with the remaining 5 myc-COG subunits (Fig 13A, row 3; Fig 13B, panel 3). Likewise, omission of both myc-COG3 and myc-COG8 did not affect the interaction of Flag-COG6 with the remaining 5 myc-COG subunits (Fig 13A, row 4; Fig 13B, panel 4). Taken together, these results suggest that COG3, COG4 and COG8 are not involved in the formation of the interacting surface for COG6.

In order to identify which components in the remaining 4 subunits (COG1, COG2, COG5 and COG7) are involved in the interaction with COG6, we systematically omitted each of these myc-COG subunits in the co-translation reactions together with Flag-COG6 (Fig 13, C and D). When these five subunits were co-translated, Flag-COG6 was efficiently coimmunoprecipitated by antibodies against the myc tagged-COGs (Fig 13C, row1; Fig 13D, panel 1, left lane). Omission of myc-COG1 did not affect co-immunoprecipiation of Flag-COG6 by myc-antibodies (Fig 13C, row 2; Fig 13D, panel 2), although the efficiency is reduced. Similarly, omission of myc-COG2 did not affect the interaction of Flag-COG6 with the remaining myc-COG subunits as assessed by co-immunoprecipitation, although the efficiency is similarly reduced (Fig 13C, row 3; Fig 13D, panel 3). When myc-COG5 was absent in the translation reaction, Flag-COG6 was not coimmunoprecipiated with anti-myc antibodies (Fig 13C, row 4; Fig 13D, panel 4). Similarly, when myc-COG7 was

omitted, anti-myc antibodies failed to co-immunoprecipiate Flag-COG6 (Fig 13C, row 5; Fig 13D, panel 5). These results suggest that COG5 and COG7, but not COG1 or COG2 are essential for interaction of Flag-COG6 with the other myc-COG subunits.

The above results also suggest that COG6 could indeed interact with COG5 and COG7 to form a sub-complex. To further substantiate this point, Flag-COG6 was co-translated with myc-COG5 and myc-COG7. The efficiency of co-immunoprecipitation of Flag-COG6 by myc antibodies (Fig. 14A, lane 1) is about 60% of that achieved by Flag antibodies (lane 2), suggesting that Flag-COG6 can be efficiently incorporated into a subcomplex with COG5 and COG7. Consistent with this, significant amount of myc-COG5 and myc-COG7 can be co-immunoprecipitated by antibodies against Flag-tag (lane 4), although the efficiency is somewhat lower. The low efficiency could indicate that COG5 and COG7 exists either as free or COG5-COG7 forms, in addition to the ternary complex consisting of COG5, COG6 and COG7. Alternatively, this low efficiency of coimmunoprecipitation of COG5 and COG7 with COG6 could be due to the possibility that COG5 and 7 are present at much higher levels after *in vitro* translation. As summarized in Fig 12B, when Flag-COG6 was co-translated with either myc-COG5 or myc-COG7 independently, Flag-COG6 was not co-immunoprecipitated with anti-myc antibodies (Fig. 14B, lane 2). Consistently, anti-Flag antibodies failed to co-immunoprecipitate myc-COG5 and myc-COG7 (lane 6). This illustrates that COG6 interacts with COG5-COG7 binary sub-complex but not COG5 or COG7 alone. This interaction is important for COG6 incorporation into the complex. The formation of the sub-complex consisting of COG5, COG6 and COG7 is depicted in Fig. 14C, where solid line indicates direct binary interaction while dashed lines indicate interaction via several subunits.

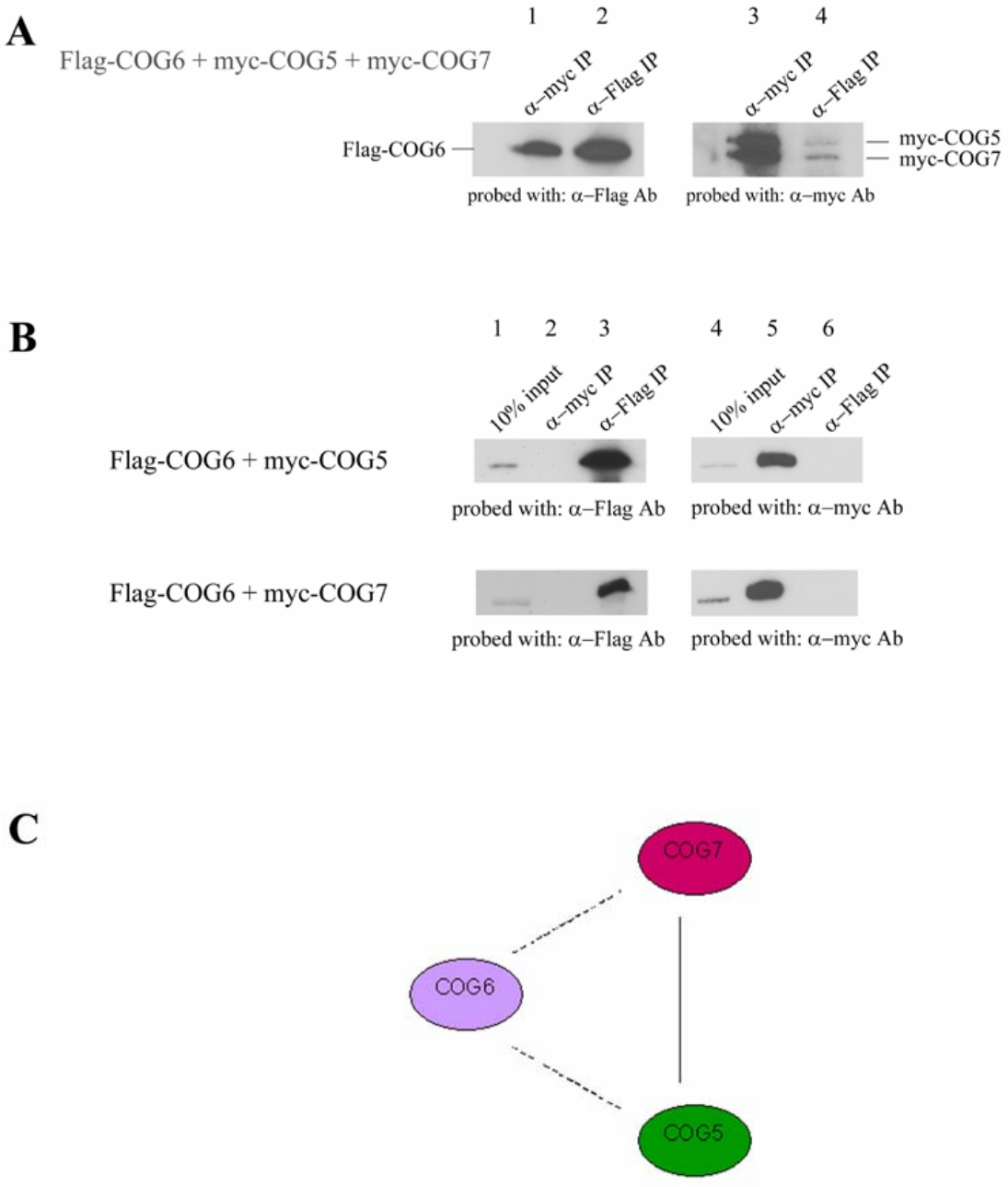

Figure 14. Formation of a subcomplex consisting of COG5, COG6 and COG7. (A), Flag-COG6, myc-COG5 and myc-COG7 were co-translated by *in vitro* translation reactions and the products were divided and immunoprecipitated with either anti-myc or anti-Flag antibodies. The immunoprecipitates were resolved by SDS-PAGE and analyzed by immunoblot with anti-Flag or anti-myc antibodies, respectively. (B), Flag-COG6 was co-translated with either myc-COG5 (upper panel) or myc-COG7 (lower panel) and the translated products were processed similarly with the respective antibodies as indicated. (C), A schematic diagram depicting the possible interactions within the ternary complex of COG5, COG6 and COG7 (direct interaction between COG5 and COG7 is shown by a solid line while interaction of COG6 with COG5-COG7 dimeric form with is indicated by dashed lines).

4.2.5 Optimal incorporation of COG8 into the COG complex depends on COG5, COG6 and COG7

We next proceeded to identify which subunits are involved in the incorporation of COG8 into the COG complex. When all 8 of the COG subunits were co-translated by *in vitro* translation (Fig 15A, row 1), Flag-COG8 was efficiently co-immunoprecipitated by antibodies against myc tag (Fig. 15B, panel 1, left lane), suggesting that Flag-COG8 is efficiently incorporated into a complex (or sub-complexes) with the other 7 myc-COGs. The efficiency of co-immunoprecipitation by myc antibodies (left lane, panel 1 of Fig 15B) is close to 90% of that achieved by Flag antibody (right lane), suggesting that the majority of Flag-COG8 has been incorporated into the complex. Omission of myc-COG1 from the translation reaction had no effect on incorporation of Flag-COG8 into the complex formed with the other 6 myc-COG subunits (Fig 15A, row 2; Fig 15B, panel 2). Similarly, omission of myc-COG2 (Fig 15A, row 3; Fig 15B, panel 3), myc-COG3 (Fig 15A, row 4; Fig 15B, panel 4) and myc-COG4 (Fig 15A, row 5; Fig 15B, panel 5) had no effect on the interaction of Flag-COG8 with the remaining 6 myc-COG subunits. Therefore, these results suggest that COG1, COG2, COG3 and COG4 are not involved in the formation of interacting surface for COG8. When COG5 (Fig 15A, row 6; Fig 15B, panel 6) and COG6 (Fig 15A, row 7; Fig 15B, panel 7) were omitted, the efficiency of co-immunoprecipitation by myc antibodies is greatly reduced. When COG7 was omitted, the efficiency of coimmunoprecipitation of Flag-COG8 by myc antibodies is about 30% of that achieved by Flag antibody (Fig 15A, row 8; Fig 15B, panel 8). Taken together, these results suggest that COG5, COG6 and COG7 are necessary for the optimal incorporation of COG8 into the COG complex, while COG1, COG2, COG3 and COG4 are dispensable.

A

	COG1	COG2	COG3	COG4	COG5	COG6	COG7	Flag-COG8	Detect COG8
1	+	+	+	+	+	+	+	+	++
2		+	+	+	+	+	+	+	++
3	+		+	+	+	+	+	+	++
4	+	+		+	+	+	+	+	++
5	+	+	+		+	+	+	+	++
6	+	+	+	+		+	+	+	+/-
7	+	+	+	+	+		+	+	+/-
8	+	+	+	+	+	+		+	+

B

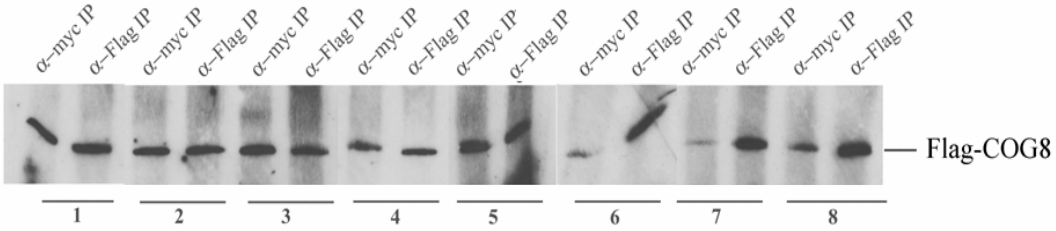

Figure 15. COG5, COG6 and COG7 are necessary for optimal incorporation of COG8 into the complex. (A), Table showing which of the 8 subunits were omitted in each set of *in vitro* translation reactions (starting from a reaction with Flag-COG8 and all other 7 myc-COG subunits). The extreme right column shows the result of the extent to which Flag-COG8 was detected in the anti-myc immunoprecipitates. (B), Immunoblot analysis with anti-Flag antibodies to detect the presence of Flag-COG8 in each of the immunoprecipitation experiments denoted by the numbers below each set, which matches the numbers shown in each reaction in Table 15A. For each *in vitro* translation reaction, the translated products were divided and co-immunoprecipitated separately with anti-myc (left lane) or anti-Flag (right lane) antibodies as indicated.

To further confirm this conclusion, we prepared co-translation reactions consisting of Flag-COG8 with myc-COG4, myc-COG5, myc-COG6 and myc-COG7 from which we sequentially omitted each of the myc-COG subunits (Fig. 16A and B). When these five subunits were co-translated, Flag-COG8 was efficiently co-immunoprecipitated by antibody against myc tag (Fig 16A, row 1; Fig 16B, panel 1). Omission of myc-COG4 did not affect co-immunoprecipiation of Flag-COG8 by the myc-antibodies (Fig 16A, row 2; Fig 16B, panel 2). When myc-COG6 was excluded from the translation reaction, the efficiency of co-immunoprecipitation of Flag-COG8 by the anti-myc antibodies was greatly diminished (Fig 16A, row 3; Fig 16B, panel 3). When myc-COG7 was omitted, anti-myc antibodies failed to co-immunoprecipiate Flag-COG8 (Fig 16A, row 4; Fig 16B, panel 4). To establish the importance of COG5 in the incorporation of COG8 into the complex, Flag-COG8 was co-translated together with myc-COG6 and HA-COG7. Flag-COG8 was not co-immunoprecipitated with anti-myc or anti-HA antibodies (Fig 16A, row 5; Fig 16B, panel 5). Hence COG5 is indeed essential to the incorporation of COG8 into the complex. In conclusion, the combined action of COG5, COG6 and COG7 are crucial for the interaction of COG8 with the other myc-COG subunits. This tetrameric relationship is illustrated in Fig. 16C.

4.3 Discussion

4.3.1 7 pairs of direct binary interactions amongst subunits of the COG complex

We have taken a systematic approach to establish the inter-subunit interactions of the mammalian COG complex. Several different methods were tried, including the yeast two-hybrid system, *in vitro* co-translation of ^{35}S-Met labeled proteins revealed by autoradiography, and *in vitro* co-translation of un-radiolabeled but tagged subunits that

A

	COG4	COG5	COG6	COG7	Flag-COG8	Detect COG8
1	+	+	+	+	+	+
2		+	+	+	+	+
3	+	+		+	+	+/-
4	+	+	+		+	-
5			+	+	+	-

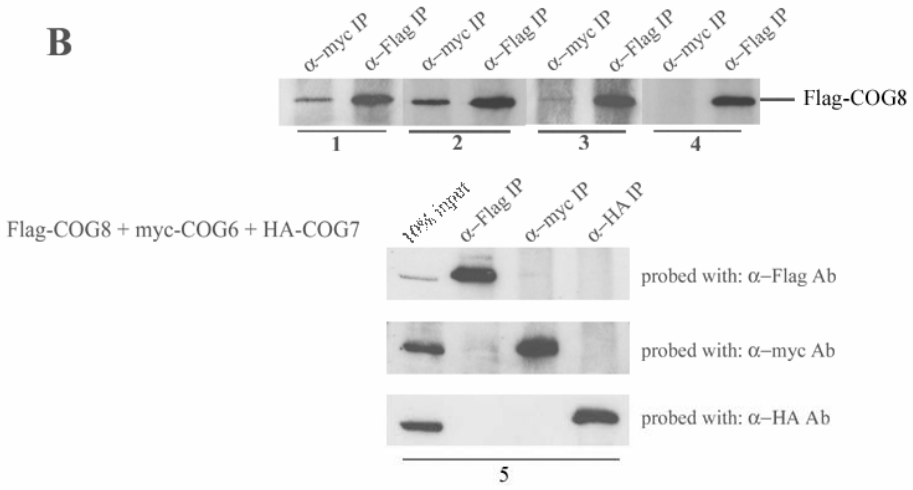

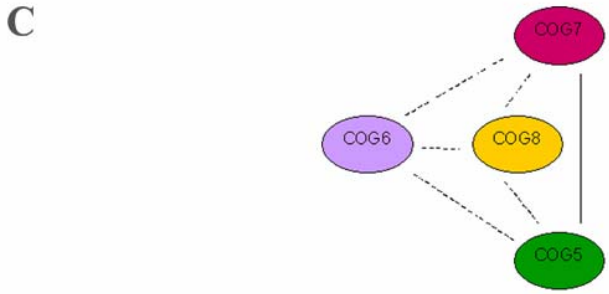

Figure 16. Formation of a tetrameric subcomplex consisting of COG5, COG6, COG7 and COG8. (A), Table showing the various subunits added (shown with symbol +) into the *in vitro* translation reaction for each experiment denoted by the numbers on the extreme left column. The extreme right column shows the result whether Flag-COG8 was detected in anti-myc immunoprecipitates. (B), For reactions 1-4, immunoblot analysis was performed with anti-Flag antibodies to detect the presence of Flag-COG8 in each of the immunoprecipitation experiments using myc or flag antibodies as indicated. For reaction 5, Flag-COG8, myc-COG6 and HA-COG7 (by omitting COG5) were co-translated and the products were divided and co-immunoprecipitated with anti-Flag, anti-myc, or anti-HA antibodies. The immunoprecipitates and 10% of the translation reactions were resolved by SDS-PAGE and analyzed by immunoblot with anti-Flag, anti-myc and anti-HA antibodies respectively. (C), A schematic diagram depicting the possible interactions within the COG5, COG6, COG7 and COG8 sub-complex (the solid line indicates a direct interaction between COG5 and COG7, while dashed lines indicate interaction of COG6 with COG5-COG7 or COG8 with COG5-COG6-COG7).

were detected by immunoblot analysis. After extensive comparisons and many trials, it turned out that the last method was most reliable and consistent. (The yeast two-hybrid system did not allow the analysis of more than two subunits at a time, and with the *in vitro* co-translation of ^{35}S-Met labeled proteins revealed by autoradiography, it was difficult to differentiate between the translated products because they were of similar sizes.) In this regard, each subunit was tagged with a few different tags for our analysis. Two strategies were employed: The first was to identify all possible binary direct interactions via co-translating two different subunits and this was evaluated by the efficiency of co-immunoprecipitation; the second approach aimed to identify interactions of a particular subunit with a sub-complex consisting of several other subunits by co-translating all 8 subunits and followed by systematically omitting each subunit. Although the reticulocyte lysate may contain some endogenous COG proteins, our results showed a high degree of specificity. This suggests that the endogenous proteins, if any, did not contribute significantly to the interactions detected. The first strategy has helped to identify 7 direct binary interactions: COG4-COG1, COG4-COG2, COG4-COG5, COG4-COG7, COG3-COG1, COG3-COG2, and COG5-COG7. As COG6 and COG8 did not exhibit any direct binary interaction, the molecular basis for their incorporation into the complex was investigated by the second strategy.

4.3.2 Incorporation of COG6 and COG8 requires interacting surfaces made up of more than 1 subunit

By systematical omission of different subunits, it was revealed that COG6 interacts with a binary COG5-COG7 sub-complex. Similarly, it was shown that COG8 interacts with a ternary COG5-COG6-COG7 sub-complex. As more and more protein complexes are being uncovered by proteomic and biochemical studies, in line with the emerging new field of systems biology, we believe our approach in defining the

interacting network of COG complex will be applicable to studies aiming to understand the inter-subunit interaction and assembly of other protein complexes.

4.3.3 A model for the assembly of the COG complex

Although multiple sub-complexes could potentially exist, we favor the following model for the assembly of the COG complex (Fig. 17). Firstly, COG4 will drive the formation of COG1-COG2-COG3-COG4 sub-complex (sub-complex I). By COG4's interaction with COG5 and COG7, COG1-COG2-COG3-COG4-COG5-COG7 sub-complex (subcomplex II) could be formed. Sub-complexes I and II could be formed at the same time and co-exist in equilibrium. COG5 and COG7, once incorporated into the sub-complex II, will create a high affinity interacting surface for COG6. Incorporation of COG6 leads to the formation of sub-complex III, which has a high affinity COG8 binding surface contributed combinatorially by COG5, COG6 and COG7. Incorporation of COG8 results in the formation of the holo-COG complex.

4.3.4 Bilobed organization of the subunits of the COG complex

Our model is not only consistent with our presented results but could also explain several other observations. Firstly, the ultrastructure of purified COG as visualized by quick freeze/deep etch/rotary shadow electron microscopy revealed that the COG complex exists as a 37-nmlong structure comprising two similarly sized globular domains (lobes A and B) connected by smaller extensions (Ungar et al., 2002). This observed bilobed structure is in good agreement with our model. Our results are also consistent with the proposal that COG1, COG2, COG3, and COG4 form one lobe (lobe A), while the other lobe consists of COG5, COG6, COG7 and COG8 (lobe B). Most importantly, our results provide a novel insight into the molecular basis that links up the two lobes. Via direct interaction of COG4 on lobe A with both COG5 and COG7 of lobe B, these two lobes are effectively and directly

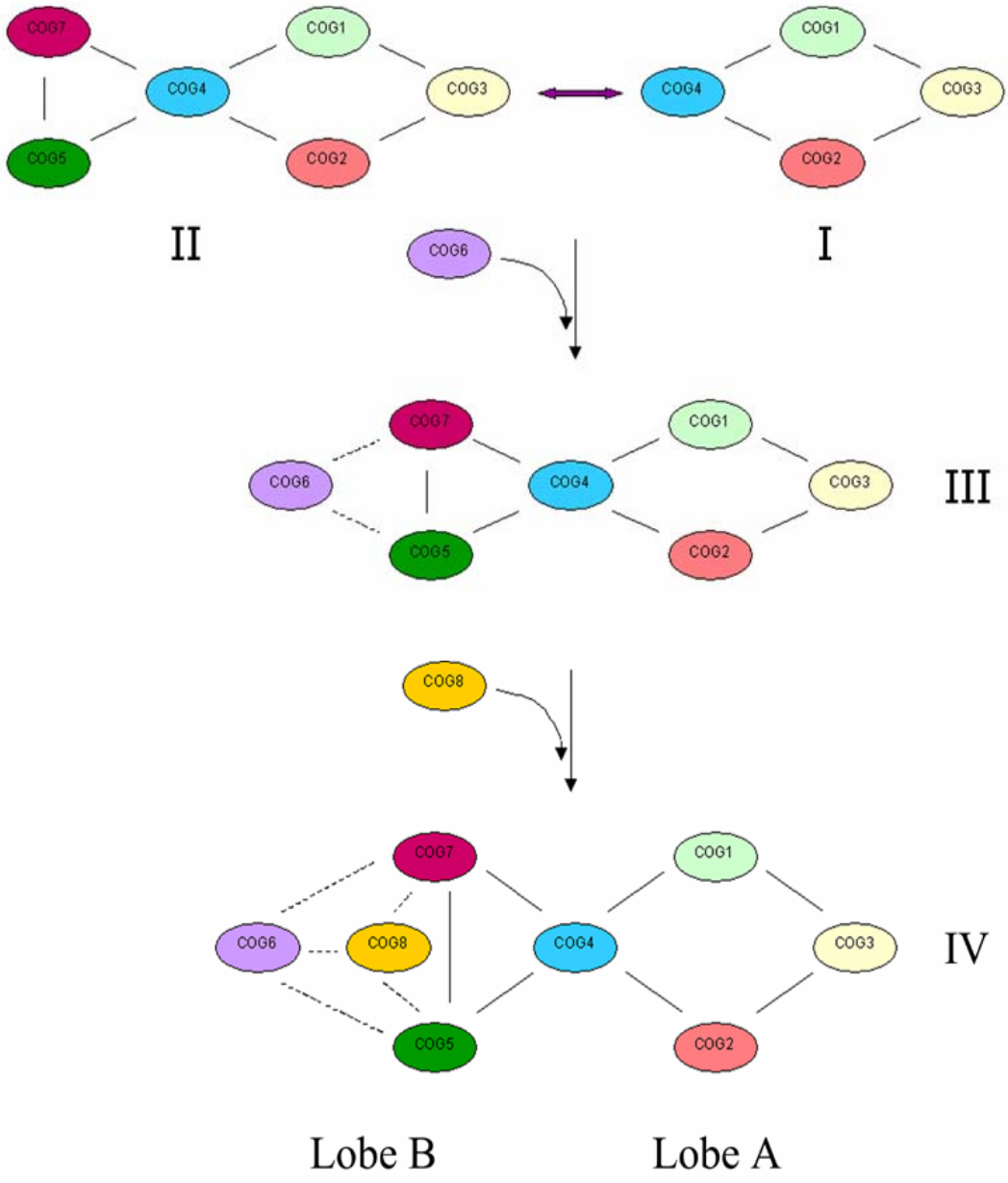

Figure 17. Diagram of a model for the assembly of the 8-subunit COG complex.

joined together. Secondly, evolutionally and structurally conserved subunits (COG3, COG4, COG5, COG6 and COG8) are located on both lobes of the complex with COG4 serving as the core for the entire complex. COG1, COG2 and COG7 from mammalian and yeast cells do not display structural homologues and they are similarly distributed in both lobes. The divergences of these subunits on both lobes enable the entire complex to evolve to accommodate specific needs of different species during evolution. Thirdly, our results also highlight the importance of the COG4 subunit in both serving as a core component of lobe A and also in the assembly of the entire complex by linking up with two subunits (COG5 and COG7) of lobe B. This important structural function revealed here could explain the essential function of COG4 in the yeast as deletion of COG4 leads to very slow growth (Whyte and Munro, 2001). We have tried to identify subdomains of COG4 that are important for each of the four direct binary interactions. Interestingly, a deletion from either the N-terminus (200-residue deletion of the 763-residue protein) or the C-terminus (163-residue) completely abolished all possible binary interactions (data not shown), suggesting that the entire molecule is necessary and the formation of interaction sites for all binary interactions is coordinated at the level of the entire structure. In addition, among the 8 COG subunits, the four essential components (COG1, COG2, COG3, and COG4) are segregated away from the other four nonessential components so that lobe A is playing a more fundamental role, despite the fact that two of the four components are not structurally conserved during evolution. This indicates that the conserved COG3 and COG4 are likely to be involved in a more fundamental role while the more divergent COG1 and COG2 serve to accommodate the needs of different architectures of the Golgi apparatus in different organisms. Since three of the four non-essential components in lobe B are structurally conserved between yeast and human, it indicates

that lobe B could play a regulatory/integrating role that is well conserved in different species while the divergent COG7 could be linked with more divergent loops of regulation. It is possible that components in lobe B could interact with proteins of other well-conserved molecular machineries to modulate the essential function played by lobe A. Consistent with this possibility, COG5 has recently been shown to be particularly important for spermatogenesis in fly and it could integrate the general function of lobe A with specialized Golgi architecture that supports rapid and extensive increases in cell surface area during spermatocyte cytokinesis and polarized elongation of differentiating spermatids (Farkas et al., 2003). Future studies along these lines, in the context of our inter-subunit network, will add more insightful understanding about the function and regulation of the COG complex.

CHAPTER 5

Mammalian Bet3 functions as a cytosolic factor participating in transport from the endoplasmic reticulum to the Golgi apparatus

5.1 Introduction

Tethering could be mediated either by multiprotein complexes (Waters and Pfeffer, 1999; Whyte and Munro, 2002; Pfeffer, 2001) or long rod-like coiled coil proteins (Gillingham and Munro, 2003; Barr, 2000). Several tethering complexes have been identified and include the exocyst (Sec6/Sec8) complex, the conserved oligomeric Golgi (COG) complex, the VFT/GARP (Vps fifty-three or Golgi-associated retrograde protein) complex, the HOPS (homotypic fusion and vacuole protein sorting) complex, and the TRAPP (transport protein particle) complex. The exocyst complex is best studied and it regulates polarized delivery of vesicles to defined regions of the plasma membrane, both in yeast and mammalian cells (Guo et al., 1999; TerBush et al., 1996). The COG complex, which I have described extensively in the previous chapters, serves to regulate traffic at the Golgi apparatus (for both ER-Golgi as well as intra-Golgi transport) in both yeast and mammalian cells. Mammalian proteins homologous to components of HOPS complex are similarly implicated in endosomal/lysosomal trafficking. Although components homologous to yeast TRAPP and VFT/GARP complexes have been identified in mammalian cells, their functional importance in mammalian cells has not been established.

During ER-Golgi transport in yeast, the TRAPP complex has been shown to function as a docking site on the early Golgi for COPII-generated vesicles derived from ER and the TRAPP complex function as a membrane machinery (Sacher et al., 2001). Components of TRAPP interact genetically with SNAREs and Ypt1p

(Guendalina et al., 1995; Jiang et al., 1998; Sacher et al., 1998). The TRAPP complex consists of 10 subunits: Bet3p, Bet5p, Trs20p, Trs23p, Trs31p, Trs33p, Trs65p/Kre11p, Trs85p/Gsg1p, Trs120p and Trs130p and the holo-complex is referred to as TRAPP II, while a sub-complex consisting of Bet3p, Bet5p, Trs20p, Trs23p, Trs31p, Trs33p, and Trs85p/Gsg1p is referred to as TRAPP I. TRAPP I and TRAPP II act in ER-Golgi and intra-Golgi transport respectively. Biochemically, TRAPP functions as a guanine nucleotide exchange factor forYpt1p, Ypt8p/Ypt31p, and Ypt11p/Ypt32p. Among the structurally homologous proteins in mammalian cells, Bet3 is the most conserved and therefore it may play a most important/conserved function of the TRAPP complexes. Among the 10 subunits, Trs33p, Trs65p and Trs85p are dispensable for cell growth, while the other 7 subunits are all essential for cell growth (Sacher et al., 2000).

To establish the functional importance of the TRAPP complex in traffic in mammalian cells, we have investigated the biochemical and functional aspects of Bet3. Our results suggest that although Bet3 is functionally conserved in ER-Golgi transport, its mode of action is significantly different in mammalian cells.

5.2 Results

5.2.1 Summary of mammalian homologues of TRAPP complex and identification of a new homologue of Trs33p

Mammalian proteins homologous to yeast TRAPP were identified by amino acid homologies or independently by biochemical characterization of Golgi associated transport steps in *in vitro* and permeabilized cell systems (Sacher and Ferro-Novick, 2001). Among the 10 TRAPP components, seven (Bet3p, Bet5p, Trs20p, Trs23p, Trs31p, Trs33p, and Trs130p) have structural homologues in human (Fig 18A).

Despite extensive database searches, mammalian proteins exhibiting significant amino acid relatedness to Trs65p, Trs85p, or Trs120p were not found. Although an early proteomic study of immunoprecipitaed TRAPP complex (via tagging Bet3) has indicated that KIAA1012 could be a counterpart of Trs85p, their amino acid sequences do not show convincing homology. Interestingly, several proteins including KIAA1012, hypothetical protein AL136752.1, CGI-85 and hypothetical protein FLJ13611 are co-immunoprecipitated with tagged Bet3. Although these proteins do not show clear homology with Trs65p, Trs85p, or Trs120p, some of these proteins could be functional counterparts of yeast Trs65p, Trs85p, or Trs120p. Similar phenomenon was observed for COG complex in that 5 of the 8 subunits are structurally conserved between yeast and human while yeast and human has 3 unique proteins that could represent functional counterparts (Ungar et al., 2002). Human Trs20 was independently identified as SEDL and has been implicated in endoplasmic reticulum-to-Golgi vesicle transport (Jang et al., 2002). Trs23 was independently identified as synbindin, which is expressed by neurons in a similar pattern to that of syndecan-2. It binds the C-terminal cytoplasmic signal Glu-Phe-Tyr-Ala (EFYA) of syndecans and is implicated in the establishment and/or function of dendritic spines synapses (Iryna et al., 2000). Synbindin is structurally related to yeast proteins known to be involved in vesicle transport.

We have searched the human genome and other databases with all the yeast and the known mammalian proteins of the TRAPP complex and have identified another novel protein homologous to Trs33p and human Trs33 (Fig. 18B). We have tentatively named the novel protein as Trs33B and the original Trs33 as Trs33A. Trs33B from human, mouse and zebrafish is well conserved and has a higher amino acid identity (33%) to Trs33p than Trs33A (24%). Trs33A and Trs33B have 56%

A

Subunit	Yeast (# of AA)	Human (# of AA)	AA identity	TRAPP I	TRAPP II
Bet5	159	145	30%	+	+
Trs20	175	140 (SEDL)	40%	+	+
Bet3	193	180	53%	+	+
Trs23	219	219 (Synbindin)	30%	+	+
Trs31	283	188	27%	+	+
Trs33	268	160 (Trs33A) 158 (Trs33B)	24% 33%	+	+
Trs65	560 (Kre11p)	-	-	+	+
Trs85	698 (Gsg1p)	-	-	-	+
Trs120	1289	-	-	-	+
Trs130	1102	1259 (EHOC-1/GT334)	12% (28%)	-	+

B

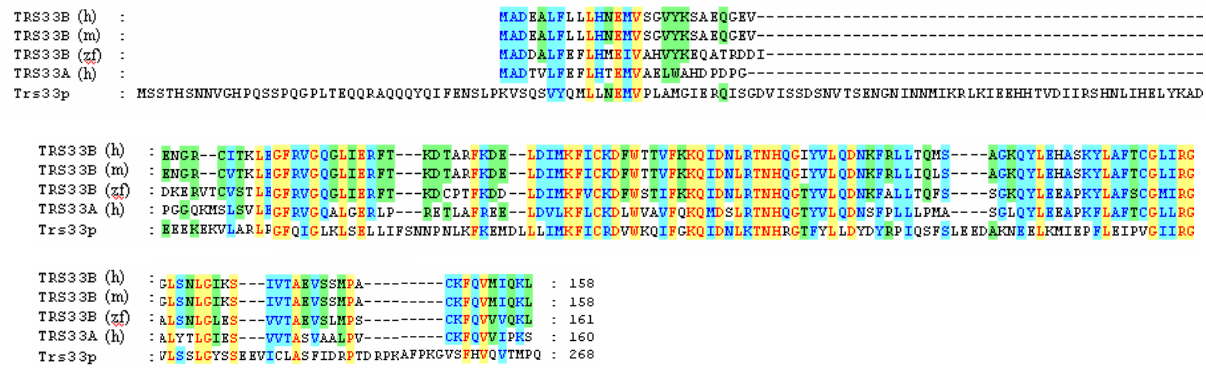

C

D

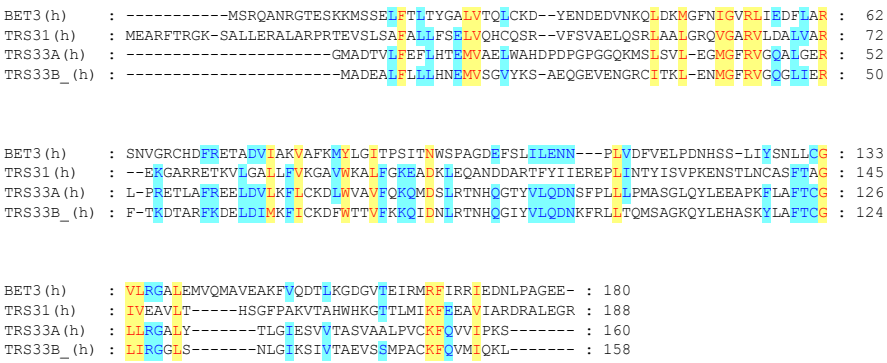

Figure 18. Analysis of the various TRAPP subunits. (A) Subunits of the TRAPP complex. (B) Sequence alignment of the various Trs33 Homologues. (C) Related sequence homology between Bet5, Trs20 and Trs23 (D) Related sequence homology between Bet3, Trs31 and Trs33.

amino acid sequence identity. Although the biochemical properties of Trs33B and the four candidate functional homologues (KIAA1012, AL136752.1, CGI-85, FLJ1361) will need to be established, these observations strongly suggest that mammalian cells have TRAPP complex with similar compositions. This information is summarized in Fig 18A. Since Bet3 is the most conserved subunit (53% identity between yeast and human), we have thus decided to focus on more detail on the biochemical, cell biological and functional aspects of Bet3.

5.2.2 Bet3 is Expressed Ubiquitously

To examine whether Bet3 is involved in a common biological process or in a specific event unique to certain tissues, the expression of Bet3 mRNA was examined in eight different mouse tissues by Northern blot analysis (Figure 19). A mouse multiple tissue Northern blot containing 2 μg poly A+ RNA of the indicated tissues was hybridized with radiolabelled Bet3 probe. A single transcript of about 1.6 kb was detected in all tissues at comparable levels except for the skeletal muscle, which expresses a lesser amount of Bet3 mRNA. The ubiquitous expression of Bet3 mRNA suggests that Bet3 may participate in a biological event that occurs in all cells.

5.2.3 Bet3 is a 22 kDa Protein Present in Both Membrane-bound and Cytosolic Forms

The entire coding region of mouse Bet3 was expressed as a carboxyl-terminally Hisx6-tagged recombinant protein (His6-Bet3) as well as an amino-terminal GST fusion (GST-Bet3) in *E. coli*. Purified His6-Bet3 was used to immunize rabbits and antibodies specific for Bet3 were isolated by affinity purification using the recombinant GST-Bet3 bound and cross-linked to glutathione-sepharose beads. The antibodies were used to determine the distribution of Bet3 in subcellular fractions obtained from rat liver. A post-nuclear supernatant (PNS) obtained after a low speed

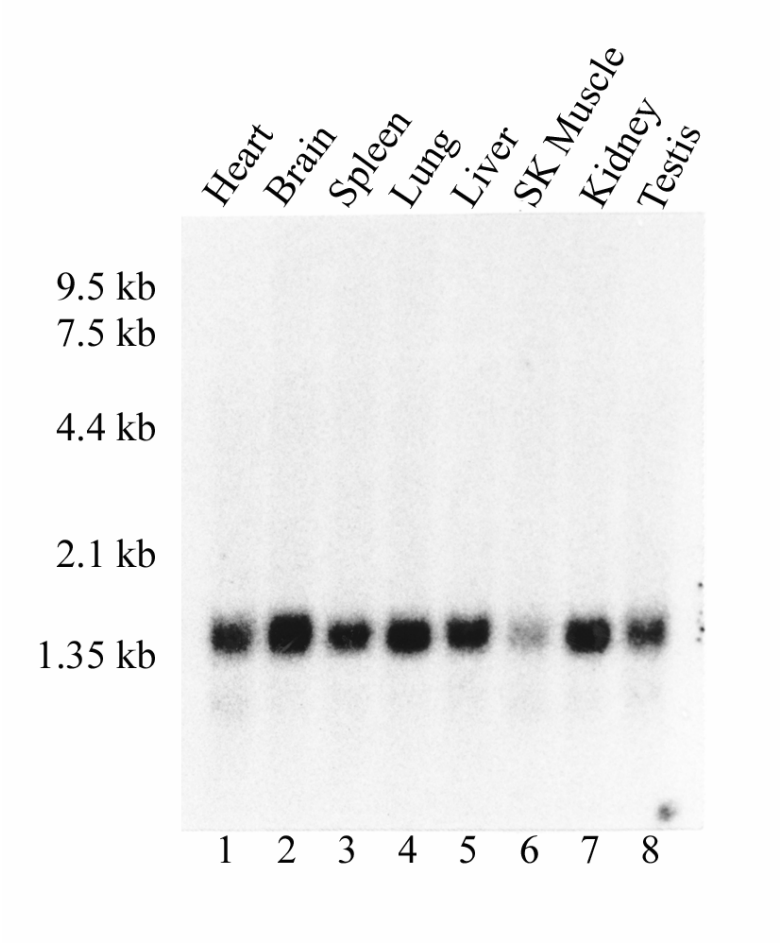

Figure 19. Northern blot analysis of Bet3 mRNA in rat tissues. A multiple tissue blot (Clontech) containing 2 μg of poly(A)+ RNA from the indicated tissues was hybridized with ^{32}P-labelled Bet3 probes and processed for autoradiography.

spin (2000xg) which removes unbroken cells, cell debris and nuclei, was centrifuged at 150,000xg to yield a total membrane pellet (TM) and a supernatant which comprises the cytosol (C). The total membrane pellet was then floated onto sucrose gradients to give a microsomal (M) pellet and the lighter Golgi-enriched membrane fraction (G). 25 μg protein from each fraction was separated by SDS-PAGE and immunoblotted to detect Bet3 and the Golgi SNARE, GS28 (Subramaniam *et al*., 1995; Subramaniam *et al*., 1996) or stained with Coomassie Blue R-250 (Figure 20). As shown by the protein profiles (Figure 20C), comparable amounts of protein from these fractions were analyzed. GS28 is detected predominantly in the G fraction as expected for an integral membrane protein of the Golgi apparatus (Figure 20B). A single polypeptide with an apparent molecular weight of 22 kDa was detected by Bet3 antibodies (Figure 20A). Detection of this 22 kDa polypeptide by Bet3 antibodies is specific because pre-incubation of the antibodies with recombinant GST-Bet3 but not with GST or other GST fusion proteins abolished its detection (data not shown). Bet3 is significantly enriched in the G fraction and also present in the cytosolic fraction (Figure 20A). These results indicate that Bet3 exists in both a soluble form in the cytosol as well as a membrane-bound form, which fractionates with the Golgi-enriched membrane.

5.2.4 The Majority of Bet3 is Present in the cytosol

Although Bet3 is present both in cytosolic and membrane-bound fractions, it is apparent that more Bet3 is associated with the cytosol because much more cytosol was obtained as compared to the amount of Golgi-enriched membranes during the subcellular fractionation of rat liver. In order to gain more insight into this, the distribution of Bet3 in cultured cells was analyzed.

Normal rat kidney cells (NRK) were processed to yield a total membrane pellet (TM) and the cytosol (C). The TM pellet was resuspended in a volume of buffer

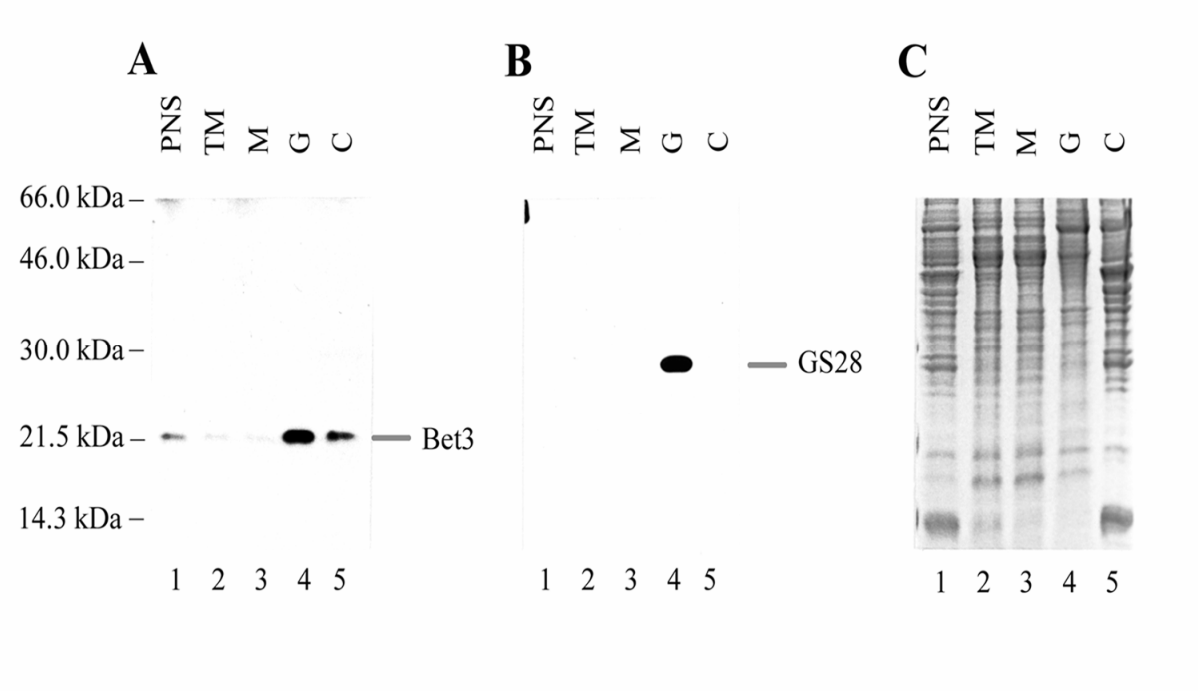

Figure 20. Distribution of Bet3 in various subcellular fractions derived from rat liver. 25 μg of protein from the indicated fractions (PNS, postnuclear supernatant; TM, total membrane; M, microsome-enriched membrane; G, Golgi-enriched membranes; and C, cytosol) was separated by SDS-PAGE and stained with Coomassie Blue R-250 (C) or transferred to filters and immunoblotted with antibodies against Bet3 (A) or GS28 (B).

equivalent to the cytosol. Equal volumes of the TM and the cytosol were resolved by SDS-PAGE, and transferred onto nitrocellulose membranes and immunoblotted with antibodies against Bet3, RhoGDI1 and GS28 (Figure 21). As shown, GS28 is found exclusively in the TM fraction (lanes 5 and 6). RhoGDI1 is a cytosolic protein (Shisheva et al., 1994) and more is present in the cytosol than the TM (lanes 3 and 4). The distribution of Bet3 is similar to that of RhoGDI1, with more protein being detected in the cytosol than the TM (lanes 1 and 2). These results suggest that although a significant amount of Bet3 is membrane-bound, the majority of Bet3 is present in the cytosol.

Using the Bet3 antibodies in immunofluorescence microscopy, Bet3 was also seen to label the cytosol (Fig 22 a) while in contrast, β-COP antibodies label the Golgi apparatus (Fig. 22 *b*) in NRK cells. Furthermore, the cytosolic labeling of Bet3 (Fig. 22, *d*) but not β-COP (Fig. 22, *e*) was abolished by preincubation of the antibodies with His6-Bet3, further confirming the specificity of the antibodies.

5.2.5 The membrane pool of Bet3 is Tightly Associated with the Membrane

The presence of a significant amount of Bet3 in the Golgi-enriched membrane fraction led us to study the nature of this association. Golgi-enriched membranes isolated from rat liver were extracted with PBS, 1 M KCl, 2.5 M urea, 0.1 M sodium carbonate (pH 11.5) and 1 % sodium deoxycholate (DOC). The extracts were centrifuged at 100,000xg. The resulting supernatants and pellets were analyzed by immunoblot to detect Bet3 and GS28 (Figure 23). As shown previously (Subramaniam et al., 1995), GS28 is not extracted by PBS (lanes 1 and 2), 1 M KCl (lanes 3 and 4), 2.5 M urea (lanes 5 and 6) or alkaline pH (lanes 7 and 8), but is efficiently extracted by detergent (lanes 9 and 10). Interestingly, Bet3 is not extracted by PBS (lanes 1 and 2) or 1 M KCl (lanes 3 and 4), suggesting that Bet3 is tightly

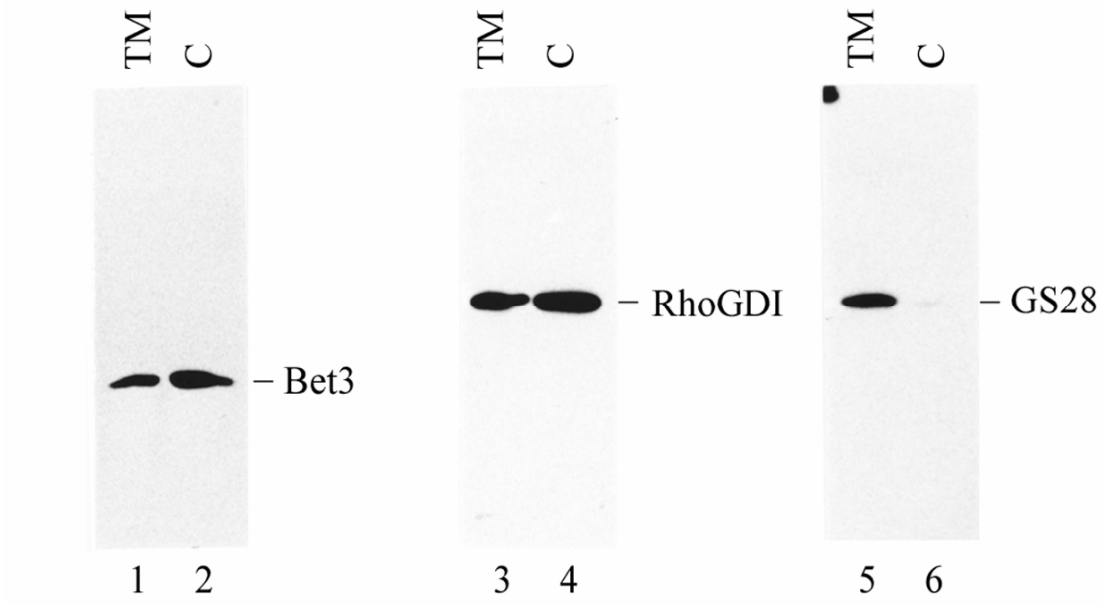

Figure 21. Bet3 is present predominantly in the cytosol. NRK cells were fractionated into total membrane (TM) and cytosol (C) fractions. Equivalent fractions of TM and C were separated by SDS-PAGE, transferred to a filter and immunoblotted to detect Bet3 (lanes 1-2), RhoGDI1 (lanes 3-4), or GS28 (lanes 5-6).

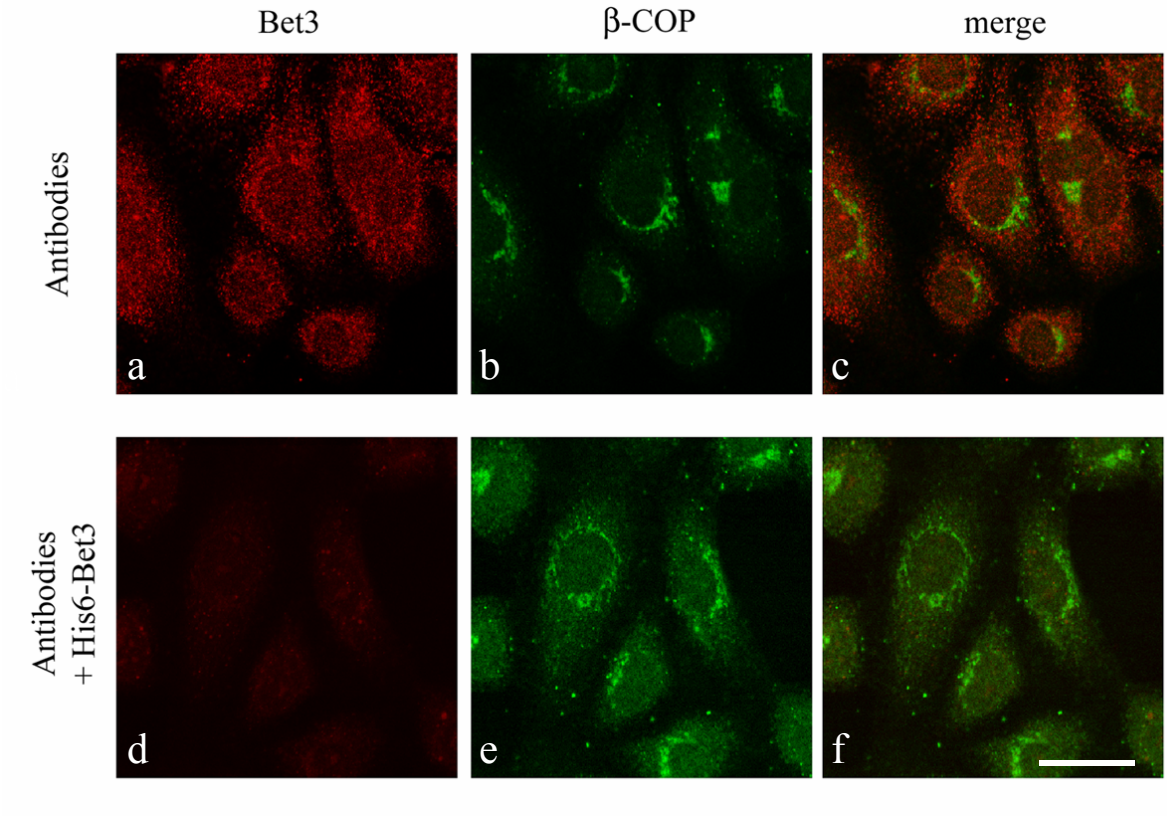

Figure 22. Anti-Bet3 antibodies label the cytosol. NRK cells were fixed, permeabilized, and double-labeled with Bet3 antibodies (*a* and *d*) and monoclonal antibodies against β-COP (*b* and *e*). The cytosolic labeling of Bet3 (*d)* but not β-COP (*e*) was abolished by prior incubation of the antibodies with His6-Bet3. The merged images are shown in *c* and *f*. *Bar*, 10 μm.

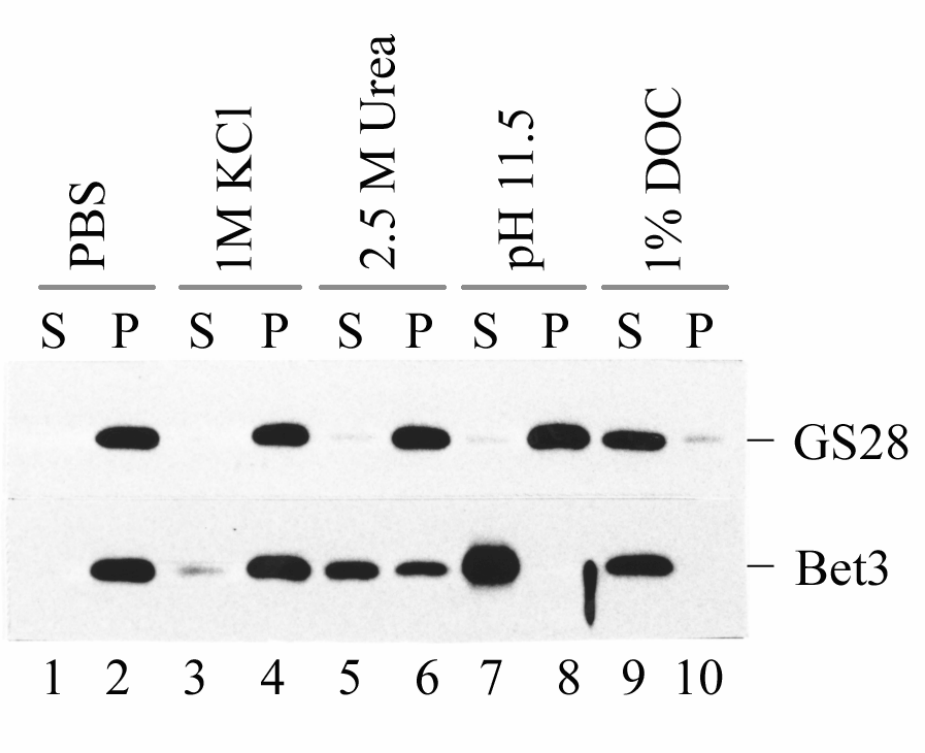

Figure 23. Bet3 is a peripheral membrane protein. Golgi-enriched membranes were extracted with PBS, 1 M KCl, 2.5 M urea, 150 mM sodium carbonate (pH 11.5), or 1% sodium deoxycholate (1% DOC), respectively. The resulting supernatants (S) and pellets (P) were separated by SDS-PAGE, transferred to a filter and immunoblotted to detect GS28 (upper panel) or Bet3 (lower panel).

associated with the membrane. However, the majority of Bet3 could be extracted by 2.5 M urea (lanes 5 and 6), while complete extraction of Bet3 from the membrane was achieved by pH 11.5 (lanes 7 and 8) or the detergent (lanes 9 and 10), suggesting that the membrane pool of Bet3 behaves like a tightly-associated peripheral membrane protein.

5.2.6 Antibodies Against Bet3 Inhibit *In Vitro* ER-Golgi Transport

To investigate the possible involvement of Bet3 in transport events in mammalian cells, we utilized a semi-intact cell system that reconstitutes the transport of the envelope glycoprotein of vesicular stomatitis virus (VSV-G) from the ER to the Golgi apparatus (Beckers *et al*., 1987; Davidson and Balch, 1993; Balch et al., 1994). The transport of VSV-G is monitored by following the extent of conversion of the endo- H sensitive ER form to the endo-H resistant Golgi form. In a standard assay in the presence of rat liver cytosol (rlc) and an ATP-regenerating system, about 70-80% of VSV-G was transported (Figure 24, lane 2) while only background levels (around 10%) of transport were detected when the assay was performed on ice (lane 1). As shown previously (Subramaniam *et al.*, 1996), *in vitro* ER-Golgi transport was potently inhibited by antibodies against GS28 (lane 3). Significantly, transport was also inhibited by Bet3 antibodies in a dose-dependent manner (lanes 4 to 9). Half-maximal inhibition was observed with approximately 1.5 μg of Bet3 antibodies (lane6), while 2 μg or more of Bet3 antibodies inhibited the transport to background levels (lanes 7 to 9). To establish that the inhibition was due to antibody binding to endogenous Bet3, the antibodies were boiled for 5 min., cooled on ice and then added into the reaction. As seen (lane 11), boiled antibodies had no inhibitory effect on the transport. Furthermore, pre-incubation of 2 μg of antibodies with 2 μg of GST-Bet3 itself did not have any significant effect on the transport (lane 12). These results

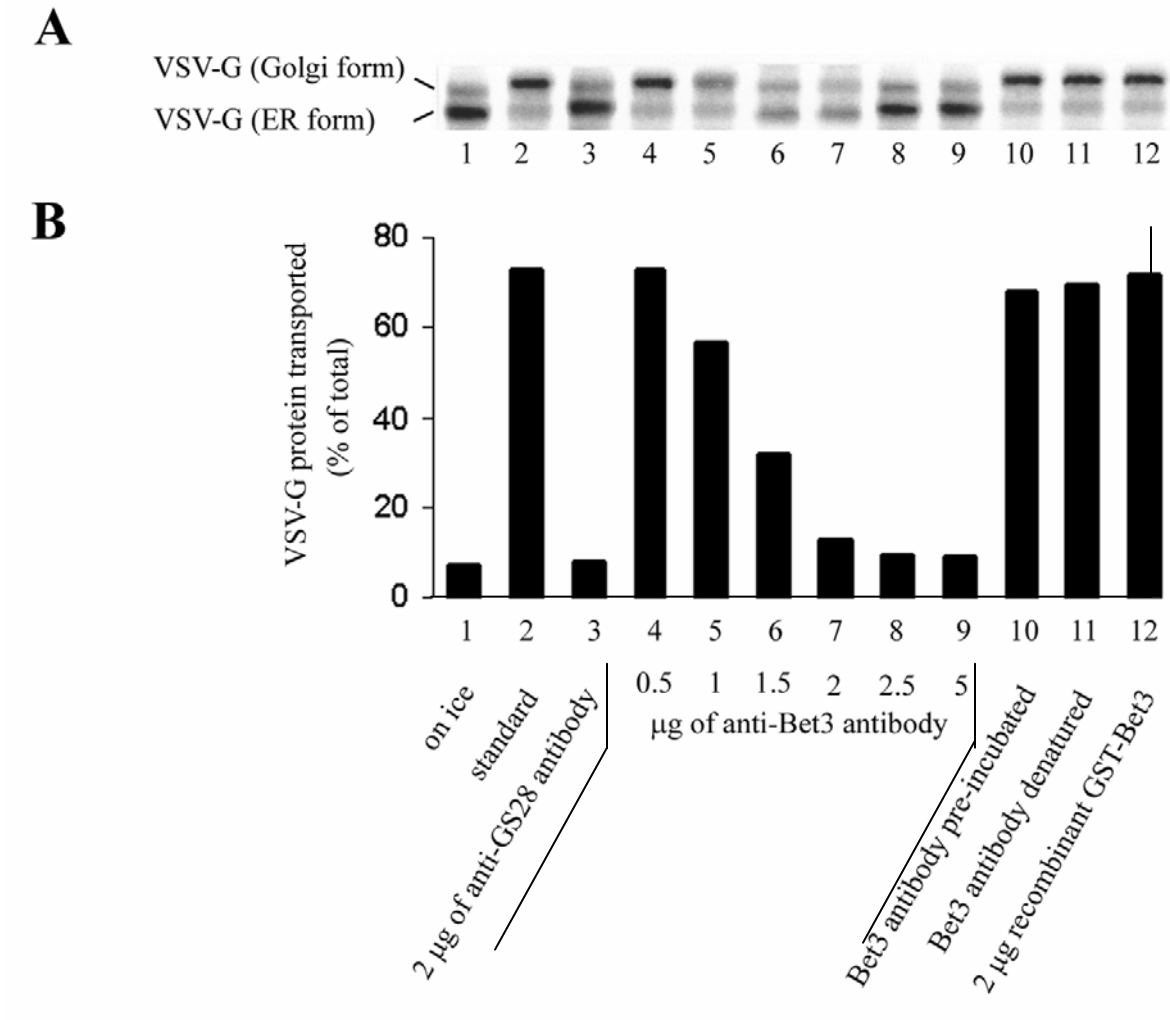

Figure 24. Antibodies against Bet3 inhibit *in vitro* transport of VSV-G from the ER to Golgi apparatus. Semi-intact NRK cells were incubated in the presence of cytosol and ATP on ice (lane 1) or at 32°C for 60 min (lanes 2-12). Increasing amounts of anti-Bet3 antibodies were added as indicated (lanes 4-9). Control assays were supplemented with 2 µg of antibody against GS28 (lane 3), 2 µg anti-Bet3 antibodies pre-incubated with 2 µg of GST-Bet3 (lane 10), 2 µg heat-inactivated anti-Bet3 antibodies (lane 11), or 2 µg GST-Bet3 (lane 12), respectively. Transport was measured by monitoring the percentage of conversion of the total pool of VSV-G from the endoH sensitive ER form to the endoH resistant Golgi form (panel A). The transport was quantified (panel B).

suggest that specific binding of antibodies to the endogenous Bet3 is the basis for the observed inhibitory effect of Bet3 antibodies and that Bet3 plays a role in ER-Golgi transport in mammalian cells.

5.2.7 Cytosolic pool of Bet3 is Required for ER-Golgi Transport

Yeast Bet3p is primarily associated with the membrane and only the membrane-bound Bet3p is functionally important for ER-Golgi transport (Sacher et al., 1998). Although the majority of Bet3 is present in the cytosol, a significant amount of Bet3 is membrane- bound and it is interesting to assess whether the membrane-bound Bet3 is sufficient for ER-Golgi transport or whether the cytosolic pool of Bet3 is also necessary for the transport. We have therefore investigated whether the inhibition by Bet3 antibodies is mediated by their binding to the cytosolic Bet3, membrane-bound Bet3, or both. As shown, when Bet3 antibodies were added to a standard transport reaction (Figure 25, lane 3, membrane plus cytosol), inhibition of ER-Golgi transport was observed. When semi-intact cells were first incubated with Bet3 antibodies for one hour on ice followed by a washing step to remove unbound antibodies and then used in the transport assay, normal transport was observed (lane 4, membrane only). This suggests that when the membrane pool of Bet3 is bound to antibodies, normal transport could still occur in the presence of cytosol which contains functional Bet3. When cytosol was preincubated with Bet3 antibodies for one hour on ice and then immediately used in the transport reaction, ER-Golgi transport was inhibited (lane 5, cytosol only). These results suggest that inhibiting membrane-bound Bet3 is not sufficient to inhibit ER-Golgi transport and that cytosolic Bet3 plays an essential role in ER-Golgi transport. In contrast, anti-GS28 potently inhibits ER-Golgi transport when only semi-intact cells were incubated with the antibody (lane 7). Similar to Bet3, antibodies against α-SNAP inhibited ER-Golgi transport when added

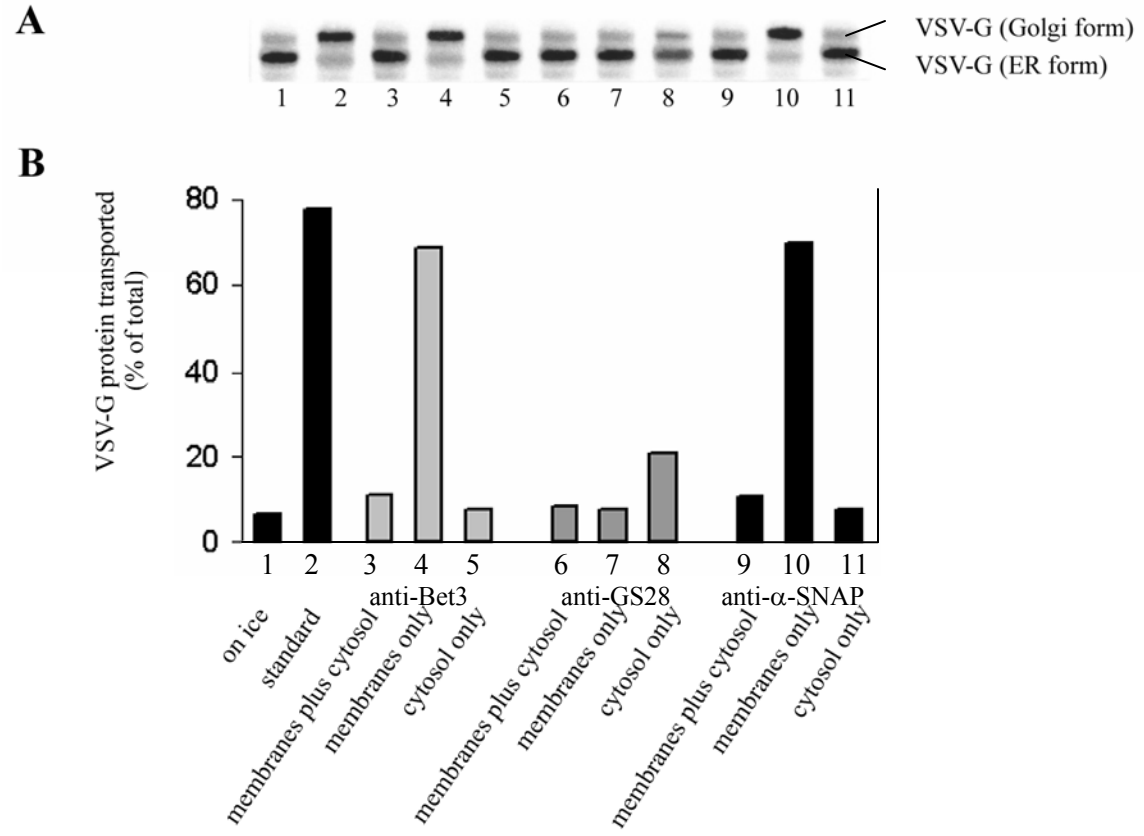

Figure 25. Antibodies against Bet3 functionally inhibit the pool of Bet3. Semi-intact NRK cells (lanes 4, 7, 10) were incubated with 2 μg of the indicated antibodies for one hr on ice, washed by centrifugation and resuspended in standard transport cocktail. Likewise, cytosol (lanes 5, 8, 11) or combinations of semi-intact cells and cytosol (lanes 3, 6, 9) were incubated with 2 μg of the indicated antibodies for one hr on ice. After supplementing with complete transport cocktail, assays were then incubated for 60 min on ice (lane 1) or at 32°C (lanes 2 to 11). The extent of VSV-G transport was monitored (panel A) and quantified (panel B).

to the standard reaction (lane 9) or the cytosol (lane 11), but not the semi-intact cells (lane 10), consistent with previous observation that cytosolic α-SNAP is necessary for ER-Golgi transport (Peter et al., 1997).

The above observation could be explained alternatively if cytosolic Bet3 could compete for the antibodies bound to the membrane Bet3 and functional Bet3 is then restored on the membrane. To further sustain the notion that cytosolic Bet3 is necessary for ER-Golgi transport, rat liver cytosol was immunodepleted of endogenous Bet3 by using anti-Bet3 antibodies coupled to Sepharose. As revealed by immunoblot analysis (Figure 26A), Bet3 is essentially undetectable in the Bet3-depleted cytosol (lane 2), while Bet3 was detected in the mock-depleted (lane 1) and α-SNAP-depleted (lane 3) cytosol. Normal levels of α-SNAP was detected in mock-depleted (lane 1) and Bet3-depleted (lane 2) cytosol but undetectable in α-SNAP depleted cytosol (lane 3). Mock-depleted cytosol (lane 2) supported normal ER-Golgi transport, while Bet3-depleted cytosol failed to support ER-Golgi transport (lane 3), suggesting that cytosolic Bet3 is indeed necessary for ER-Golgi transport. More importantly, the defect of Bet3-depleted cytosol could be rescued by relatively high concentrations of recombinant GST-Bet3 (lanes 4-7).

5.2.8 Bet3 Functions Prior to the EGTA-sensitive Stage during ER-Golgi transport

To gain mechanistic insight into the function of Bet3 in ER-Golgi transport, we have performed several experiments to define the stage at which Bet3 functions in ER-Golgi transport. We have first established that antibodies against Bet3 must be added before the EGTA-sensitive stage during *in vitro* ER-Golgi transport. EGTA has been shown to reversibly inhibit the *in vitro* ER-Golgi transport at a stage after docking of transport intermediates but before the actual fusion (Rexach and Schekman, 1991;

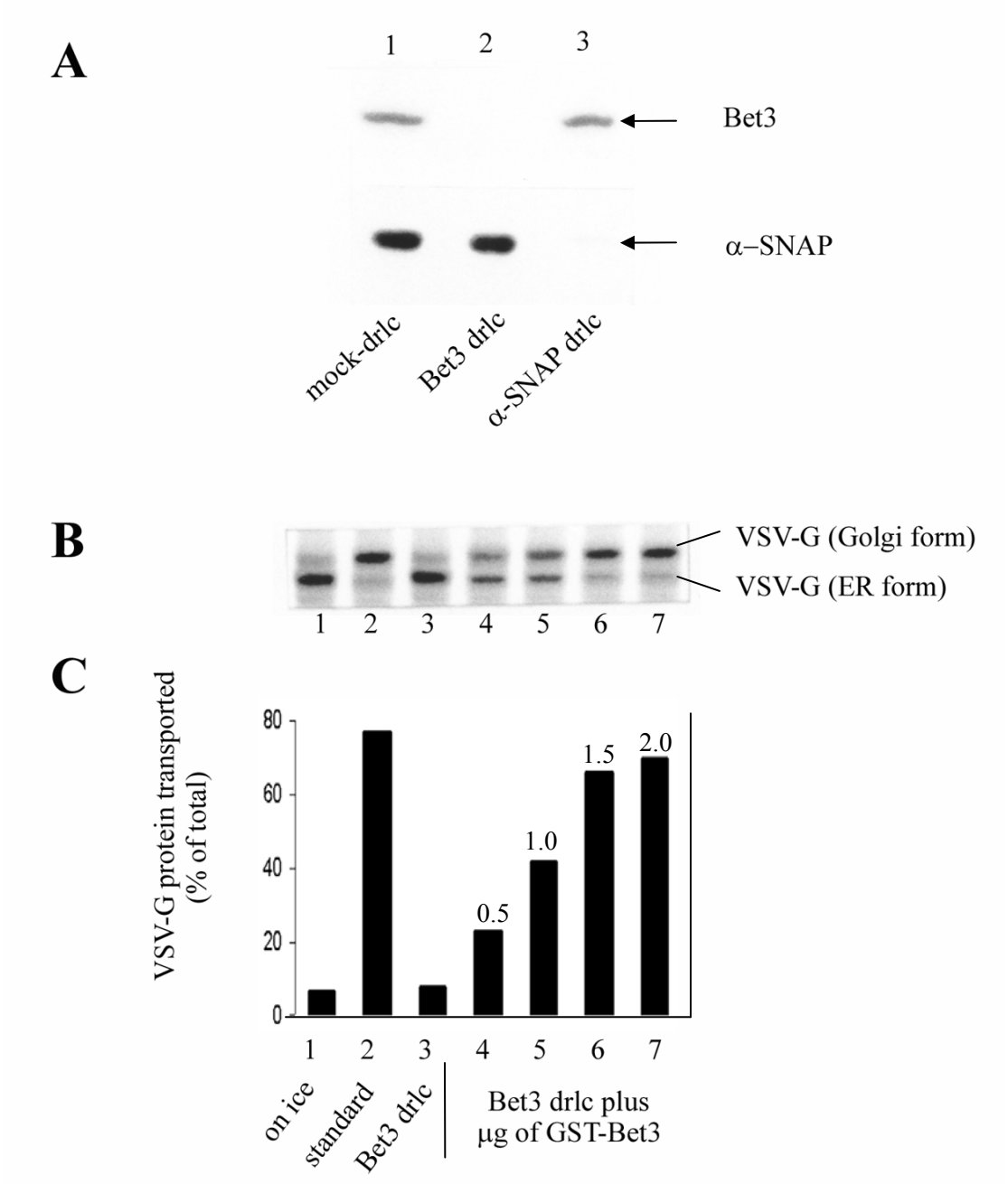

Figure 26. Cytosolic Bet3 is necessary for ER to Golgi transport. (A): Rat liver cytosol (rlc) was immunodepleted with anti-HA antibodies (lane 1, mock-drlc), anti-Bet3 antibodies (lane 2, Bet3-drlc), or anti-α-SNAP antibodies (lane 3, α-SNAP drlc). The immunodepleted cytosols were analysed by immunoblot to detect Bet3 (upper panel) or α-SNAP (lower panel). (B) and (C): Semi-intact NRK cells were incubated in transport cocktail with mock-drlc (lanes 1-2) or Bet3-drlc (lanes 3-7) supplemented with the indicated amounts (μg) of GST-Bet3 (lanes 4-7). Transport reactions were incubated for 60 min on ice (lane 1) or at 32°C (lanes2-7). The extent of VSV-G transport was monitored (B) and quantified (C).

Balch et al., 1994; Pind et al., 1994; Aridor et al., 1995; Lupashin et al., 1996). In a typical experiment, ER-Golgi transport is initially performed in the presence of EGTA to arrest transport at the EGTA-sensitive step (stage I). The semi-intact cells are then washed to remove the inhibitor and resuspended in fresh transport cocktail containing fresh cytosol and ATP (stage II)(Fig 27A). In the presence of EGTA, VSV-G was arrested in the endo-H sensitive ER form (Figure 27B and C, lane 3). However, a second stage of incubation in fresh transport cocktail allowed VSV-G to be converted to the endo-H resistant Golgi form (lane 4). As shown previously (Subramaniam et al., 1996), antibodies against GS28 inhibited ER-Golgi transport when they were added to the reaction either in the first stage (lane 5) or the second stage (lane 6). This is consistent with the notion that antibodies against GS28 can still inhibit ER-Golgi transport after the EGTA-sensitive stage (Subramaniam et al., 1996). Bet1 has previously been shown to be present in the pre-Golgi intermediate compartment and it may participate in the ER-Golgi transport before the EGTA-sensitive stage (Zhang *et al.*, 1997), because antibodies against Bet1 potently inhibited ER-Golgi transport when they were added in the stage I (lane 7) but not in the stage II (lane 8) of the reaction. Similarly to Bet1, antibodies against Bet3 inhibited ER-Golgi transport only when they were added at stage I (lane 9) but not stage II (lane 10), suggesting that Bet3 antibodies can no longer block the function of Bet3 when they are added after the EGTA-sensitive stage. Furthermore, like normal rlc (lane 11), Bet3-depleted rlc (lane 12) can support stage II transport, suggesting that cytosolic Bet3 is no longer required after the EGTA-sensitive stage.

5.2.9 Bet3 acts after COPII but before Rab1 and α-SNAP during ER-Golgi transport

To define more precisely the stage at which Bet3 acts during ER-Golgi

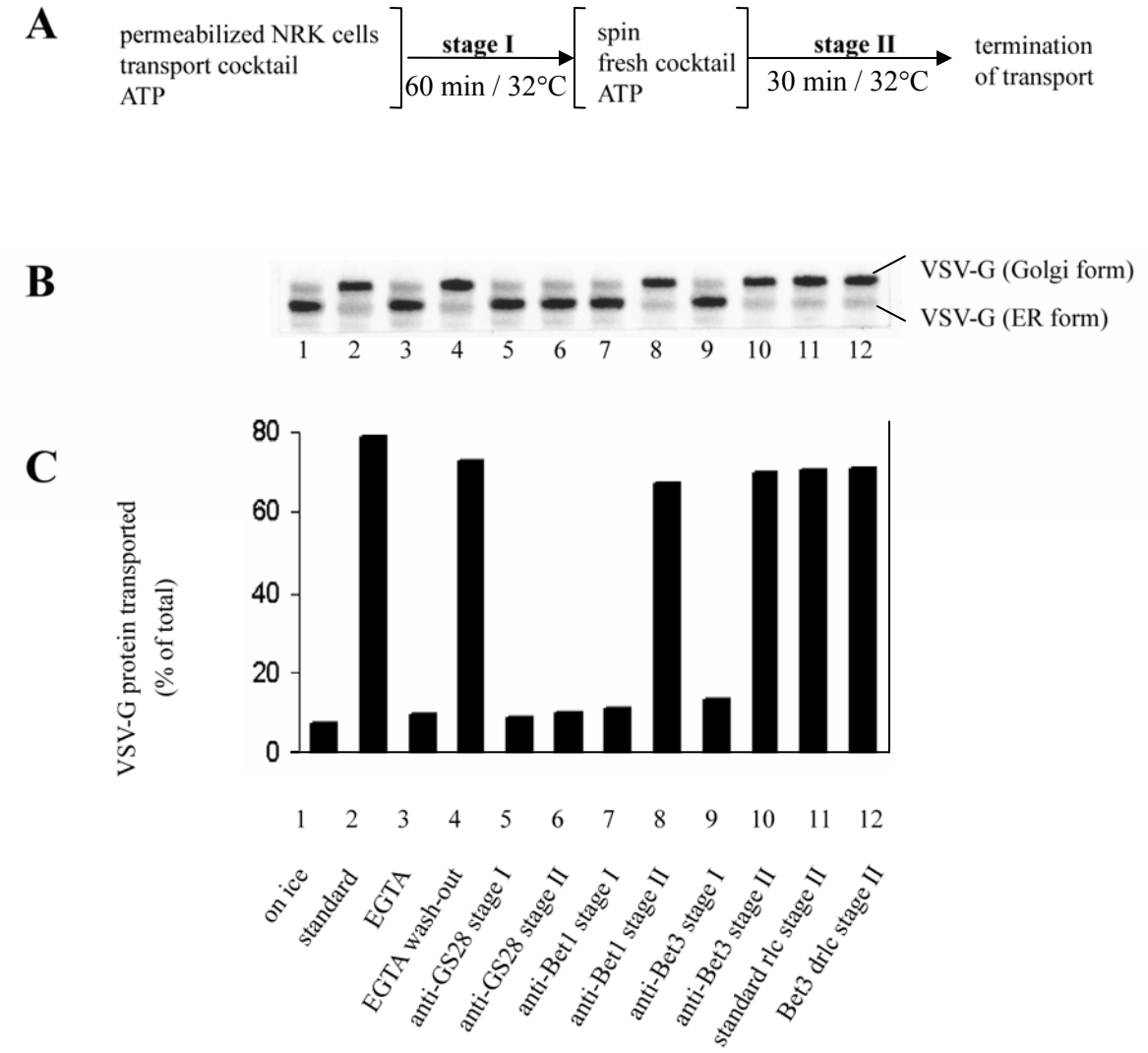

Figure 27. Antibodies against Bet3 act before the EGTA sensitive step in ER to Golgi transport *in vitro*. As outlined in panel (A), permeabilized NRK cells, cytosol and ATP were incubated in the absence (lanes 1 and 2) or presence of 8 mM EGTA (lanes 2 to12) on ice (lane 1) or at 32°C (lanes 2 to 12) for 60 min (stage I). The membranes were then collected by a brief spin and resuspended in fresh transport cocktail including fresh ATP and cytosol (lanes 2 to 11) or Bet3 immunodepleted cytosol (Bet3 drlc, lane 12). Reagents were added at stage I or stage II as indicated in panel (C). Transport was measured by the conversion of the VSV-G protein to the Endoglycosidase H resistant form (panel B) and quantified (panel C).

transport, we have used combinations of Bet3-depleted cytosol and cytosols depleted of various essential components using a modified two stage assay (Fig 28). Transport assay of semi-intact cells was first performed in the presence of cytosol depleted of an essential component (for example X) at 32°C for 90 min so that the transport is arrested at the stage that requires X component. After a brief spin and a washing stage, a second stage of incubation was performed in the presence of cytosol depleted of another essential component (such as Y). If component Y acts before X, the first stage of reaction with X-depleted cytosol (which contains Y component) will drive the transport to a point that no longer requires component Y and therefore normal transport will be observed during the second stage using Y-depleted cytosol. If Y acts after X component, first stage incubation using X-depleted cytosol will drive the transport to a point that is before the action of Y component and therefore a second stage reaction using Y-depleted cytosol will not support normal transport. Sec13 is a component of COPII involved in ER export (Schekman and Orci, 1996; Aridor et al., 1998; Tang et al., 1987). When Bet3-depleted cytosol was used in stage I and Sec13-depleted cytosol used in stage II, normal transport was observed (Fig 28B, I), suggesting that Bet3-depleted cytosol could drive transport to a point that no longer require Sec13 and that Sec13 therefore acts before Bet3. This result suggests that Bet3 participates in a stage after the action of COPII. Consistent with this notion, when Sec13-depleted and Bet3-depleted cytosols were used in stage I and II, respectively, only a background level of transport was observed (II). When Bet3-depleted cytosol was used for the first stage while α-SNAP-depleted cytosol used in the second stage, only background levels of transport was observed (III), suggesting that Bet3 depleted cytosol could not drive transport to the point that no longer requires α-SNAP and therefore Bet3 acts before α-SNAP. Furthermore, when α-SNAP-depleted cytosol and Bet3-depleted cytosols were

A

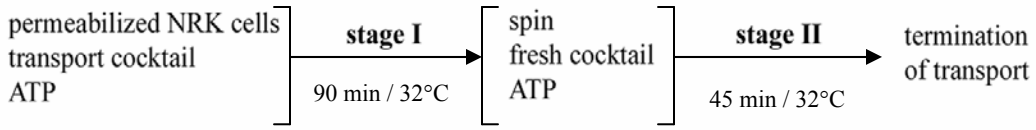

B

	stage I	stage II	VSV-G protein transported (%)
I	Bet3 drlc	mSEC13 drlc	71
II	mSEC13 drlc	Bet3 drlc	11
III	Bet3 drlc	α-SNAP drlc	12
IV	α-SNAP drlc	Bet3 drlc	64
V	Bet3 drlc	Rab1 drlc	10
VI	Rab1 drlc	Bet3 drlc	67

Figure 28. Bet3 is functionally required after Sec13 but before Rab1 and α-SNAP. Semi-intact NRK cells were incubated in transport cocktail with the indicated immunodepleted cytosols for 90 min at 32°C (stage I). The cells were subsequently washed by centrifugation and resuspended in fresh transport cocktail supplemented with the indicated immunodepleted cytosols for an additional 45 min (stage II). The extent of VSV-G transported to the Golgi was quantified.

used for the first and second stages respectively, normal transport was achieved (IV), consistent with the notion that α-SNAP-depleted cytosol (which contains Bet3) could drive the transport to a point that no longer requires Bet3 and therefore α-SNAP acts after Bet3. Similar experiments using combinations of Bet3-depleted cytosol with Rab1-depleted cytosol (V and VI) suggest that Bet3 also acts before Rab1. We have previously established that both Rab1 and α-SNAP act before the EGTA-sensitive stage and that Rab1 acts before α-SNAP (Peter et al., 1998). In this regards, Bet3, Rab1 and α-SNAP function after COPII but before the EGTA-sensitive stage in a sequential manner during ER-Golgi transport.

5.2.10 Cytosolic Bet3 exists in two distinct pools

In yeast, Bet3p exists in a large protein complex termed TRAPP (Sacher et al., 1998). To see whether a similar protein complex also exists in mammalian cells, we have analysed Bet3 distribution by gel-filtration (Fig 29). Two pools of Bet3 were observed, one high molecular weight pool (pool I) is distributed in fractions 2-4, while the other (pool II) in fractions 8-10 (A, panel a). Since pool I has sizes about that of coatomer which is found in fractions 2-5 (panel b), it may represent a Bet3-containing protein complex equivalent to yeast TRAPP. When cytosol was first denatured with SDS, pool I was no longer detected and Bet3 is only detected in pool II (Panel c), suggesting that pool II may represent the free form of Bet3. These results suggest that Bet3 may exist in a dynamic equilibrium between a TRAPP-equivalent complex and the free form. Recombinant GST-Bet3 is mainly distributed in fractions 6-8 (B, panel a), similar to denatured β-COP (A, panel d). However, when GST-Bet3 is mixed with the Bet3-depleted cytosol and then analysed by gel-filtration, a significant amount of GST-Bet3 is shifted to fractions 2-4, suggesting that GST-Bet3 could be incorporated into a TRAPP-equivalent protein complex.

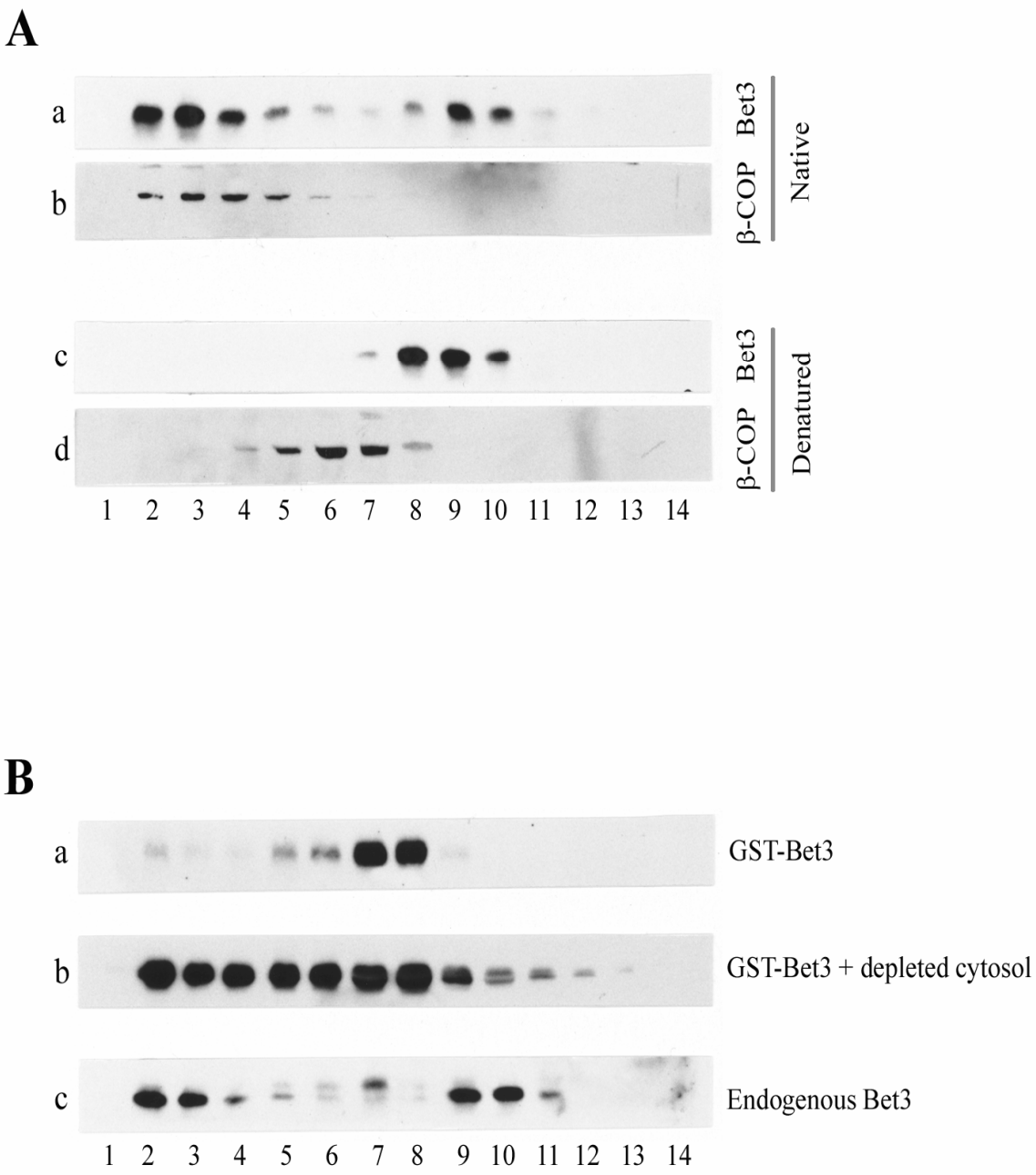

Figure 29. Two pools of Bet3 in the cytosol as revealed by gel filtration analysis. (A): Rat liver cytosol (panels a and b) or denatured cytosol (panels c and d) was resolved by gel filtration and the resulting fractions were analyzed by immunoblotting to detect Bet3 (panels a and c) or β-COP (panels b and d). (B): GST-Bet3 alone (panel a) or GST-Bet3 pre-incubated with Bet3-depleted rlc (panel b) were resolved by gel filtration and the resulting fractions were analyzed by immunoblotting to detect GST-Bet3. Shown also is the distribution of endogenous Bet3 (panel c).

5.3 Discussion

5.3.1 Identification of mammalian Bet3 and other subunits of the TRAPP complex

EST data-base searches using yeast Bet3p sequence resulted in the identification of a homologous mammalian protein, mouse Bet3 (Bet3). Since Bet3 is over 50% identical to Bet3p in the amino acid sequence, Bet3 is likely to be a mammalian equivalent of Bet3p. The mouse Bet3 homologue is 100% identical to human Bet3. By immunoblot analysis, antibodies raised against recombinant Bet3 recognize specifically a 22 kDa protein that is present in both cytosol and in Golgi-enriched membranes derived from rat liver. Since detection of this 22 kDa protein is totally abolished by pre-incubation of antibodies with recombinant Bet3 but not with GST or other recombinant proteins, we conclude that the 22 kDa protein is the endogenous Bet3. The membrane-associated fraction of Bet3 is tightly associated with the membrane because it is not extracted by 1 M KCl. When NRK cells were fractionated into total membrane and cytosol, it was found that the majority of Bet3 is present in the cytosol when equal fractions of total membrane and cytosol were used for the immunoblot analysis. These results suggest that Bet3 exists primarily in the cytosol and is recruited to the membrane in a dynamic manner. In contrast to what was observed in yeast Bet3p where the majority of the protein is membrane-associated (Sacher et al., 1998), hbet3 and htrs20 were largely soluble under the conditions used to prepare the lysate (Sacher et al., 2000). TRAPP subunits are resistant to extraction with Triton X-100, suggesting that TRAPP may bind to a matrix (Sacher et al., 2000). TRAPP has also been shown to stably associate with the Golgi and is required for vesicle docking (Barrowman et al., 2000).

Analysis of multiprotein complexes will provide a better knowledge of the

organization of a higher-order of network interactions and also enable us to understand and appreciate that the complex composition between human and other organisms is largely conserved. Analysis of yeast complexes can often predict the composition of the human counterparts. TRAPP subunits have been shown to exist in many different mammalian organisms (Sacher et al., 2000). Extremely high evolutionary conservation between yeast and mammalian subunits indicates that TRAPP plays a critical role in the secretory pathway in both yeast and man (Sacher et al., 1998). We have searched the human genome and other data-bases with all the yeast and the known mammalian proteins of the TRAPP complex and have identified another novel protein homologous to Trs33p and human Trs33, thereby suggesting that mammalian cells have TRAPP complex subunits with similar compositions. Human orthologs are smaller in size compared to their yeast counterparts possibly explaining the size difference noted between yeast and mammalian TRAPP (~1000 vs ~670 kD) (Sacher and Ferro-Novick, 2001)

Functional mammalian counterparts of yeast proteins have also been identified for Trs20 and Trs23. Human Trs20 was independently identified as SEDL which reveals an unexpected similarity to the structures of the N-terminal regulatory domain of two SNAREs, Ykt6p and mouse Sec22b, despite no sequence homology to these proteins (Jang et al., 2002). The N-terminal domain of Ykt6p influences the kinetics and proper assembly of SNARE complexes (Tochio et al., 2001). The N-terminal domain of mSec22b is also likely to provide some important regulatory functions, because expression of the N-terminal deletion mutant of VAMP-7, a homologue of mSec22b, was found to increase SNARE complex formation and strongly stimulate neurite outgrowth from PC12 cells (Martinez-Arca et al., 2000). The structural similarity of SEDL to the N-terminal domain of these SNAREs suggests a regulatory

function of the protein, perhaps an intramolecular regulatory role because it inhibits the C-terminal SNARE motif from forming the core complex with other SNAREs (Tochio et al., 2001 and Nicholson, et al., 1998). The three structures share an identical folding topology. In addition, the common hydrophobic surface on the similar structures of the three proteins, all involved in ER-to-Golgi vesicle transport, suggests that they may interact with different partners that belong to the same family of proteins (Jang et al., 2002). It was proposed based on the structure similarity of SEDL and Ykt6p-NT that SEDL binds to a target SNARE, thereby providing a regulatory role in the pairing of SNAREs along the transport pathway. (Jang et al., 2002). Synbindin is highly conserved across species and has 29% amino acid identity with Trs23. Synbindin forms clusters in dendritic spines when syndecan-2 is co-expressed in neurons. Immunoelectron microscopy localized synbindin on postsynaptic membranes and intracellular vesicles within dendrites, suggesting a role in postsynaptic membrane trafficking (Iryna et al 2000).

All the low molecular weight TRAPP subunits (Bet5, Trs20, Bet3, Trs23, Trs31 and Trs33p) are structurally conserved, while only one of the four high molecular weight subunits (Trs130) is conserved, suggesting that the large subunits may evolve more rapidly to accommodate the needs of different architectures and mechanisms in different organisms. Trs130p shares significant homology to a protein called GT334 (Lafreniere et al., 1997). Trs130p contains a region which has potential to be involved in a coiled-coil interaction, and overlaps with the region of highest homology to GT334. Similar to the COG complex, it is possible that the more divergent subunits of the TRAPP complex could interact with proteins of other well-conserved molecular machineries to moderate and enhance the essential and more fundamental roles played by the more conserved subunits.

The function of Bet3p and TRAPP in ER-Golgi transport may be analogous to that of the exocyst in post-Golgi secretion (Sacher et al 1998). An alignment of Trs33p, Trs31p and Bet3p from yeast and humans revealed several conserved features – two shared motifs as well as several conserved bulky, hydrophobic residues were detected (Sacher et al 2000). The alignment of Bet3, Trs31, Trs33A and Trs33B is shown in Fig. 18D. In addition, Trs20p showed relatively good alignment with Trs23p along the entire length of the protein, particularly strongest between their carboxy terminal halves. The alignment of Bet5, Trs20 (h) and synbindin is shown in Fig. 18C.

5.3.2 Role of Bet3 in ER-Golgi transport

Several lines of evidence suggest that Bet3 plays an essential role in ER-Golgi transport in mammalian cells. First, VSV-G transport in semi-intact cells could be inhibited by Bet3 antibodies in a dose-dependent manner and this inhibition is specific because denatured antibodies had no effect on VSV-G transport and the inhibitory effect of the antibodies could be neutralized by pre-incubation with recombinant Bet3. The importance of cytosolic Bet3 is established by the observation that cytosol could support normal protein transport, shown when only the membrane pool of Bet3 in semi-intact cells was decorated with the antibodies suggesting that the membrane pool of Bet3 is not necessary for ER-Golgi transport. It is most likely that cytosolic Bet3 could be recruited to the membrane so that functional Bet3 could be restored in the membrane. When cytosol was pre-incubated with Bet3 antibodies, inhibition of ER-Golgi transport of VSV-G was observed. In addition, the membrane pool is not sufficient to support ER-Golgi transport, because Bet3-depleted cytosol could not support this transport, establishing an essential role of cytosolic Bet3 in ER-Golgi transport. Furthermore, Bet3-depleted cytosol could be rendered competent in supporting ER-Golgi transport when supplemented with recombinant GST-Bet3.

However, relatively high concentrations of recombinant GST-Bet3 are required to rescue transport competence of the Bet3-depleted cytosol. Several possibilities could explain this point. One possibility is that only a fraction of GST-Bet3 is folded properly and exists in a functional conformation. The second possibility relates to the observation that cytosolic Bet3 exists in two distinct pools. One high molecular weight pool has a size comparable to that of coatomer, while the other reflects the free form of Bet3. Since Bet3p in yeast is found in the TRAPP protein complex (Sacher et al., 1998), the high molecular weight complex containing Bet3 may be equivalent to TRAPP and is the functional form of Bet3 associated with other components of this complex. Importantly, a significant amount of GST-Bet3 was incorporated into the high molecular weight form when incubated with Bet3-depleted cytosol. This suggests that Bet3-depleted cytosol may contain sufficient amounts of free form of other components of this protein complex. Interaction of GST-Bet3 with Bet3-depleted cytosol may have resulted in association of the GST-Bet3 with the free forms of other components in such a way that a functional TRAPP-equivalent complex could be formed. This could account for the fact that GST-Bet3 could rescue the transport defect of Bet3-depleted cytosol and that high concentrations of GST-Bet3 are required for this activity because only a fraction of GST-Bet3 could be incorporated into the functional protein complex. This observation is in line with the results obtained from the identification of mammalian TRAPP from HeLa lysates. hBet3 and htrs20 proteins co-eluted in a peak with an estimated size of about 670 kDa. In addition, a second more abundant peak of material was found, likely representing monomeric hBet3 and htrs20. Yeast lysates contain a 1094 kDa complex and no free pool of any subunits were detected (Sacher et al., 2000; Sacher and Ferro-Novick, 2001). It was suggested that the large pool of unassembled TRAPP subunits in mammalian cells may reflect

differences in how Golgi dynamics are regulated in mammalian cells versus yeast.

Mechanistic understanding of the participation of Bet3 in ER-Golgi transport came from the observation that it functions after COPII but before Rab1, α-SNAP and the EGTA-sensitive stage during ER-Golgi transport. EGTA has been shown previously to inhibit *in vitro* ER-Golgi transport after docking of transport intermediates but before actual fusion (Rexach and Schekman, 1991; Balch et al., 1994; Pind et al., 1994; Aridor et al., 1995; Lupashin et al., 1996). Several lines of evidence suggest that Bet3 functions before the EGTA-sensitive stage. Although Bet3 antibodies potently inhibited ER-Golgi transport when added before the EGTA-sensitive stage, addition of Bet3 antibodies to the *in vitro* transport reaction after the EGTA-sensitive stage had no effect on ER-Golgi transport. Secondly, Bet3-depleted cytosol can support events downstream of the EGTA-sensitive stage, suggesting that cytosolic Bet3 is no longer required after the EGTA-sensitive stage. In addition, Rab1 and α-SNAP have both been shown to participate in ER-Golgi transport before the EGTA-sensitive stage but downstream of the action of Sec13 (Peter et al., 1997). The demonstration that Bet3 acts before Rab1 and α-SNAP further supports this conclusion. Based on these observations, it is reasonable to suggest that Bet3 and/or its associated complex is most likely involved in the transport/targeting of ER-derived vesicles to the Golgi apparatus and in initiating the first stage of the docking event (the tethering) so that subsequent docking mediated by SNAREs can be faithfully and efficiently achieved. Additionally, Bet3 may also participate in the regulatory events mediated by SNAREs.

The TRAPP complex was shown to act as the GEF for Ypt1 and Ypt31/32 GTPases both *in vitro* and *in vivo* (Jones et al., 2000). The function of Ypt1 GTPase is required at the cis-Golgi for the targeting and fusion of ER-derived vesicles (Cao and

Barlowe, 2000; Segev, 1991), while the function of Ypt31/32 GTPases is essential for the formation of trans Golgi vesicles (Jedd et al., 1997). It has also been shown that increasing gene dosage of YPT31/32 suppressed the lethality resulting from deletion of the essential TRS130 gene and also partially suppresses the deletion of GCS1, an Arf GAP (Zhang et al., 2002) TRAPP has also been shown to be required for ER-to-Golgi transport (Barrowman et al., 2000, Sacher et al., 1998, plus this study). TRAPP could therefore potentially reside at the Golgi, thereafter activating GTP binding proteins which then lead to recruitment of other tethering factors or perhaps TRAPP could regulate several transport events and may serve as a general transport factor in regulating vesicle traffic.

CHAPTER 6

Preferential association of syntaxin 8 with the early endosome

6.1 Introduction

Protein transport along the secretory and endocytotic pathways is primarily mediated via various types of transport vesicles that bud from a donor compartment and fuse with a target compartment (Hong, 1996; Palade, 1975; Pryer et al., 1992; Rothman, 1994; Rothman and Wieland, 1996; Schekman and Orci, 1996). Soluble *N*-ethylmaleimide-sensitive factor (NSF; or its yeast counterpart, Sec18p) and soluble NSF attachment proteins (SNAPs; or the yeast counterpart, Sec17p) have been shown to participate in many different transport events (Clary et al., 1990; Graham and Emr, 1991; Griff et al., 1992; Whiteheart and Kubalek, 1995). The action of NSF and SNAP is mediated through SNAP receptors (SNAREs) that participate in vesicle docking and fusion events (Rothman, 1994; Whiteheart and Kubalek, 1995). It is generally believed that the specific docking and fusion of vesicles with the target compartment require interaction between v-SNAREs on the vesicles and t-SNAREs on the target membrane (Ferro-Novick and Jahn, 1994; Pfeffer, 1996; Rothman, 1994; Rothman and Warren, 1994; Scheller, 1995; Söllner et al., 1993; Südhof, 1995). Because of the importance of SNAREs in vesicle docking and fusion, identification and characterization of novel SNAREs is of significance because these studies will not only uncover new proteins participating in various trafficking events but also provide a novel molecular avenue for the detailed molecular and morphological studies of the respective trafficking events. Members of the syntaxin family represent an important class of t-SNAREs involved in diverse trafficking events (Bennett et al., 1993; Bock and Scheller, 1997; Hay et al., 1996, 1997). Syntaxin 1, the first member of this

family, was originally identified by its co-immunoprecipitation with synaptotagmin and is enriched in the presynaptic plasma membrane (Bennett et al., 1992). Syntaxin 1 is a substrate for botulinum neurotoxin C (BoNT/C), which is known to act at the motor neuron to inhibit the exocytotic release of acetylcholine from the synaptic vesicles and cause the clinical manifestation of botulism, providing solid evidence for the role of syntaxin 1 in synaptic vesicle docking and fusion (Blasi et al., 1993). Syntaxin 1, SNAP-25 and synaptobrevin/VAMP are known to be the major components involved in the docking and fusion of synaptic vesicles (Pevsner et al., 1994; Söllner et al., 1993; Scheller 1995; Südhof, 1995). Several other members of the syntaxin family have been identified, suggesting that members of this family are key molecules in docking and fusion processes of diverse transport events (Bennett et al., 1993; Bock et al., 1997; Wang et al, 1997; Wong et al., 1998; Tang et al., 1998a,b,c,d).

In addition to the tethering complexes described in chapters 3-5, I have also undertook to study the identification and characterization of novel SNAREs. In this present study, I describe the molecular characterization of a novel member (syntaxin 8) of the syntaxin family and have biochemically established that syntaxin 8 does behave like a SNARE. Immunofluorescence microscopy and immunogold labeling establish that syntaxin 8 is enriched in the early endosome.

6.2 Results

6.2.1 Syntaxin 8, a novel member of the syntaxin family

Searching the expressed sequence tags (ESTs) data-base using the Blast program (Altschul et al., 1997) with the amino acid sequence of syntaxin 6 (Bock et al., 1996) revealed the existence of several EST clones (accession numbers AA000586, W41301, W63907 and W83363) that could potentially encode protein fragments

homologous to syntaxin 6. A PCR fragment of the EST clone W833633 was used to screen a rat brain cDNA library, resulting in the isolation of full length cDNA clones for this protein. While our work was in progress, Scheller and Bock presented a series of EST clones that could potentially encode novel syntaxins (Bock and Scheller, 1997). Since the EST clones revealed during our database search correspond to what they have termed syntaxin 8, we have retained the name syntaxin 8 for this protein. The nucleotide and the derived amino acid sequence of rat syntaxin 8 is shown in Fig. 30A. Syntaxin 8 is a protein of 236 residues with a calculated molecular mass of 26894 dalton. There exists an 18-residue hydrophobic region (boxed in Fig. 30A) at the C terminus that could function as a carboxyl-terminal membrane anchor, a characteristic of the majority of known SNAREs (Pfeffer, 1996; Rothman and Warren, 1994).

Similar to other SNAREs, there exist three regions (residues 13-37, 44-68 and 166-204) that have the potential to form coiled-coil structures as predicted using the COILS program with a window of 21. The region around the third potential coiled-coil region (underlined in Fig. 30A) bears the highest amino acid identity with syntaxin 6 and to a lesser extent with SNAP-25. The amino acid sequences of the corresponding regions of syntaxin 8, syntaxin 6 and SNAP-25 are aligned and shown in Fig. 30B.

6.2.2 The transcript of syntaxin 8 is widely expressed

Syntaxin 8 could potentially participate in a common trafficking event that occurs in every cell or in a trafficking event that is unique to specific cells of certain tissues. To distinguish between these two possibilities, we have analyzed the mRNA levels of syntaxin 8 by northern blot (Fig. 31). A single transcript of about 1.2 kb was detected, at comparable levels, in all the tissues examined. The widespread expression of syntaxin 8 transcript is more consistent with the notion that syntaxin 8 is likely to be involved in a common transport event.

A

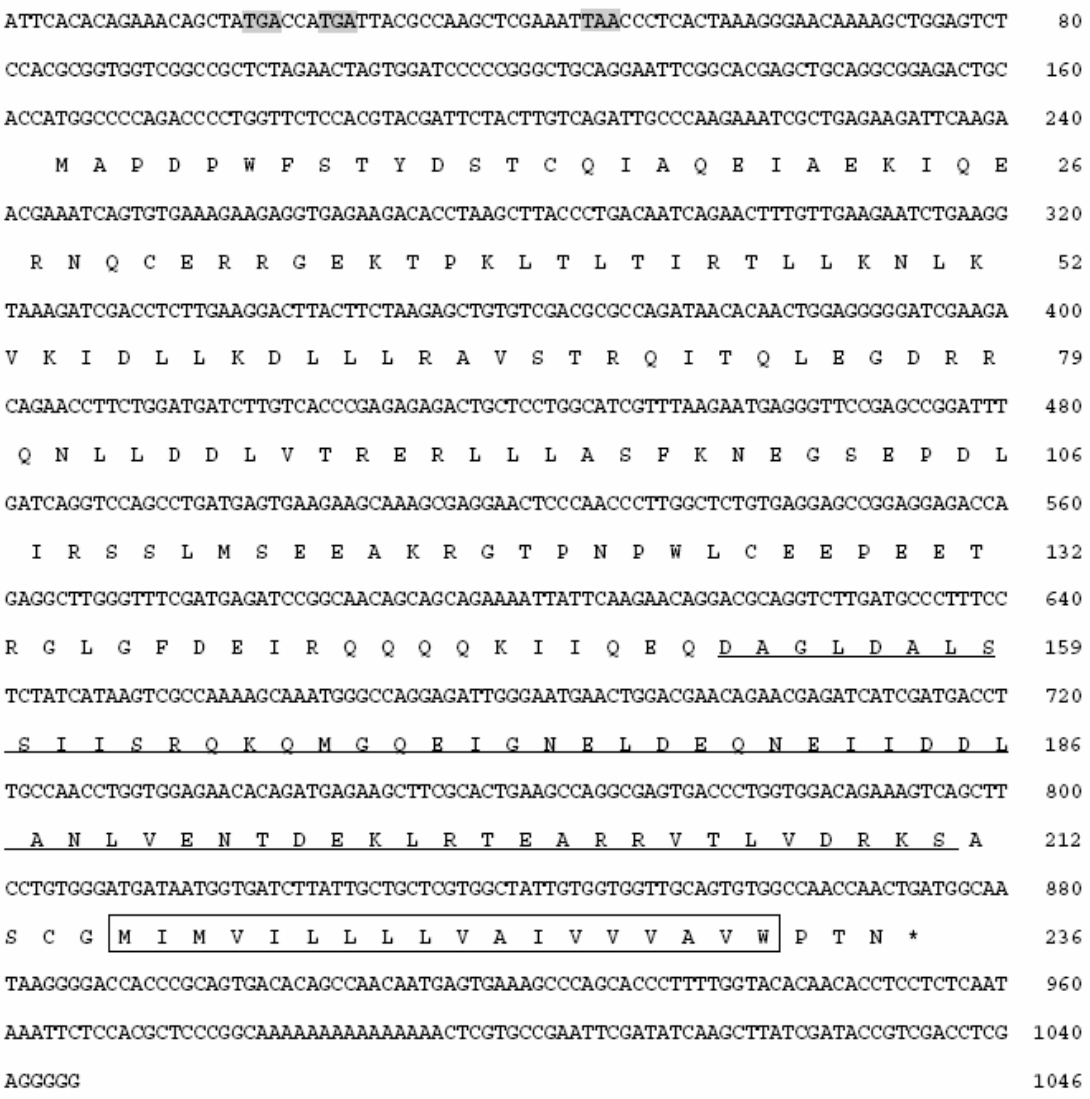

B

Figure 30. A novel SNARE protein, syntaxin 8. (A) Nucleotide and derived amino acid sequences of rat syntaxin 8. The carboxyl-terminal membrane anchor sequence is boxed. The region around the third potential coiled-coil region is underlined. (B) Alignment of the amino acid sequences (corresponding regions) of syntaxin 8, syntaxin 6 and SNAP-25. Identical residues are shaded.

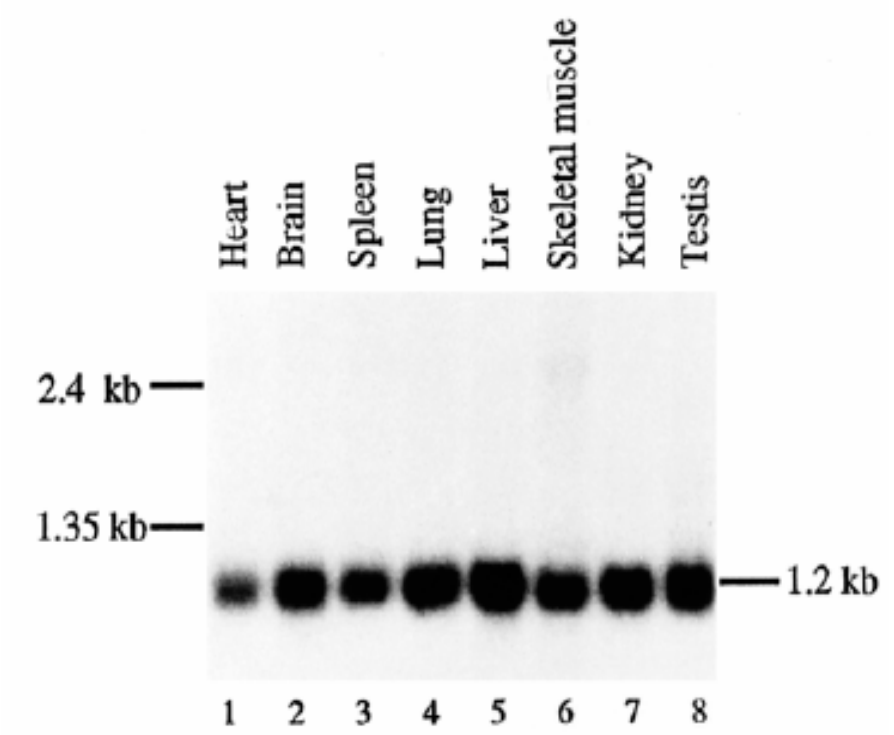

Figure 31. Syntaxin 8 transcript is ubiquitously expressed. A transcript of 1.2 kb is detected in all rat tissues examined by northern blot analysis of a rat mRNA mutiple tissue Northern blot containing 2 μg of poly (A)+ mRNA.

6.2.3 Syntaxin 8 is an integral membrane protein enriched in the endosomal fraction

The predicted cytoplasmic domain (residues 1-210) of syntaxin 8 was expressed in bacteria as a HisX6-tagged protein and purified HisX6-syntaxin 8 was used to immunize rabbits. Antibodies specific for syntaxin 8 were affinity-purified. The total membrane (TM) derived from rat liver was floated onto step sucrose gradient, resulting in the isolation of four membrane fractions (M fraction at the 1.25/1.1 M sucrose interface, G1 fraction at the 1.1/1.0 M sucrose interface, G2 fraction at the 1.0/0.8 M sucrose interface, and EM fraction at the 0.8/0.25 M sucrose interface). 20 μg of TM, M, G1, and G2 as well as 5 μg of EM fractions were analysed by immunoblot to detect syntaxin 8, GS28 (Subramaniam et al., 1995, 1996), cell surface asialoglycoprotein receptor subunits R2 and R3 (Spiess and Lodish, 1985), endosomal syntaxin 7 (Wang et al., 1997; Wong et al., 1998) and lysosomal integral membrane protein Lamp2/lgp96/lgpB/LIMPIV/lgp110 (Sandoval and Bakke, 1994). As shown in Fig. 32, GS28 is enriched in G1 and G2 fractions and to a lesser extent in the EM fraction. Asialoglycoprotein receptor subunits R2 and R3 are similarly enriched in the G1 and G2 fractions. Although the endosomal syntaxin 7 is also enriched in G1 and G2, it is about four times more enriched in the EM fraction as compared to the G1 and G2 fractions as four times less proteins of the EM fraction was analysed. A 27 kDa protein was detected with syntaxin 8 antibodies and detection of this protein was abolished by pre-incubation of antibodies with recombinant syntaxin 8 but not with other recombinant proteins (such as syntaxin 7; data not shown). As seen, syntaxin 8 is also about four times more enriched in the EM fraction than the G1 and G2 fractions. The lysosomal Lamp2 is more enriched in the G2 and EM fractions. These results indicate that syntaxin 8 is enriched in fractions that are also enriched for

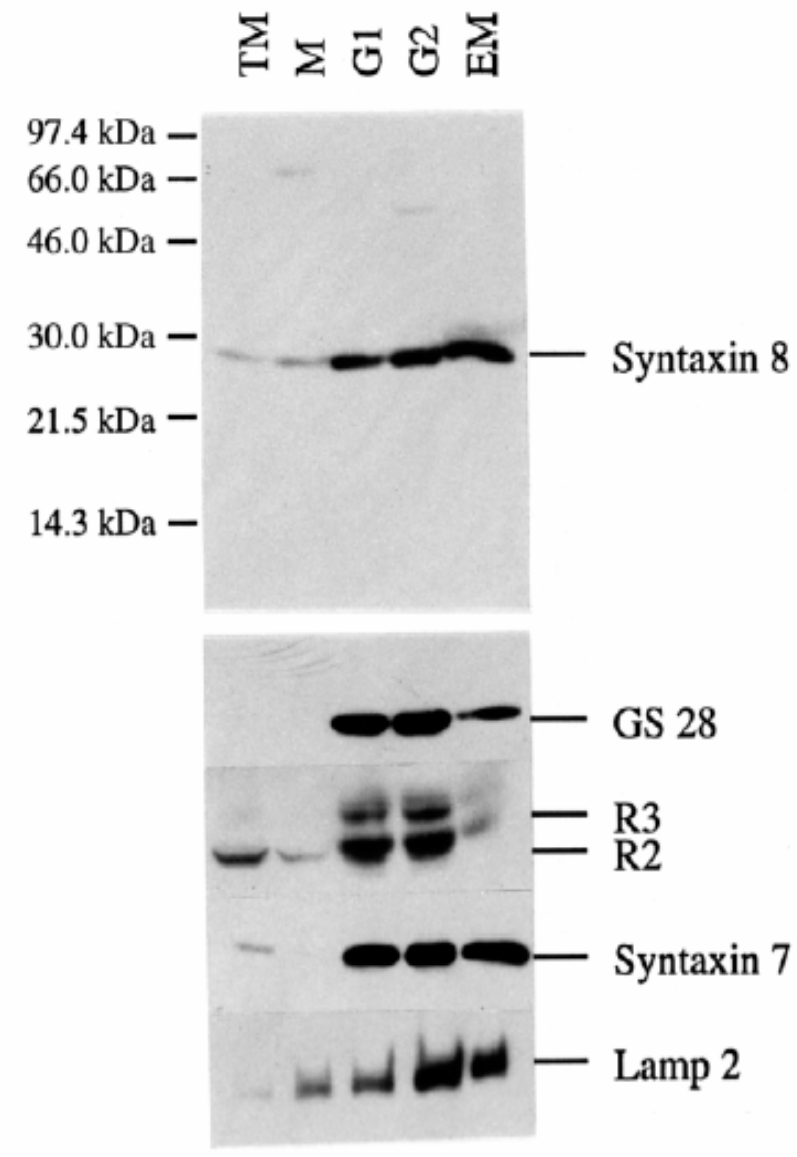

Figure 32. Syntaxin 8 is a 27 kDa protein enriched in the endosomal fraction. 20 μg of total (TM), microsomal (M), Golgi (G1 and G2), and 5 μg of endosomal (EM) fractions were analyzed by immunoblot to detect syntaxin 8, GS28, asialoglycoprotein receptor subunits R2 and R3, syntaxin 7 and lamp-2.

markers of the endosomal pathway.

As predicted from the derived amino acid sequence, syntaxin 8 is most likely an integral membrane protein. When a membrane fraction enriched in the Golgi, endosome and lysosome (GEM fraction in the 1.1/0.5 M sucrose interface) was extracted with various reagents, it was found that syntaxin 8 is not extracted with PBS, 1 M KCl, 2.5 M urea, or 0.15 M sodium bicarbonate (pH 11.5), but was effectively extracted by detergents such as 1% NP-40 or 1% DOC (Fig. 33). These results establish that syntaxin 8 is indeed an integral membrane protein.

6.2.4 Syntaxin 8 behaves as a SNARE

The common property of known SNAREs is that they can be incorporated into SNARE complexes with a sedimentation coefficient of 20S in the presence of NSF and α-SNAP under conditions that prevent ATP hydrolysis by NSF (Söllner et al., 1993; Subramaniam et al., 1996). To provide evidence that syntaxin 8 is indeed a SNARE, we have investigated whether syntaxin 8 also possess this property (Fig. 34A). When the GEM membrane extract was resolved with a glycerol gradient, syntaxin 8 was found to have a sedimentation coefficient of 7-8 S (upper row). In the presence of NSF and α-SNAP, under conditions that prevent ATP hydrolysis by NSF, syntaxin 8 was shifted to positions of about 20 S (middle row). However, in conditions that promote ATP hydrolysis of NSF, NSF and α-SNAP shifted syntaxin 8 to positions of about 5-6 S (lower row). Since NSF and α-SNAP are known to disrupt SNARE complexes (Subramaniam et al., 1997), the shifting of syntaxin 8 from 7-8 S to 5-6 S by NSF and α-SNAP in conditions that faciliate ATP hydrolysis suggest that syntaxin 8 in the membrane extract exists in a protein complex that is disassembled by NSF and α-SNAP. These effects of NSF and α-SNAP on syntaxin 8 are characteristic of known SNAREs and suggest that syntaxin 8 is indeed a SNARE.

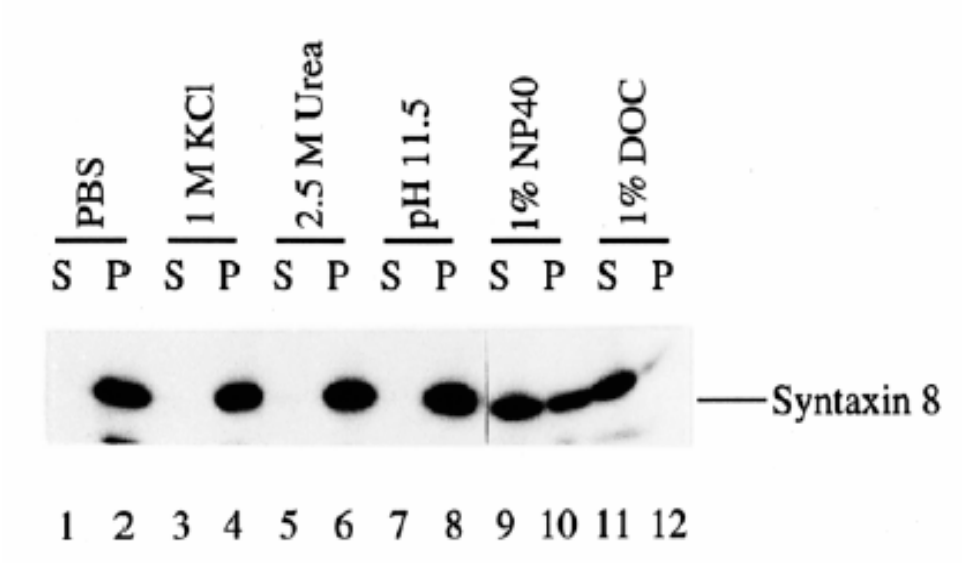

Figure 33. Syntaxin 8 is an integral membrane protein. 25 μg of Golgi/endosomal-enriched membrane fractions (GEM) were extracted with PBS, 1 M KCl, 2.5 M urea, 0.15 M sodium carbonate pH 11.5, 1% NP-40, or 1% sodium deoxycholate (DOC). After centrifugation, the supernatant (S) and pellets (P) were analyzed by immunoblot to detect syntaxin 8.

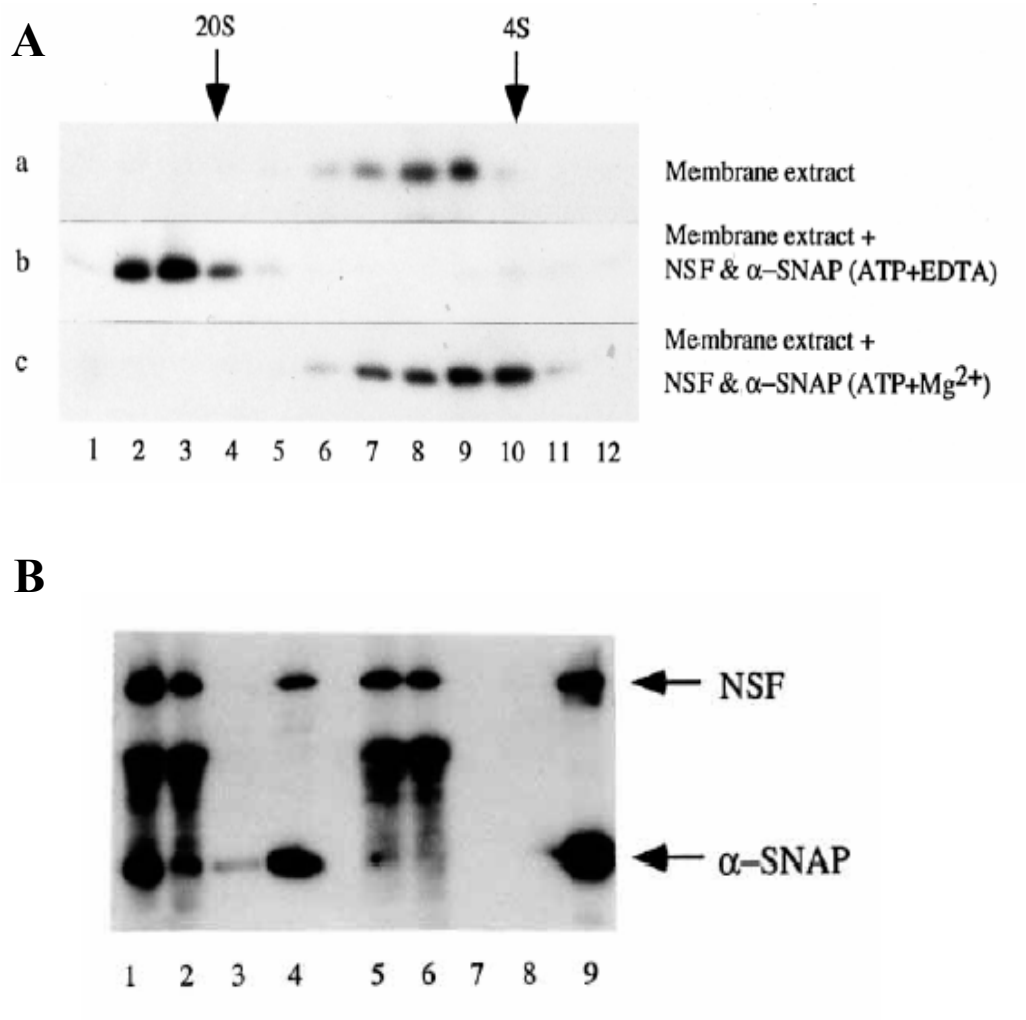

Figure 34. Syntaxin 8 is a SNAP Receptor. (A) GEM Triton X-100 extracts were incubated without (a) or with (b and c) NSF and α-SNAP in assembly (a and b) or disassembly buffer (c) and then separated on a 15-40% glycerol gradient. Gradient fractions were analyzed for the distribution of syntaxin 8 by immunoblotting. (B) The syntaxin 8 containing 20S fractions were immunoprecipitated with antibodies against syntaxin 8 (lanes 1-4) or control antibodies (lanes 5-8) under assembly conditions. The immunoprecipitates were eluted with assembly buffer (lanes 1, 3, 5, and 7) or disassembly buffer (lanes 2, 4, 6, and, 8). The eluates (lanes 3, 4, 7, and 8) and beads (lanes 1, 2, 5 and 6) were resolved by SDS-PAGE along with 100 ng of recombinant NSF and α-SNAP (lane 9) and analyzed for the presence of α-SNAP and NSF by immunoblot analysis.

To provide additional evidence for the notion that syntaxin 8 is a SNARE, the 20 S fractions were immunoprecipitated with antibodies against syntaxin 8 (lanes 1-4, Fig. 34B) or control rabbit IgG (lanes 5-8). The immunoprecipitates were eluted either in assembly buffer (lanes 1, 3, 5, 7) or disassembly buffer (lanes 2, 4, 6, 8). The beads (lanes 1, 2, 5, 6) and the eluates (lanes 3, 4, 7, 8), together with 100 ng of recombinant NSF and 100 ng of recombinant α-SNAP (lane 9) were resolved by SDS-PAGE and processed for immunoblotting to detect NSF and α-SNAP. Some non-specific association of NSF but not α-SNAP with control rabbit IgG was observed (lanes 5-6) and the associated NSF was not released from the control beads either in assembly (lane 7) or disassembly buffer (lane 8). Both NSF and α-SNAP were seen to be co-immunoprecipitated by antibodies against syntaxin 8 (lanes 1-2). Significantly, both NSF and α-SNAP could be released from the immunoprecipitates in disassembly buffer (lane 4) but not in assembly buffer (lane 3). These results suggest that syntaxin 8 does exist in a SNARE complex with NSF and α-SNAP in the 20S fraction and this SNARE complex can be dissociated in conditions that promote ATP hydrolysis by NSF, thus dissociating the SNARE complexes. Further evidence for syntaxin 8 as a SNARE came from our observation that a significant fraction of α-SNAP could be co-immunoprecipitated with syntaxin 8 from total NRK cell lysate (Fig. 35). Total NRK cell lysate was immunoprecipitated with control rabbit IgG (lanes 2, 4) and antibodies against syntaxin 8 (lanes 3, 5). The beads (lanes 2-3) and 10% of the supernatants (lanes 4-5), together with 10% of starting lysate (lane 1) were analysed by immunoblot to detect syntaxin 8 and α-SNAP. Syntaxin 8 is efficiently immunoprecipitated by its antibodies (lanes 3, 5) but not by control rabbit IgG (lanes 2, 4). Furthermore, a significant amount of α-SNAP was specifically co-immunoprecipitated by antibodies against syntaxin 8 (lane 3) but not by control IgG (lane 2). Given the fact that α-SNAP

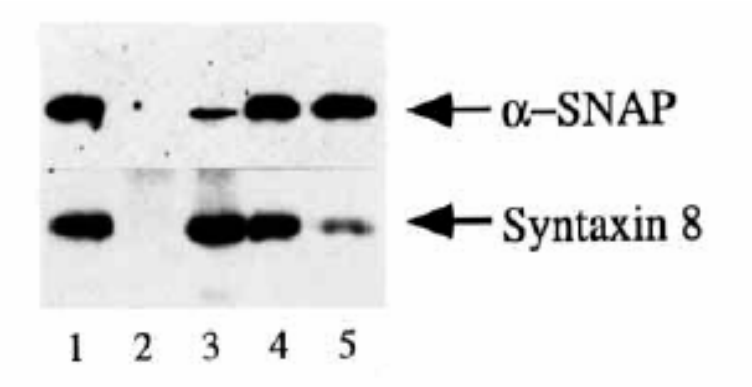

Figure 35. Co-immunoprecipitation of α-SNAP with syntaxin 8 from total NRK cell lysate. NRK cell lysate was incubated with antibodies against syntaxin 8 (lanes 3 and 5) or control rabbit IgG (lanes 2 and 4). The immunoprecipitates (lanes 2-3) and 10% of the supernatants (lanes 4-5), along with 10% of starting lysates (lane 1) were resolved by SDS-PAGE, transferred to a filter, and probed with antibodies against syntaxin 8 and α-SNAP.

is involved essentially in all the transport events and is associated with all the SNARE complexes in the cells, the clear co-immunoprecipitation of a significant amount of α-SNAP with syntaxin 8 from total cell lysate further supports that syntaxin 8 does function as a SNARE.

6.2.5 Co-immunoprecipitation of Vti1-rp1 with syntaxin 8

To investigate which SNAREs could potentially interact with syntaxin 8, we have performed a large-scale immunoprecipitation of detergent extract derived from rat liver Golgi/endosome-enriched membranes (Fig. 36). As shown, control rabbit IgG did not immunoprecipitate any specific proteins (lane 2), while several distinct polypeptides were specifically immunoprecipitated with antibodies against syntaxin 8 (lane 3). Since SNAREs typically have sizes below 40 kDa and the region below 40 kDa was resolved better than higher molecular mass region (lane 3), polypeptides with sizes of 40 kDa or less were individually excised out from the gel and subjected to trypsin digestion. Tryptic peptides were resolved by HPLC and purified peptides were subjected to protein microsequencing. It was revealed that the 40, 35, 32 and 28 kDa proteins represent γ-SNAP, α-SNAP, Vit1-rp1, and syntaxin 8, respectively. The co-immunoprecipitation of γ-SNAP, α-SNAP with syntaxin 8 in this experiment further supports the notion that syntaxin 8 is a SNARE. Vti1-rp1 is one of the two mammalian homologues (Xu et al., 1998) of yeast Vti1p, which functions in both retrograde intra-Golgi transport as well as several events in the endosomal pathway (von Mollard et al., 1999). The other mammalian homologue of Vti1p (Vit1-rp2) is associated with the Golgi apparatus and is apparently important for protein transport along the secretory pathway (Xu et al., 1998). Although detailed studies of Vit1-rp1 have not been reported, it was speculated that it may participate in the endosomal pathway (Xu et al., 1998). Consistent with this view, our preliminary studies suggest

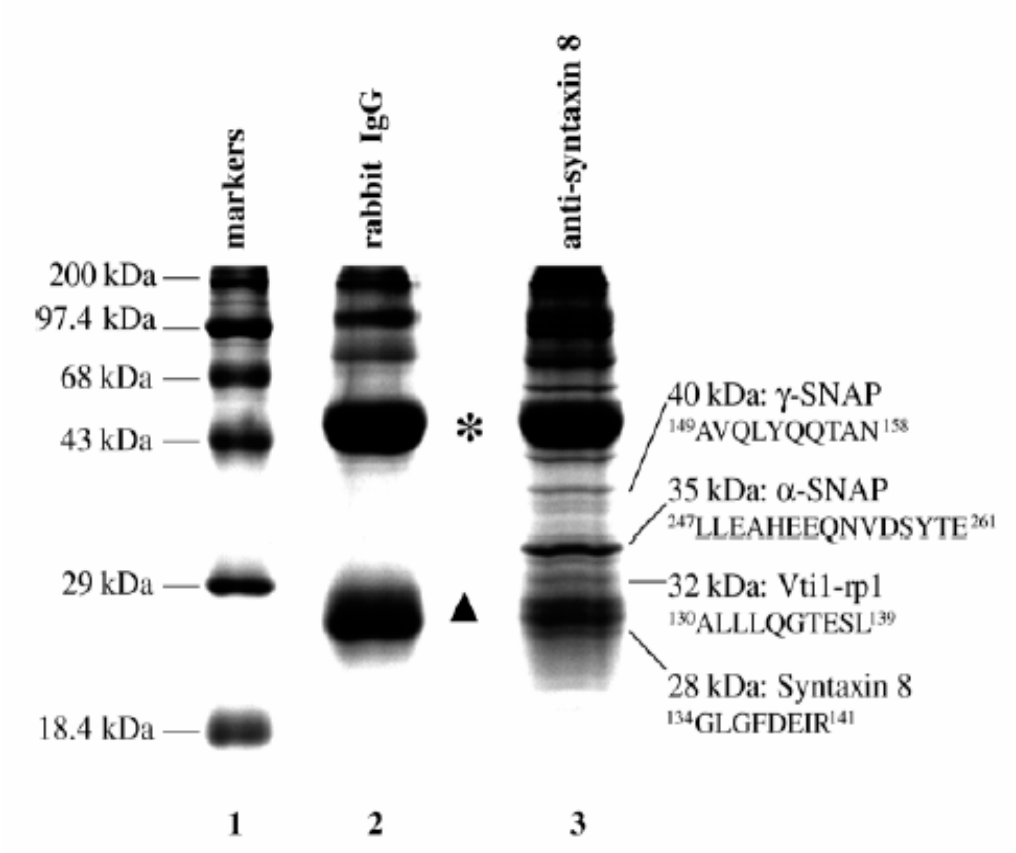

Figure 36. Co-immunoprecipitation of Vti1-rp1 with syntaxin 8. Detergent extract of Golgi/endosome-enriched membranes were incubated with beads containing control rabbit IgG (lane 2) or affinity-purified antibodies against syntaxin 8 (lane 3). The immunoprecipitates were resolved by SDS-PAGE and specific proteins with sizes of 40 kDa or less were analysed by amino acid microsequencing. The identities and the amino acid sequences of tryptic peptides are indicated.

that Vti1-rp1 is associated both with the Golgi apparatus (particularly the TGN) as well as endosomal compartments (Xu et al., unpublished observations).

6.2.6 Immunofluorescence microscopy showing colocalization of syntaxin 8 with early endosomal markers Rab5 and Rabaptin5

Using the affinity-purified antibodies against syntaxin 8, we investigated its subcellular localization by indirect immunofluorescence microscopy. Double-labeling of syntaxin 8 with several markers of the secretory and endocytotic pathways showed that syntaxin 8 (Fig. 37, a and d) colocalized well with Rab5 (b) and Rabaptin5 (e), two markers of the early endosome (Stenmark et al., 1995; Simonsen et al., 1998; Christoforidis et al., 1999). However, syntaxin 8 (g) did not colocalize with TGN38 (h), a marker for the Golgi apparatus and the trans-Golgi network (Luzio et al., 1990).

6.2.7 Immunogold labeling showing preferential localization of syntaxin 8 in the early endosome

The early and late endosomes of NRK cells were marked by internalized 5 nm and 15 nm gold-conjugated BSA, respectively. Cryosections of these cells were processed for immunogold labeling for syntaxin 8 and then examined by electron microscopy as described (Griffiths, 1993; Liou et al., 1996). Syntaxin 8 labeling was found in both the multivesicular (Fig. 38A and Fig. 39A, large arrowheads) as well as vesicular tubular structures (Fig. 38B) of the early endosome (EE, small arrows). To a lesser extent, syntaxin 8 labeling was also found in the late endosome (Fig. 39B), the cell surface and the coated pits (Fig. 39A). The immunogold labeling of syntaxin 8 was quantified (Fig. 40) and the highest density of syntaxin 8 labeling was found in the early endosome. Significant densities were found also in the late endosome and the plasma membrane. These results suggest that syntaxin 8 is preferentially enriched in the early endosome with some also present in structures preceding it (the plasma

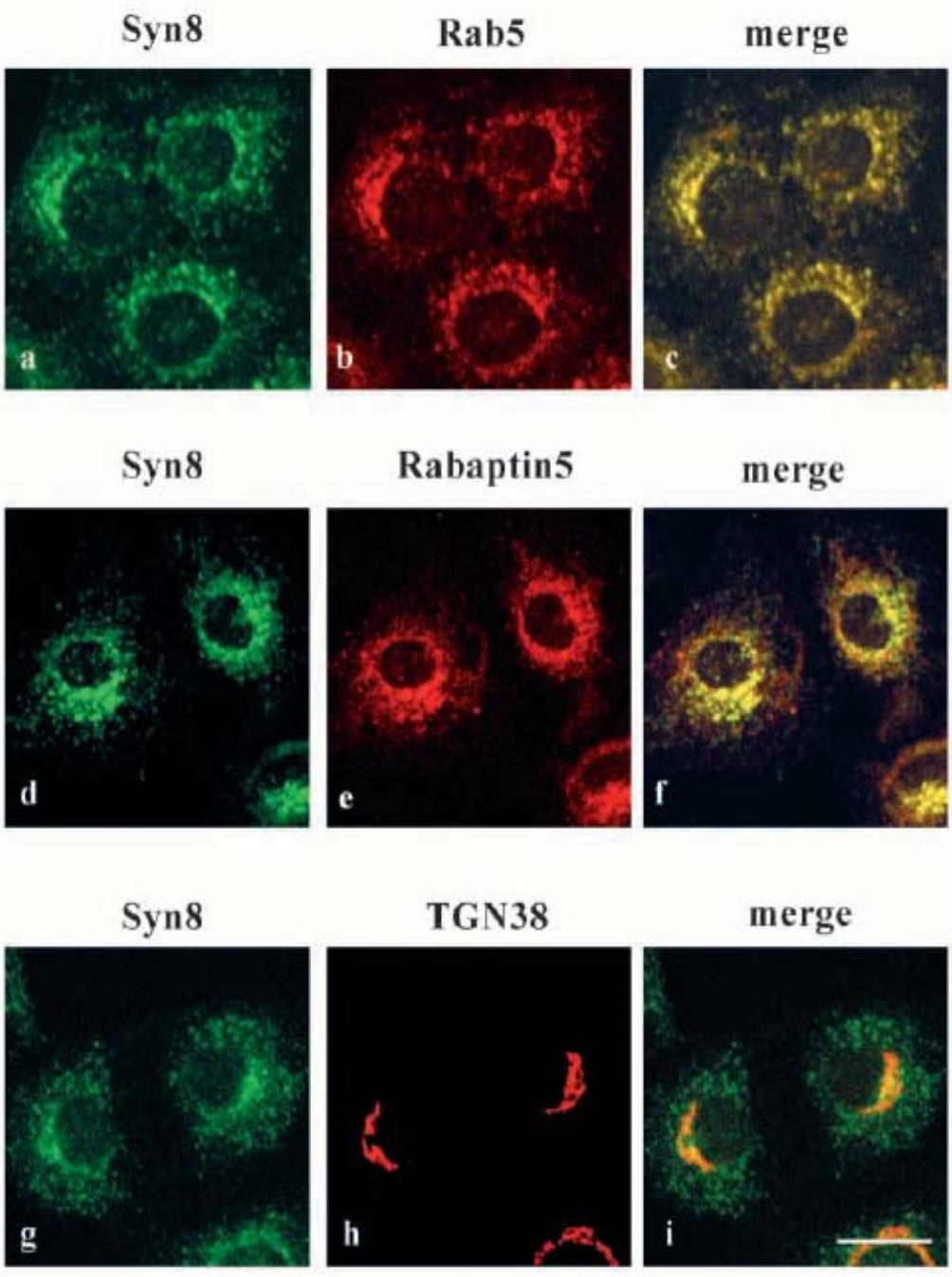

Figure 37. Colocalization of syntaxin 8 with markers of the early endosome. NRK cells were proceesed for double-labeling using antibodies against syntaxin 8 and Rab 5 (panels a-c), syntaxin 8 and rabaptin 5 (d-f), syntaxin 8 and TGN38 (g-i). Bar, 10 μm.

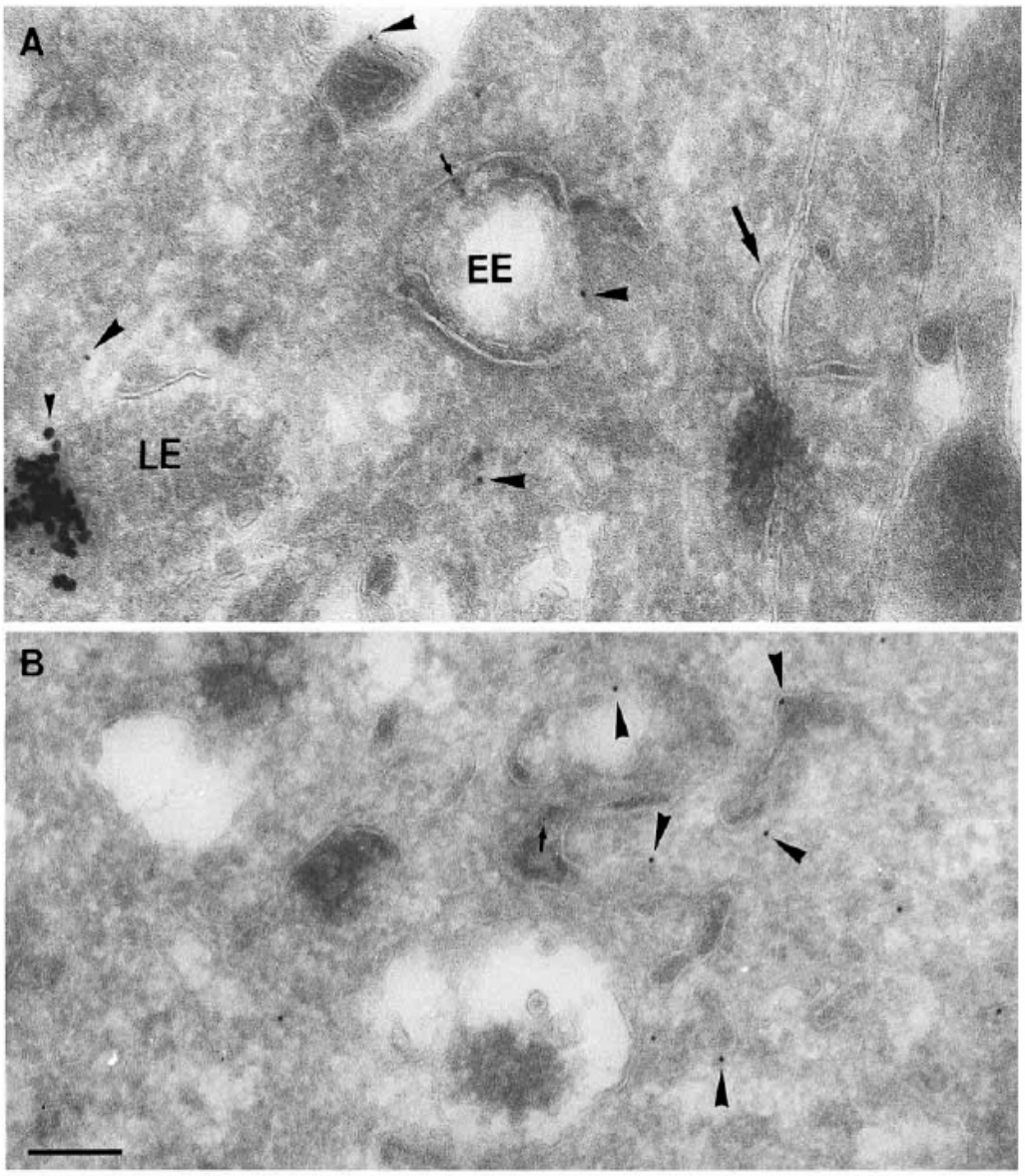

Figure 38. Preferential association of syntaxin 8 in the early endosomes. Cryosections from NRK cells with 15 nm gold-BSA (small arrowheads) internalized into late endocytic structures and 5 nm gold-BSA (small arrows) internalized into the early endosomes were labeled with antibodies against syntaxin 8 followed by 10 nm gold-Protein A (large arrowheads). (A) One gold particle for syntaxin 8 in an early endosome, the remaining syntaxin 8 labelling in A is probably in late endosomes. (B) Syntaxin 8 labelling over extended regions of early endosomes. The cell surface is indicated by the large arrow. Bar, 200 nm.

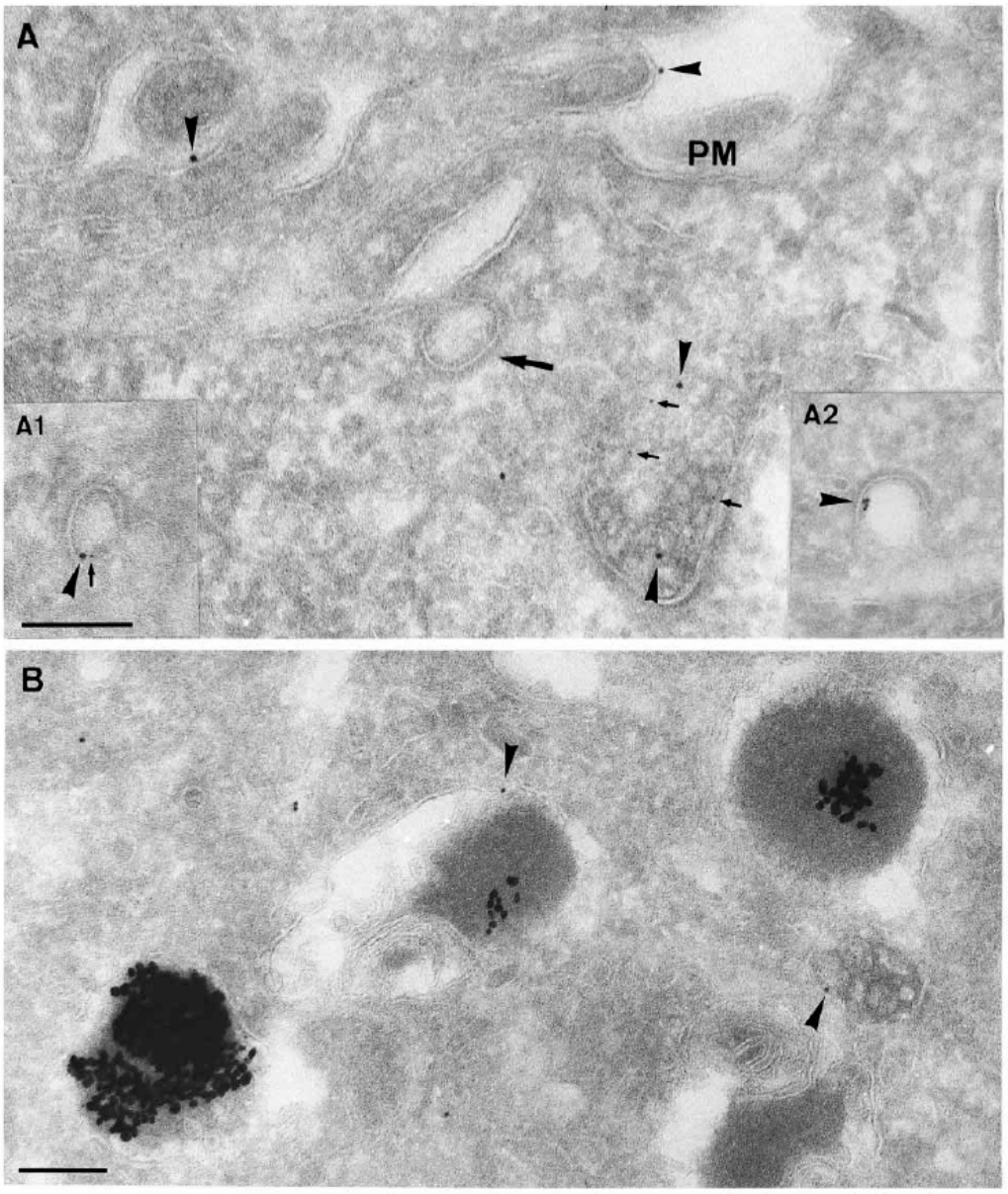

Figure 39. Some association of syntaxin 8 in the late endosome, cell surface and coated pits. Cryosections from NRK cells with 15 nm gold-BSA internalized into late endocytic structures and 5 nm gold-BSA (small arrows) internalized into the early endosomes were labeled with antibodies against syntaxin 8 followed by 10 nm gold-Protein A (large arrowheads). (A) Syntaxin 8 labeling on the plasma membrane (PM) and in an early endosome. A1 and A2 show two examples of syntaxin 8 labeling over coated pits. (B) Labeling over late endocytic structures. Bar, 200 nm.

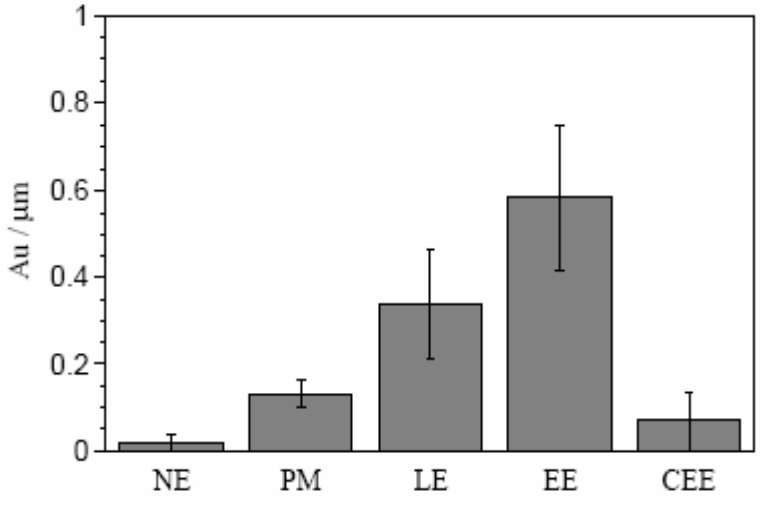

Figure 40. Quantification of immunogold labeling of syntaxin 8 Immunogold labeling of syntaxin 8 was highest in the early endosomes (EE) as compared with other regions namely nuclear envelope (NE), plasma membrane (PM), late endosomes (LE). Labeling in early endosome in the absence of syntaxin 8 antibodies was used as negative control (CEE). Au/µm = number of gold particle/µm.

membrane and the coated pits) and its downstream structure (the late endosome).

6.2.8 Colocalization of syntaxin 8 and Rab5 in the early endosome as revealed by double immunogold labeling

To gain additional support for the notion that syntaxin 8 is enriched in the early endosome, double immuno-gold labeling of syntaxin 8 and Rab5 was performed on sections derived from rapidly-frozen PC12 cells that have been processed for freeze-substitution and embeding in Lowicry HM-20 (Neuhaus et al., 1998). Ultra-thin sections were double-labeled with syntaxin 8 and Rab5 antibodies. The majority of syntaxin 8 labeling (large arrowheads) is found in the endosomal structures marked by Rab5 labeling (small arrowheads; Fig. 41). These results, taken together, establish that syntaxin 8 is indeed enriched in the early endosome.

6.3 Discussion

6.3.1 Syntaxin 8 is a novel SNARE protein

We have cloned full-length rat cDNAs encoding a novel member of the syntaxin family. It is a member of the syntaxin family based on the homology of its amino acid sequence with known members of the family, the presence of regions with the potential to form coiled-coil domains, and the existence of a carboxyl-terminal hydrophobic tail anchor. Its identity as a member of the syntaxin family is further supported by our demonstration that it behaves like a SNARE because it could be incorporated into a 20S SNARE complex by NSF and α-SNAP in conditions that promote formation of SNARE complexes and its complex in membrane extract is disrupted by NSF and α-SNAP under conditions that facilitate disassembly of SNARE complexes. The coimmunoprecipitation of a significant amount of α-SNAP by antibodies against syntaxin 8 from total NRK cell lysates further supports our findings.

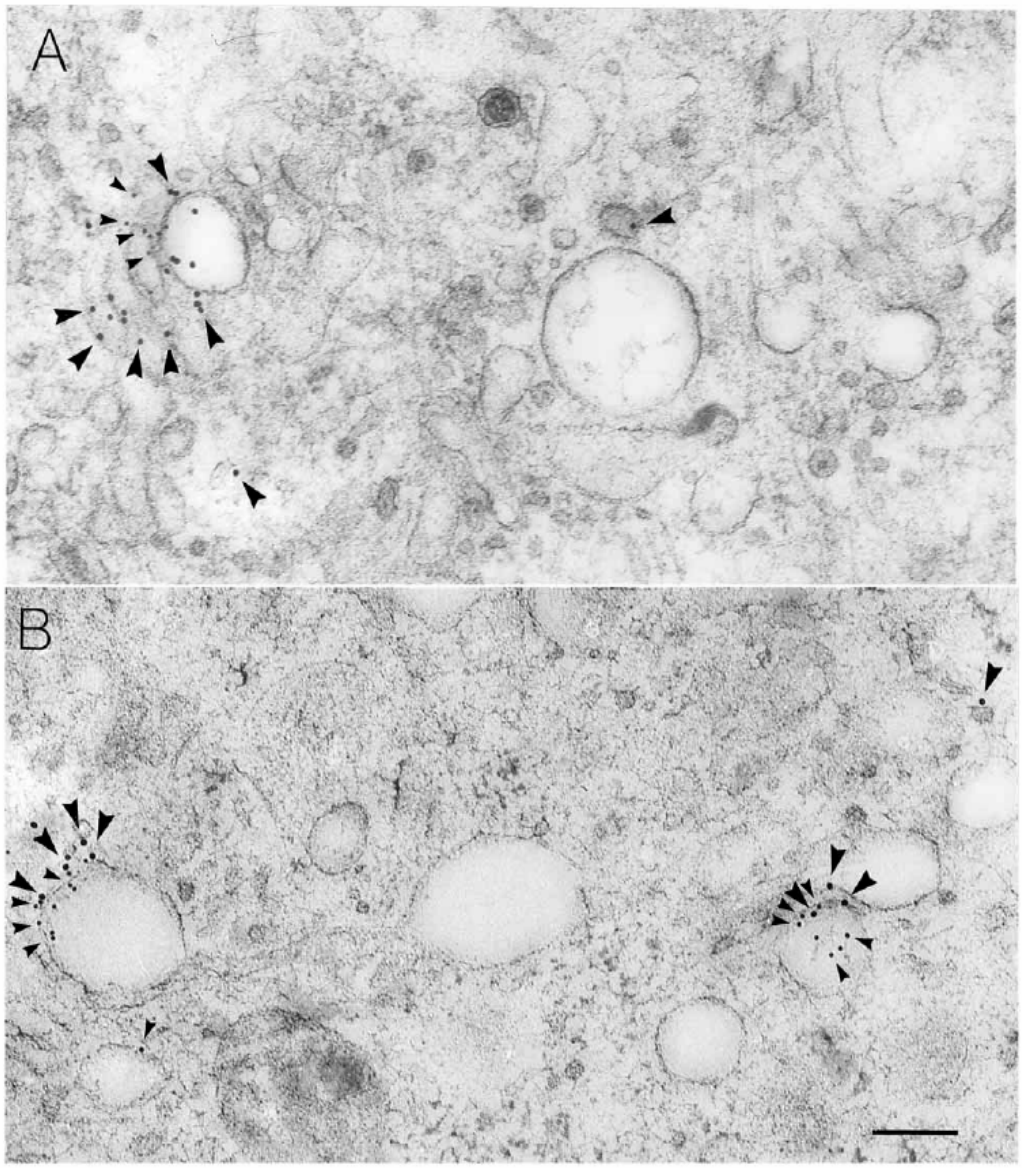

Figure 41. Double immunogold labeling of syntaxin 8 and Rab5 in the early endosome. Ultra-thin sections derived from rapidly-frozen PC12 cells were double-labeled with syntaxin 8 (followed by 14 nm gold-Protein A) and Rab5 antibodies (followed by 9 nm gold Protein A). The majority of syntaxin 8 labeling (large arrowheads) is found in the endosomal strucutres marked by Rab5 labeling (small arrowheads). Bar, 200 μm.

6.3.2 Association of syntaxin 8 with the early endosome

The endosomal pathway is generally believed to be composed of the early endosome, the late endosome and the lysosome, with the early endosome possibly containing distinct subcompartments (sorting endosome and recycling endosome; Gruenberg and Maxfield, 1995; Mellman, 1996). Although it was proposed that trafficking through the endocytic pathway is achieved through compartment maturation, recent studies favor the idea that early endosome and late endosome are distinct compartments. Endocytotic vesicles derived from the plasma membrane will fuse selectively with the early endosome and protein movement from the early to the late endosome is mediated by transport intermediates referred to as endosomal carrier vesicle (ECV) or multivesicular bodies (MVB). The late endosome and the lysosome are believed to be in a dynamic equilibrium and fuse to form hybrid organelles, which will regenerate to form the late endosome and the lysosome by fission (Bright et al., 1997). Several lines of evidence established that syntaxin 8 is preferentially associated with the early endosome. Firstly, immunoblot analysis of subcellular membrane fractions derived from rat liver showed that syntaxin 8 is present at highest levels in membrane fractions enriched for endosomal syntaxin 7 (Wang et al., 1997; Wong et al., 1998). Secondly, double-labeling of syntaxin 8 with several markers of the secretory and endocytotic pathways by indirect immunofluorescence microscopy revealed that syntaxin 8 colocalizes well with Rab5 and Rabaptin5, two well established proteins of the early endosomes (Stenmark et al., 1995; Simonsen et al., 1998; Christoforidis et al., 1999). Thirdly, immunogold labelling at the electron microscopy level revealed that highest levels of syntaxin 8 are present in the early endosome. To lesser extents, syntaxin 8 is also present in late endosome, the plasma membrane and coated pits. This observation is further supported by colocalization of

syntaxin 8 in early endosomal structures marked by Rab5 by immunogold electron microscopy.

6.3.3 Syntaxins associated with the endosomal pathway

Currently, several other syntaxins are known to exist in the endosomal pathway. Although syntaxin 7 is present in early endosome in A431 cells (Wong et al., 1998), it is also present in late compartments of the endosomal pathway in NRK cells (Wong et al., unpublished results). Syntaxin 12/13 is another endosomal syntaxin (Advani et al., 1998; Tang et al., 1998d) and a recent study suggests that it may participate in recycling of plasma membrane proteins via tubulovesicular recycling endosome (Prekeris et al., 1998). Syntaxin 11 is associated with the late endosomes (Valdez et al., 1999). The establishment of syntaxin 8 as an additional syntaxin associated with the endosomal pathway suggests that there exist many different docking/fusion events in the endosomal pathway and these three syntaxins may differentially participate in various docking and fusion events. Future studies aiming to establish the interacting partners for these endosomal syntaxins and to explore the various functional aspects in the endosomal pathway will enhance our understanding of the molecular mechanisms of membrane traffic in the endosomal pathway.

6.3.4 Existence of syntaxin 8 with vti1-rp1 in a SNARE complex

Steegmaier et al. (1998) and Thoreau et al. (1999) have also reported the cloning of human syntaxin 8. Based on the localization studies using epitope-tagged syntaxin 8 transiently expressed in transfected cells, Steegmaier et al. (1998) have suggested that syntaxin 8 is localized to the ER. Interestingly, syntaxin 8 was identified by Thoreau et al. using the regulator domain of the cystic fibrosis transmembrane conductance regulator in the yeast two-hybrid system (Thoreau et al., 1999). In our present study, we have investigated the subcellular localization of

endogenous syntaxin 8 using both immunofluorescence microscopy as well as immunogold labeling. Our results suggest that syntaxin 8 is preferentially localized to the early endosome. Significantly, we have revealed that syntaxin 8 exists in a SNARE complex with Vti1-rp1. Vti1-rp1 and Vti1-rp2 are two homologous proteins (Advani et al., 1998; Lupashin et al., 1998; von Mollard and Stevens, 1998; Xu et al., 1998) related to yeast Vti1p, which is essential for intra-Golgi retrograde transport (von Mollard et al., 1997). In addition, Vti1p participate in several events in the endocytotic pathway in yeast, including transport from the trans-Golgi to the endosome, direct transport from the trans-Golgi to the vacuole, and other transport events linked to the vacuole (von Mollard and Stevens, 1999). Vti1-rp2 is associated with the Golgi apparatus and participates in the biosynthetic pathway (Xu et al., 1998), while Vti1-rp1 is mainly associated with the TGN and the endosomes (Y. Xu et al., unpublished observations). The coexistence of syntaxin 8 and Vti1-rp1 in the same SNARE complex indicates that TGN derived vesicles containing Vti1-rp1 may dock and fuse with syntaxin 8-containing endosomal compartment through their interaction. Since the recycling compartment of the early endosome is the major endosomal site linked to the TGN, syntaxin 8 may have a function in the recycling early endosome.

CHAPTER 7

Conclusion

The main characteristic feature which distinguishes eukaryotic and prokaryotic cells is that eukaryotic cells maintain numerous membrane-bound compartments within which highly specialized processes are carried out with high efficiency. The integrity of each compartment is maintained through specific intracellular membrane transport processes which are mainly mediated via small membrane-bound transport carriers/vesicles. We have come a long way in understanding the complex process of intracellular membrane trafficking, mainly due to the tremendous rate of discovery of many novel proteins involved in the various transport pathways. In this thesis, I have reported the identification and characterization of several novel proteins and their mechanisms that would contribute to the increasing knowledge in this area. We made use of a simple general approach, which is the homologous searching of EST databases, in order to spot novel proteins involved in protein trafficking. We chose to focus on the mammalian system as many proteins in yeast have already been identified and we were interested to define the mechanisms of trafficking involved in the more complex eukaryotic system. The thesis thus centers around three proteins involved in many aspects of vesicle docking and fusion, two are implicated in the tethering process, Bet3 and Sec34/Cog3; while one is a SNARE associated with the early endosome, syntaxin 8.

7.1 The role of COG in secretory pathway

The Golgi apparatus is the central organelle of the exocytic pathway. It receives cargo from the ER via the intermediate compartment and further redirects cargo to different destinations by packaging them into specific transport vesicles. It also has an important role in retrograde transport as it recycles proteins back to the ER.

In general, transport between Golgi compartments is initiated by the formation of transport vesicles on one side of the Golgi membrane, mediated by complex interactions between small GTP-binding proteins, COPI coat components, cargo and cargo receptors. The transport vesicles dock to the other side of the Golgi membranes and subsequently fusion occurs. This entire process requires the participation of coat proteins, phospholipids, small and large G-proteins, Rabs, tethering molecules and SNAREs.

I undertook to study the mammalian homologue (Sec34/Cog3) of Sec34p, to ascertain its role in membrane traffic in mammalian cells, and its interacting partners. Antibodies prepared against N-terminal Sec34/Cog3 recognize a polypeptide of about 93 kDa and label the Golgi apparatus. The anti-Sec34/Cog3 antibodies also inhibited the transport of the VSVG from the ER to the Golgi in a dose-dependent way in a well-characterized semi intact cell assay. Of significance is our discovery that Sec34, GTC-90 and ldlBp/ldlCp are components of the same protein complex. GTC-90, ldlBp, Dor1 and Cod1 were efficiently and specifically co-immunoprecipitated from rat liver cytosol by antibodies against Sec34/Cog3. In addition, upon expression by transient transfection, myc-tagged ldlBp, ldlCp, Dor1, Cod1 and Cod2 was similarly co-immunoprecipitated by anti-Sec34/Cog3 antibodies. While our work on Sec34/Cog3 was in progress, other labs has also established that Sec34 exists in a multi-subunit complex. With the consensus of the various investigators studying this protein complex, it was renamed the conserved oligomeric Golgi (COG) complex. (Krieger et al., 1981; Kingsley et al., 1986; Podos et al., 1994; Wuestehube et al., 1996; VanRheenen et al., 1998, 1999; Walter et al., 1998, Chatterton et al., 1999; Spelbrink and Nothwehr, 1999; Kim et al., 1999, 2001; Whyte and Munro, 2001; Ram et al., 2002; Ungar et al., 2002, Suvorova et al., 2002, Loh and Hong, 2002; Farkas et al.,

2003). Sec34/Cog3 was identified initially as a human homologue of yeast Sec34p, which was identified in a genetic screen for genes whose products are important for ER-Golgi transport. GTC-90/Cog5 was isolated as a component of a protein complex that supports intra-Golgi transport *in vitro*, and LdlBp/Cog1 and LdlCp/Cog2 were identified by genetic approaches and are important for surface expression of LDL receptor and for Golgi structure and function. Since these are one and the same complex, the COG complex could therefore be an evolutionary conserved modulator of Golgi traffic.

COG has been assigned many roles. Mutations in COG subunits (Cog1-8) have been shown to affect the structure and function of the Golgi in yeast, *Drosophila melanogaster* sperm and mammalian somatic cells. Compromising COG function can cause defects in glycoconjugate synthesis, intracellular protein sorting, protein secretion and, in some cases, cell growth. COG mutations seem to affect the regulation, compartmentalization, or activity of multiple Golgi glycosylation enzymes and/or their substrate transporters without substantially disrupting secretion or endocytosis (Kingsley et al., 1986; Reddy and Krieger, 1989). The activities of these proteins depend on their proper intra-Golgi localization and appropriate intralumenal environments (e.g., pH) (Harris and Waters, 1996; Skrincosky et al., 1997; Axelsson et al., 2001; Martinez-Menarguez et al., 2001; Mironov et al., 2001; Opat et al., 2001; Berger, 2002; Roth, 2002; Puri et al., 2002; Zerfaoui et al., 2002). Thus, COG might play a role directly or indirectly in the transport to, retention at or retrieval of resident Golgi proteins to appropriate sites, or otherwise determine the Golgi's structure and/or lumenal environment (Kingsley et al., 1986). In summary, COG has been implicated in the localization, transport and/or function of multiple Golgi processing proteins.

A direct role for COG in controlling anterograde or retrograde membrane

trafficking was suggested by its ability to stimulate an in *vitro* intra-Golgi transport and glycosylation assay (Walter et al., 1998) and by genetic studies in yeast that have identified a large number of COG-interacting genes that encode proteins implicated in Golgi trafficking (VanRheenen et al., 1998, 1999; Kim et al., 1999, 2001; Spelbrink and Nothwehr, 1999; Whyte and Munro, 2001; Ram et al., 2002; Suvorova et al., 2002). Yeast COG has been proposed to function as a vesicle tethering factor in anterograde ER to Golgi trafficking (VanRheenen et al., 1998, 1999), in COPI-mediated retrograde trafficking (Ram et al., 2002; Suvorova et al., 2002), and in cargo sorting during exit from the ER (Morsomme and Riezman, 2002; Morsomme et al., 2003). The role of COG in concert with COPI in ensuring the proper trafficking and localization of COG-mutation sensitive Golgi resident integral membrane proteins (GEARs) was recently highlighted (Oka et al 2004). The abundance of GEARs were reduced in COG-deficient mutant cells and, in some cases, increased in COG-overexpressing cells. The current study of the mammalian COG complex helps to further define the function of this peripheral Golgi associated hetero-octameric protein complex in cells. It seems likely that a major function of COG is to work in concert with COPI to control retrograde trafficking (retrieval), thereby ensuring the proper intra-Golgi distribution and abundance of the GEARs. Thus, in the absence of normal COG function in the mutants, some GEARs are abnormally transported by retrograde traffic from the Golgi to the ER. The effects of COG on retrograde trafficking and proteasomal degradation of some GEARs may provide insights into the broader issue of how the steady state levels of Golgi-resident proteins are controlled. The GEAR/COG/COPI system provides new tools to study both this relatively unexplored area of membrane cell biology as well as other aspects of the structure and function of the Golgi apparatus.

In order to define the structural and molecular basis underlying the assembly/function of the COG complex, we undertook systematic investigation of the inter-molecular interactions between the various subunits. Our results suggest that COG4 serves as a core component of the complex by interacting directly with COG1, COG2, COG5 and COG7. COG3 is incorporated by its direct interaction with COG1 and COG2, while COG6 and COG8 do not interact with any individual subunit. Incorporation of COG6 into the complex requires the concerted interaction of both COG5 and COG7, while optimal incorporation of COG8 depends on the concerted interaction of COG5, COG6 and COG7. These results enabled us to present a working model for the assembly of the complex.

Very recently, an interesting study linking the mutation of the COG complex subunit COG7 with a lethal congenital disorder was reported (Wu et al., 2004). The mutation causes a fatal form of congenital disorders of glycosylation (CDG) in two siblings, as it impairs the integrity of the COG complex and alters Golgi trafficking, resulting in disruption of multiple glycosylation pathways. This provides evidence that the COG complex mediates functions essential for survival in humans. From this and the many reported studies on COG, it is evident that COG is an important modulator of Golgi function and that COG abnormalities probably affects many Golgi functions. COG deficiency may be considered as either a defect in glycosylation or in intracellular trafficking. It is also interesting to delineate the mechanism by which the mutations in the COG subunits causes the multiple glycosylation defects and lead to a lethal phenotype.

From the numerous publications that resulted from the study of the COG complex in the past two years, this topic is of great importance and has contributed significantly to the understanding of the role of a single complex in numerous areas of

intracellular protein trafficking. This opens up many exciting potential avenues of research to further dissect and understand the role of the COG complex. One possible future line of investigation would be to selectively "knock down" each subunit in mammalian cells and to study its effects.

7.2 The role of the Bet3-containing TRAPPI complex

Similar to the COG complex, the TRAPPI complex has been implicated with a role in the ER-Golgi tethering event. However, the similarity seems to end there. While the function of the COG complex seems multifold and more likely to be a general modulator of Golgi function, the role of the TRAPP complex seems more specific. The TRAPP complex has been proposed to act as a docking site at the early Golgi for COPII-generated vesicles that derive from the ER. In addition, TRAPP functions as a guanine nucleotide exchange factor (GEF) for Ypt1p, Ypt8p/Ypt31p, and Ypt11p/Ypt32p.

Our biochemical and functional analysis of the most conserved component of the TRAPP complex, Bet3 has established that it is involved in ER-Golgi transport. Moreover, action of Bet3 comes after COPII but before Rab1, α-SNAP and the EGTA-sensitive stage during ER-Golgi transport. Our results also show that mammalian Bet3 exists both in a free cytosolic form as well as part of a complex, as opposed to that in yeast lysates where no free pool of any subunits were detected.

The notion that TRAPP could potentially regulate several transport events and perhaps serve as a general transport factor in regulating vesicle traffic is still likely. In light of the fact that some of its subunits are structurally conserved across species while some are not, there remains the prospect that the TRAPP complex could interact with proteins involved in other transport machineries and potentiate further roles in the

various trafficking pathways. Future work shall be focused on establishing the detailed mechanical function of Bet3 pertaining to ER-Golgi transport. One question of interest is whether Bet3 or its associated complex may be a GEF for ER-Golgi Rab proteins.

7.3 The role of syntaxin 8 in endosomal SNARE complex

Assembly of the neuronal SNARE complex is mediated by the SNARE motifs. The bundle of four intertwined α-helices is contributed by syntaxin 1 and synaptobrevin 2, each contributing one helix while SNAP-25 contributes two helices. The characteristics of the neuronal SNARE complex was compared to that of a SNARE complex operating in the endosomal system (Antonin et al 2000). It was observed that the R-SNARE, endobrevin, forms a SNARE complex with the Q-SNAREs, syntaxin 7, syntaxin 8 and vti1b, which functions in the homotypic fusion of late endosomes. The features of the neuronal core complex therefore serves as a paradigm for all SNARE complexes and are essential for understanding SNARE function in membrane fusion.

With the genome sequence now known, all yeast and mammalian SNAREs have been identified. Yeast and mammalian SNAREs share about 20-30% sequence identities. We have demonstrated that syntaxin 8 is indeed an endosomal SNARE containing regions with the potential to form coiled-coil structures and that it co-precipitates with vti1b/vti1-rp1. Our studies are consistent with the view that syntaxin 8 and vti1b exists in the same endosomal SNARE complex. Substitution experiments, sequence and structural comparisons revealed that each protein occupies a unique position in the complex, with syntaxin 7 corresponding to syntaxin 1, and vti1b and syntaxin 8 corresponding to the N- and C-terminal domains of SNAP-25 respectively. The structure of the core complexes and their molecular mechanism in membrane

fusion is highly conserved between distant SNAREs (Antonin et al., 2000). Mice deficient in vti1b had reduced amounts of syntaxin 8 due to degradation of the syntaxin 8 protein, while the amounts of syntaxin 7 and endobrevin did not change. These data indicate that vti1b is specifically required for the stability of a single SNARE partner. Vti1b-deficient mice were viable and fertile (Atlaskin et al., 2003). Most vti1b-deficient mice were indistinguishable from wild-type mice and did not display defects in transport to the lysosome. However, 20% of the vti1b-deficient mice were smaller. Lysosomal degradation of an endocytosed protein was slightly delayed in hepatocytes derived from these mice. Multivesicular bodies and autophagic vacuoles accumulated in hepatocytes of some smaller vti1b-deficient mice. This suggests that other SNAREs can compensate for the reduction in syntaxin 8 and for the loss of vti1b in most mice by replacement with syntaxin 6 and vti1a respectively in an endobrevin and syntaxin 7-containing SNARE complex (Atlaskin et al., 2003). Further understanding of the role of syntaxin 8 in endosomal traffic may be obtained from future "knock down" analysis in cells as well as knockout experiments in mice. The studies presented here have helped to further define the molecules and mechanisms involved in transport of cargo and membrane components in the exocytic and endocytic pathways.

REFERENCES

Advani, R.J., Bae, H.R., Bock, J.B., Chao, D.S., Doung, Y.C., Prekeris, R., Yoo, J.S. and Scheller, R.H. (1998). Seven novel mammalian SNARE proteins localize to distinct membrane compartments. J. Biol. Chem. 273, 10317-10324.

Allan, B.B., and Balch, W.E. (1999). Protein sorting by directed maturation of Golgi compartments. Science 285, 63–66.

Altschul, S.F., Gish, W., Miller, W., Myers, E.W., and Lipman, D.J. (1990). Basic local alignment search tool. J. Mol. Biol. 215, 403–410.

Altschul, S.F., Madden, T.L, Schaffer, A.A, Zhang, J., Zhang, Z., Miller, W., and Lipman, D.J. (1997). Gapped BLAST and PSI-BLAST: a new generation of protein database search programs. Nucleic Acids Res. 25, 3389-3402.

Aridor, M., Weissman, J., Bannykh, S., Nuoffer, C., and Balch, W.E. (1998). Cargo selection by the COPII budding machinery during export from the ER. J. Cell Biol. 141, 61-70.

Atlashkin, V., Kreykenbohm, V., Eskelinen, E.L., Wenzel, D., Fayyazi, A., and Fischer, von Mollard G. (2003). Deletion of the SNARE vti1b in mice results in the loss of a single SNARE partner, syntaxin 8. Mol. Cell Biol. 23, 5198-5207.

Balch, W.E., McCaffery, J.M., Plutner, H., and Farquhar, M.G. (1994). Vesicular stomatitis virus glycoprotein is sorted and concentrated during export from the endoplasmic reticulum. Cell 76, 841–852

Barlowe, C., and Schekman, R. (1993). SEC12 encodes a guanine-nucleotide-exchange factor essential for transport vesicle budding from the ER. Nature 365, 347-349

Barlowe, C., Orci, L., Yeung, T., Hosobuchi, M., Hamamoto, S., Salama, N., Rexach, M.F., Ravazzola, M., Amherdt, M. and Schekman, R. (1994). COPII: a membrane coat formed by Sec proteins that drive vesicle budding from the endoplasmic reticulum. Cell 77, 895-907.

Barr, F. (2000). Vesicular transport. Essays Biochem 36, 37-46. Review

Barrowman, J., Sacher, M. and Ferro-Novick, S. (2000). TRAPP stably associates with the Golgi and is required for vesicle docking. EMBO J. 19, 862-869.

Beckers, C.J., and Balch, W.E. (1989). Calcium and GTP: essential components in vesicular trafficking between the endoplasmic reticulum and Golgi apparatus. J. Cell Biol. 108, 1245-1256.

Beckers, C.J., Keller, D.S., and Balch, W.E. (1987). Semi-intact cells permeable to macromolecules: use in reconstitution of protein transport from the endoplasmic reticulum to the Golgi complex. Cell 50, 523-534.

Bennett, M.K., Calakos, N. and Scheller, R.H. (1992). Syntaxin: a synaptic protein implicated in docking of synaptic vesicles at presynaptic active zones. Science 257, 255-259.

Bennett, M.K., Garcia-Arraras, J.E., Elferink, L.A., Peterson, K., Fleming, A.M., Hazuka, C.D. and Scheller, R.H. (1993). The syntaxin family of vesicular transport receptors. Cell 74, 863-873.

Bennett, M.K. (1995). SNAREs and the specificity of transport vesicle targeting. Curr. Opin. Cell Biol. 7, 582-586.

Blasi, J., Chapman, E.R., Yamasaki, S., Binz, T., Niemann, H. and Jahn, R. (1993). Botulinum neurotoxin C1 blocks neurotransmitter release by means of cleaving HPC-1/syntaxin. EMBO J. 12, 4821-4828.

Bock, J.B., Matern, H.T., Peden, A.A., and Scheller, R.H. (2001). A genomic perspective on membrane compartment organization. Nature 409, 839-41.

Bock, J.B. and Scheller, R.H. (1997). Protein transport. A fusion of new ideas. Nature 387, 133-135.

Bock, J.B., Klumperman, J., Davanger, S. and Scheller, R.H. (1997). Syntaxin 6 functions in trans-Golgi network vesicle trafficking. Mol. Biol. Cell 8, 1261-1271.

Bock, J.B., Lin, R.C. and Scheller, R.H. (1996). A new syntaxin family member implicated in targeting of intracellular transport vesicle. J. Biol. Chem. 271, 17961-17965.

Bonifacino, J.S. and Lippincott-Schwartz, J. (2003). Coat proteins: shaping membrane transport. Nat Rev Mol Cell Biol 4, 409-414.

Bonifacino, J.S., and Glick, B.S. (2004). The mechanisms of vesicle budding and fusion. Cell 116, 153-166.

Brennwald, P. and Novick, P. (1993). Interactions of three domains distinguishing the Ras-related GTP-binding proteins Ypt1 and Sec4. Nature 362; 560-563.

Bright, N.A., Reaves, B.J., Mullock, B.M. and Luzio, J.P. (1997). Dense core lysosomes can fuse with late endosomes and are re-formed from the resultant hybrid organelles. J. Cell Sci. 110, 2027-2040.

Bucci, C., Parton, R.G., Mather, I. H., Stunnenberg, H., Simons, K., Hoflack, B., and Zerial, M. (1992). The small GTPase rab5 functions as a regulatory factor in the early endocytic pathway. Cell 70, 715-728.

Callaghan, J., Simonsen, A., Gaullier, J.M., Toh, B.H., and Stenmark, H. (1999). The endosome fusion regulator early-endosomal autoantigen 1 (EEA1) is a dimer. Biochem. J. 338, 539-43.

Cao, X., Ballew, N., and Barlowe, C. (1998). Initial docking of ER-derived vesicles requires Uso1p and Ypt1p but is independent of SNARE proteins. EMBO J. 17, 2156–2165.

Chatterton, J.E., Hirsch, D., Schwartz, J.J., Bickel, P.E., Rosenberg, R.D., Lodish, H.F., and Krieger, M. (1999). Expression cloning of LDLB, a gene essential for normal Golgi function and assembly of the ldlCp complex. Proc. Natl. Acad. Sci. U. S. A. 96, 915–920.

Chen, Y.A. and Scheller, R.H. (2001). SNARE-mediated membrane fusion. Nat. Rev. Mol. Cell Biol. 2, 98-106. Review.

Christoforidis, S., McBride, H.M., Burgoyne, R.D. and Zerial, M. (1999). The Rab5 effector EEA1 is a core component of endosome docking. Nature 397, 621-625.

Clary, D.O., Griff, I.C. and Rothman, J.E. (1990). SNAPs, a family of NSF attachment proteins involved in intracellular membrane fusion in animals and yeast. Cell 61, 709-721.

Conibear, E., and Stevens, T.H. (2000). Vps52p, Vps53p, and Vps54p form a novel multisubunit complex required for protein sorting at the yeast late Golgi. Mol. Biol. Cell. 11, 305-323.

Conibear, E., Cleck, J.N., and Stevens, T.H. (2003). Vps51p mediates the association of the GARP (Vps52/53/54) complex with the late Golgi t-SNARE Tlg1p. Mol. Biol. Cell. 14, 1610-1623.

Dascher, C., and Balch, W.E. (1996). Mammalian Sly1 regulates syntaxin 5 function in endoplasmic reticulum to Golgi transport. J. Biol. Chem. 271, 15866-15869.

Davidson, H.W., and Balch, W.E. (1993). Differential inhibition of multiple vesicular transport steps between the endoplasmic reticulum and trans Golgi network. J Biol. Chem. 268, 4216-4226.

Donaldson, J.G., Cassel, D., Kahn, R.A., and Klausner, R.D. (1992). ADP-ribosylation factor, a small GTP-binding protein, is required for binding of the coatomer protein beta-COP to Golgi membranes. Proc. Natl. Acad. Sci. USA 89, 6408-6412.

Donaldson, J.G., Kahn, R.A., Lippincott-Schwartz, J., and Klausner, R.D. (1991). Binding of ARF and beta-COP to Golgi membranes: possible regulation by a trimeric G protein. Science 254, 1197-1199.

Dumas, J.J., Merithew, E., Sudharshan, E., Rajamani, D., Hayes, S., Lawe, D., Corvera, S., and Lambright, D.G. (2001). Multivalent endosome targeting by homodimeric EEA1. Mol. Cell 8, 947–58.

Dunn, B., Stearns, T., Botstein, D. (1993). Specificity domains distinguish the Ras-related GTPases Ypt1 and Sec4. Nature 362, 563-565.

Espenshade, P., Gimeno, R.E., Holzmacher, E., Teung, P. and Kaiser, C.A. (1995). Yeast SEC16 gene encodes a multidomain vesicle coat protein that interacts with Sec23p. J. Cell Biol. 131, 311-324

Farkas, R.M., Giansanti, M.G., Gatti, M., and Fuller, M.T. (2003). The Drosophila Cog5 homologue is required for cytokinesis, cell elongation, and assembly of specialized Golgi architecture during spermatogenesis. Mol. Biol. Cell. 14, 190-200.

Farquhar, M.G., and Palade, G.E. (1981). The Golgi apparatus (complex) –(1954-1981)-from artifact to center stage. J. Cell Bio. 91, 77s-103s.

Fasshauer, D., Sutton, R.B., Brunger, A.T., and Jahn, R. (1998). Conserved structural features of the synaptic fusion complex: SNARE proteins reclassified as Q- and R-SNAREs. Proc. Natl. Acad. Sci. USA 95, 15781-86.

Faundez, V., Horng, J.T., and Kelly, R.B. (1998). A function for the AP3 coat complex in synaptic vesicle formation from endosomes. Cell 93, 423-32.

Ferro-Novick, S. and Jahn, R. (1994). Vesicle fusion from yeast to man. Nature 370, 191-193. Review.

Ferro-Novick, S. and Novick, P. (1993). The role of GTP-binding proteins in transport along the exocytotic pathway. Annu. Rev. Cell Biol. 9, 575-599.

Gillingham, A.K., and Munro, S. (2003). Long coiled-coil proteins and membrane traffic. Biochim. Biophys. Acta. 1641, 71-85. Review.

Gimeno, R.E., Espenshade, P. and Kaiser, C.A. (1995). SED4 encodes a yeast endoplasmic reticulum protein that binds Sec16p and participates in vesicle formation. J. Cell Biol. 131, 325-338.

Glickman, J.N., Conibear, E., and Pearse, B.M. (1989). Specificity of binding of clathrin adaptors to signals on the mannose-6-phosphate/insulin-like growth factor II receptor. EMBO J. 8, 1041-1047.

Gorvel, J., Chavrier, P., Zerial, M., and Gruenberg, J. (1991). Rab5 controls early endosome fusion in vitro. Cell 64, 915-925.

Gotte, M., and von Mollard, G.F. (1998). A new beat for the SNARE drum. Trends Cell Biol. 8, 215-218. Review.

Graham, T.R. and Emr, S.D. (1991). Compartmental organization of Golgi specific protein modification and vacuolar protein sorting events defined in a yeast sec18 (NSF) mutant. J. Cell Biol. 114, 207-218.

Griff, I.C., Schekman, R., Rothman, J.E. and Kaiser, C.A. (1992). The yeast SEC17 gene product is functionally equivalent to mammalian α-SNAP protein. J. Biol. Chem. 267, 12106-12115.

Griffiths, G. (1993). Cryo and Replica techniques for immunolabelling. In Fine Structure Immunocytochemistry, 137-203. Springer Verlag, Berlin.

Grindstaff, K.K., Yeaman, C., Anandasabapathy, N., Hsu, S.C., Rodriguez-Boulan, E., Scheller, R.H., and Nelson, W.J. (1998). Sec6/8 complex is recruited to cell-cell contacts and specifies transport vesicle delivery to the basal-lateral membrane in epithelial cells. Cell 93, 731-40.

Gruenberg, J. and Maxfield, F.R. (1995). Membrane transport in the endocytic pathway. Curr. Opin. Cell Biol. 7, 552-563.

Guan, K.L., and Dixon, J.E. (1991). Eukaryotic proteins expressed in Escherichia coli: an improved thrombin cleavage and purification procedure of fusion proteins with glutathione S-transferase. Anal. Biochem. 192, 262-267.

Guo, Q., Vasile, E., and Krieger, M. (1994). Disruptions in Golgi structure and membrane traffic in a conditional lethal mammalian cell mutant are corrected by epsilon-COP. J. Cell Biol. 125, 1213–1224.

Guo, W., Roth, D., Walch-Solimena, C., and Novick, P. (1999). The exocyst is an effector for Sec4p, targeting secretory vesicles to sites of exocytosis. EMBO J. 18, 1071-1080.

Guo, W., Sacher, M., Barrowman, J., Ferro-Novick, S., and Novick, P. (2000). Protein complexes in transport vesicle targeting. Trends Cell Biol. 10, 251-55

Hammer, J.A. 3rd, and Wu, X.S. (2002). Rabs grab motors: defining the connections between Rab GTPases and motor proteins. Curr. Opin. Cell Biol. 14, 69–75.

Hata, Y., Slaughter, C.A., and Sudhof, T.C. (1993). Synaptic vesicle fusion complex contains unc-18 homologue bound to syntaxin. Nature 366, 347-351.

Hauri, H.P., Kappeler, F., Andersson, H., and Appenzeller, C. (2000). ERGIC-53 and traffic in the secretory pathway. J. Cell Sci. 113, 587–596.

Hay, J.C., and Scheller, R.H. (1997). SNAREs and NSF in targeted membrane fusion. Curr. Opin. Cell Biol. 9, 505-512.

Hay, J.C., Chao, D.S., Kuo, C.S. and Scheller, R.H. (1997). Protein interactions regulating vesicle transport between the endoplasmic reticulum and Golgi apparatus in mammalian cells. Cell 89, 147-158.

Hay, J.C., Harald, H. and Scheller, R.H. (1996). Mammalian vesicle trafficking proteins of the endoplasmic reticulum and Golgi apparatus. J. Biol. Chem. 271, 5671-5679.

Hobbie, L., Fisher, A.S., Lee, S., Flint, A., and Krieger, M. (1994). Isolation of three classes of conditional lethal Chinese hamster ovary cell mutants with temperature-dependent defects in low density lipoprotein receptor stability and intracellular membrane transport. J. Biol. Chem. 269, 20958–20970.

Hobbs, H.H., Brown, M.S., and Goldstein, J.L. (1992). Molecular genetics of the LDL receptor gene in familial hypercholesterolemia. Hum. Mutat. 1, 445–466. Review.

Holthuis, J.C., Nichols, B.J., Dhruvakumar, S., Pelham, H.R. (1998). Two syntaxin homologues in the TGN/endosomal system of yeast. EMBO J. 17, 113-126.

Hong, W. (1996). Protein Trafficking along the Exocytotic Pathway. R. G. Landes Company, Austin, USA.

Hong, W. (1998) Protein transport from the endoplasmic reticulum to the Golgi apparatus. J. Cell Sci. 111, 2831–2839. Review.

Horn, M., and Banting, G. (1994). Okadaic acid treatment leads to a fragmentation of the trans-Golgi network and an increase in expression of TGN38 at the cell surface. Biochem. J. 301, 69-73.

Hsu, S.C., Hazuka, C.D., Roth, R., Foletti, D.L., Heuser, J., and Scheller, R.H. (1998). Subunit composition, protein interactions, and structures of the mammalian brain sec6/8 complex and septin filaments. Neuron 20, 1111-1122.

Hsu, S.C., Ting, A.E., Hazuka, C.D., Davanger, S., Kenny, J.W., Kee, Y., and Scheller, R.H. (1996). The mammalian brain rsec6/8 complex. Neuron 17, 1209-1219.

Huber, L.A., Pimplikar, S., Parton, R.G., Virta, H., Zerial, M., and Simons, K. (1993). Rab8, a small GTPase involved in vesicular traffic between the TGN and the basolateral plasma membrane. J. Cell Biol. 123, 35-45.

Iryna, M.E., Kazuki, H., Yoshiaki, M., Fumitoshi, I., and Yu, Y. (2000). Synbindin, A Novel Syndecan-2–binding Protein in Neuronal Dendritic Spines. J. Cell Biol. 151, 53-68

Jackson, T. (1998). Transport vesicles: coats of many colors. Curr. Biol. 8, R609-12.

Jahn, R., Lang, T., and Sudhof, T.C. (2003). Membrane fusion. Cell 112, 519-533 Review.

Jang, S.B., Kim, Y.G., Cho, Y.S., Suh, P.G., Kim, K.H., and Oh, B.H. (2002). Crystal structure of SEDL and its implications for a genetic disease spondyloepiphyseal dysplasia tarda. J. Biol. Chem. 277, 49863-49869.

Jedd, G., Mulholland, J., and Segev, N.(1997). Two new Ypt GTPases are required for exit from the yeast trans-Golgi compartment. J. Cell Biol. 137, 563-580.

Jiang, Y., Scarpa, A., Zhang, L, Stone, S., Feliciano, E., and Ferro-Novick, S. (1998). A high copy suppressor screen reveals genetic interactions between BET3 and a new gene. Evidence for a novel complex in ER-to-Golgi transport. Genetics 149, 833-841.

Jones, S., Newman, C., Liu, F. and Segev, N. (2000). The TRAPP complex is a nucleotide exchanger for Ypt1 and Ypt31/32. Mol. Biol. Cell.11, 4403-4411.

Kavalali, E.T. (2002). SNARE interactions in membrane trafficking: a perspective from mammalian central synapses. Bioassays 24, 926-936. Review.

Kee, Y., Yoo, J.S., Hazuka, C.D., Peterson, K.E., Hsu, S.C., and Scheller, R.H. (1987). Subunit structure of the mammalian exocyst complex. Proc. Natl. Acad. Sci. 94, 14438-14443.

Kim, D.W., Massey, T., Sacher, M., Pypaert, M., and Ferro-Novick, S. (2001). Sgf1p, a new component of the Sec34p/Sec35p complex. Traffic 2, 820–830.

Kim, D.W., Sacher, M., Scarpa, A., Quinn, A.M., and Ferro-Novick, S. (1999). High-copy suppressor analysis reveals a physical interaction between Sec34p and Sec35p, a protein implicated in vesicle docking. Mol. Biol. Cell 10, 3317–3329.

Kingsley, D.M., Kozarsky, K.F., Hobbie, L., and Krieger, M. (1986). Reversible defects in O-linked glycosylation and LDL receptor expression in a UDP-Gal/UDP-GalNAc 4-epimerase deficient mutant. Cell 44, 749–759.

Kingsley, D.M., Kozarsky, K.F., Segal, M., and Krieger, M. (1986). Three types of low density lipoprotein receptor-deficient mutant have pleiotropic defects in the synthesis of N-linked, O-linked, and lipid-linked carbohydrate chains. J. Cell Biol. 102, 1576–1585.

Kirchhausen, T. (1993). Coated pits and vesicles-Sorting it all out. Curr. Opin. Struct. Biol. 3, 182-188.

Kirchhausen, T. (2000). Three ways to make a vesicle. Nat. Rev. Mol. Cell Biol. 1, 187-198.

Kozarsky, K.F., Brush, H.A., and Krieger, M. (1986). Unusual forms of low density lipoprotein receptors in hamster cell mutants with defects in the receptor structural gene. J. Cell Biol. 102, 1567–1575.

Lafreniere, R.G., Kibar, Z., Rochefort, D.L., Han, F.Y., Fon, E.A., Dube, M.P., Kang, X., Baird, S., Korneluk, R.G., Rommens, J.M., and Rouleau, G.A. (1997). Genomic structure of the human GT334 (EHOC-1) gene mapping to 21q22.3. Gene. 198, 313-321.

Le Borgne, R., and Hoflack, B. (1998). Protein transport from the secretory to the endocytic pathway in mammalian cells. Biochim. Biophys. Acta. 1404, 195-209.

Letourneur, F., Gaynor, E.C., Hennecke, S., Demolliere, C., Duden, R., Emr, S.D., Riezman, H. and Cosson, P. (1994). Coatomer is essential for retrieval of dilysine-tagged proteins to the endoplasmic reticulum. Cell 79, 1199-1207.

Lian, J.P., Stone, S., Jiang, Y., Lyons, P., and Ferro-Novick, S. (1994). Ypt1p implicated in v-SNARE activation. Nature 372, 698–701.

Liou, W., Geuze, H.J., Geelen, M.J. and Slot, J.W. (1997). The autophagic and endocytic pathways converge at the nascent autophagic vacuoles. J. Cell Biol. 136, 61-70.

Lipschutz, J.H., and Mostov, K.E. (2002). Exocytosis: the many masters of the exocyst. Curr. Biol. 12, R212-214. Review.

Loh, E., and Hong, W. (2002). Sec34 is implicated in traffic from the endoplasmic reticulum to the Golgi and exists in a complex with GTC-90 and ldlBp. J. Biol. Chem. 277, 21955-21961.

Loh, E., and Hong, W. (2004). The binary interacting network of the conserved oligomeric Golgi (COG) tethering complex. J. Biol. Chem. Mar 26 [Epub ahead of print]

Lombardi, D., Soldati, T., Riederer, M.A., Goda, Y., Zerial, M., and Pfeffer, S.R. (1993). Rab9 functions in transport between late endosomes and the trans-Golgi network. EMBO J. 12, 677-682.

Lowe, S.L., Wong, S.H. and Hong, W. (1996). The mammalian ARF-like protein 1 (Arl1) is associated with the Golgi complex. J. Cell Sci. 109, 209-220.

Lupashin, V.V., Pokrovskaya, I.D., McNew, J.A. and Waters, M.G. (1997). Characterization of a novel yeast SNARE protein implicated in Golgi retrograde traffic. Mol. Biol. Cell 8, 2659-2676.

Lupashin, V.V., and Waters, M.G. (1997). t-SNARE activation through transient interaction with a rab-like guanosine triphosphatase. Science 276, 1255-1258.

Luzio, J.P., Brake, B., Banting, G., Howell, K.E., Braghetta, P. and Stanley, K.K. (1990). Identification, sequencing and expression of an integral membrane protein of the trans-Golgi network (TGN38). Biochem. J. 270, 97-102.

Malmstrom, K., and Krieger, M. (1991) Use of radiation suicide to isolate constitutive and temperature-sensitive conditional Chinese hamster ovary cell mutants with defects in the endocytosis of low density lipoprotein. J. Biol. Chem. 266, 24025–24030.

Martinez, O., Schmidt, A., Salamero, J., Hoflack, B., Roa, M., and Goud, B. (1994). The small GTP-binding protein rab6 functions in intra-Golgi transport, J. Cell Biol. 127, 1575-1588.

Martinez-Arca, S., Alberts, P., Zahraoui, A., Louvard, D., and Galli, T. (2000). Role of tetanus neurotoxin insensitive vesicle-associated membrane protein (TI-VAMP) in vesicular transport mediating neurite outgrowth. J. Cell Biol. 149, 889-900.

Mayer, T., Touchot, N., and Elazar, Z. (1996). Transport between cis and medial Golgi cisternae requires the function of the Ras-related GTPase Rab6. J. Biol. Chem. 271, 16097-16103.

McBride, H.M., Rybin, V., Murphy, C., Giner, A., Teasdale, R., and Zerial, M. (1999). Oligomeric complexes link Rab5 effectors with NSF and drive membrane fusion via interactions between EEA1 and syntaxin 13. Cell 98, 377–386.

McMahon, H.T., Missler, M., Li, C., and Sudhof, T.C. (1995). Complexins: cytosolic proteins that regulate SNAP receptor function. Cell 83, 111-119.

McNew, J.A., Parlati, F., Fukuda, R., Johnston, R.J., Paz, K., Paumet, F., Sollner, T.H., and Rothman, J.E. (2000) Compartmental specificity of cellular membrane fusion encoded in SNARE proteins. Nature 407, 153-159.

Mellman, I. (1996). Endocytosis and molecular sorting. Annu. Rev. Cell Dev. Biol. 12, 575-625.

Mellman, I., and Simons, K. (1992). The Golgi complex: in vitro veritas? Cell. 68, 829-840.

Mills, I.G., Jones, A.T., and Clague, M.J. (1998). Involvement of the endosomal autoantigen EEA1 in homotypic fusion of early endosomes. Curr. Biol. 8, 881-884.

Morsomme, P., Prescianotto-Baschong, C., and Riezman, H. (2003). The ER v-SNAREs are required for GPI-anchored protein sorting from other secretory proteins upon exit from the ER. J. Cell Biol. 162, 403-412.

Morsomme, P., and Riezman, H. (2002). The Rab GTPase Ypt1p and tethering factors couple protein sorting at the ER to vesicle targeting to the Golgi apparatus. Dev. Cell. 2, 307-317.

Mu, F.T., Callaghan, J.M., Steele-Mortimer, O., Stenmark, H., Parton, R.G., Campbell, P.L., McCluskey, J., Yeo, J.P., Tock, E.P., and Toh, B.H. (1995). EEA1, an early endosome-associated protein. EEA1 is a conserved alpha-helical peripheral membrane protein flanked by cysteine “fingers” and contains a calmodulin-binding IQ motif. J. Biol. Chem. 270, 13503-13511.

Mukhopadhyay, A., Funato, K., and Stahl, P.D. (1997). Rab7 regulates transport from early to late endocytic compartments in Xenopus oocytes. J. Biol. Chem. 272, 13055-13059.

Nagahama, M., Orci, L., Ravazzola, M., Amherdt, M., Lacomis, L., Tempst, P., Rothman, J.E., and Sollner, T.H. (1996). A v-SNARE implicated in intra-Golgi transport. J. Cell Biol. 133, 507–516.

Nakajima, H., Hirata, A., Ogawa, Y., Yonehara, T., Yoda, K., and Yamasaki, M. (1991). A cytoskeleton related gene, uso1, is required for intracellular protein transport in Saccharomyces cerevisiae. J. Cell Biol. 113, 245–260.

Nakajima, H., Hirata, A., Ogawa, Y., Yonehara, T., Yoda, K., and Yamasaki, M. (1991). A cytoskeleton-related gene, uso1, is required for intracellular protein transport in Saccharomyces cerevisiae. J. Cell Biol. 113, 245–260.

Nelson, D.S., Alvarez, C., Gao, Y.S., Garcia-Mata, R., Fialkowski, E., and Sztul, E. (1998). The membrane transport factor TAP/p115 cycles between Golgi and earlier secretory compartments and contains distinct domains required for its localization and function. J. Cell Biol. 143, 319-331.

Neuhaus, E.M., Horstmann, H., Almers, W., Maniak, M. and Soldati, T. (1998). Ethane-freezing/methanol-fixation of cell monolayers: a procedure for improved preservation of structure and antigenicity for light and electron microscopies. J. Struct. Biol. 121, 326-342.

Nicholson, K.L., Munson, M., Miller, R.B., Filip, T.J., Fairman, R., and Hughson, F.M. (1998). Regulation of SNARE complex assembly by an N-terminal domain of the t-SNARE Sso1p. Nat. Struct. Biol 5, 793-802.

Novick, P., Field, C., and Schekman, R. (1980). Identification of 23 complementation groups required for post-translational events in the yeast secretory pathway . Cell 21, 205-215.

Novick, P., and Schekman, R. (1979). Secretion and cell-surface growth are blocked in a temperature-sensitive mutant of Saccharomyces cerevisiae. Proc. Natl. Acad. Sci. USA 76, 1858-1862.

Novick, P., and Zerial, M. (1997). The diversity of Rab proteins in vesicle transport. Curr. Opin. Cell Biol. 9, 496-504.

Oka, T., Ungar, D., Hughson, F.M., and Krieger, M. (2004). The COG and COPI complexes interact to control the abundance of GEARs, a subset of Golgi integral membrane proteins. Mol. Biol. Cell. 15, 2423-2435.

Ooi, C.E., Moreira, J.E., Dell'Angelica, E.C., Poy, G., Wassarman, D.A., Bonifacino, J.S. (1997). Altered expression of a novel adaptin leads to defective pigment granule biogenesis in the Drosophila eye color mutant garnet. EMBO J. 16, 4508-4518.

Orci, L., Stamnes, M., Ravazzola, M., Amherdt, M., Perrelet, A., Sollner, T.H., and Rothman, J.E. (1997). Bidirectional transport by distinct populations of COPI-coated vesicles. Cell. 90, 335-349.

Ortiz, D., Medkova, M., Walch-Solimena, C., and Novick, P. (2002). Ypt32 recruits the Sec4p guanine nucleotide exchange factor, Sec2p, to secretory vesicles: evidence for a Rab cascade in yeast. J. Cell Biol. 157, 1005–1015.

Ossig, R., Dascher, C., Trepte, H.H., Schmitt, H.D., and Gallwitz, D. (1991). The yeast SLY gene products, suppressors of defects in the essential GTP-binding Ypt1 protein, may act in endoplasmic reticulum-to-Golgi transport. Mol. Cell Biol. 11, 2980-2993.

Palade, G.E. (1975). Intracellular aspects of the processing of protein synthesis. Science 189, 347-354.

Palmer, D.J., Helms, J.B., Beckers, C.J.M., Orci, L., and Rothman, J. (1993). Binding of coatomer to Golgi membranes requires ADP-ribosylation factor. J Biol Chem 268, 12083-12089.

Panic, B., Whyte, J.R., and Munro, S. (2003). The ARF-like GTPases Arl1p and Arl3p act in a pathway that interacts with vesicle-tethering factors at the Golgi apparatus Curr. Biol. 13, 405-410.

Pelham, H.R. (2001). SNAREs and the specificity of membrane fusion. Trends Cell Biol. 11, 99-101.

Peterson, M.R, and Emr, S.D. (2001). The class C Vps complex functions at multiple stages of the vacuolar transport pathway. Traffic 2, 476-486.

Peterson, M.R., Burd, C.G., and Emr, S.D. (1999). Vac1p coordinates rab and phosphatidlyinositol 3-kinase signaling in Vps45p-dependent vesicle docking/fusion at the endosome. Curr. Biol. 11, 159-162.

Pevsner, J., Hsu, S.C., Braun, J.E., Calakos, N., Ting, A.E. Bennett, M.K., and Scheller, R.H. (1994). Specificity and regulation of a synaptic vesicle docking complex. Neuron 13, 353-361.

Pevsner, J., Hsu, S., and Scheller, R.H. (1994). n-Sec1: a neural-specific syntaxin-binding protein. Proc. Natl. Acad. Sci. USA. 91, 1445-1449.

Pfeffer, S. (2001). Vesicle tethering factors united. Mol. Cell 8, 729-730.

Pfeffer, S.R. (1996). Transport vesicle docking: SNAREs and associates. Annu. Rev. Cell Dev. Biol. 12, 441-461.

Pfeffer, S.R. (1999) Transport-vesicle targeting: tethers before SNAREs. Nat. Cell Biol.1, E17-E22.

Pfeffer, S.R (1994). Rab GTPases: master regulators of membrane trafficking. Curr. Opin. Cell Biol. 6, 522-526.

Plutner, H., Cox, A.D., Pind, S., Khovravi-Far, R., Bourne, J.R., Schwaninger, R., Der, C.J., and Balch, W. E. (1991). Rab1b regulates vesicular transport between the endoplasmic reticulum and successive Golgi compartments. J. Cell Biol. 115, 31-43.

Podos, S.D., Reddy, P., Ashkenas, J., and Krieger, M. (1994). LDLC encodes a brefeldin A-sensitive, peripheral Golgi protein required for normal Golgi function J. Cell Biol. 127, 679–691.

Poirier, M.A., Xiao, W., Macosko, J.C., Chan, C., Shin, Y.K., Bennett, M.K. (1998). The synaptic SNARE complex is a parallel four-stranded helical bundle. Nat. Struc. Biol. 5, 765-769.

Prekeris, R., Klumperman, J., Chen, Y.A. and Scheller, R.H. (1998). Syntaxin 13 mediates cycling of plasma membrane proteins via tubulovesicular recycling endosomes. J. Cell Biol. 143, 957-971.

Prekeris, R., Yang, B., Oorschot, V., Klumperman, J. and Scheller, R.H. (1999). Differential roles of syntaxin 7 and syntaxin 8 in endosomal trafficking. Mol. Biol. Cell 10, 3891-3908.

Preston, R.A., Manolson, M.F., Becherer, K., Weidenhammer, E., Kirkpatrick, D., Wright, R., and Jones, E.W. (1991) Isolation and characterization of PEP3, a gene required for vacuolar biogenesis in Saccharomyces cerevisiae. Mol Cell Biol. 11, 5801-5612.

Prigent, M., Dubois, T., Raposo, G., Derrien, V., Tenza, D., Rosse, C., Camonis, J., and Chavrier, P. (2003). ARF6 controls post-endocytic recycling through its downstream exocyst complex effector. J. Cell Biol. 163, 1111-1121.

Pryer, N.K., Wuestehube, L.J. and Schekman, R. (1992). Vesicle-mediated protein sorting. Annu. Rev. Biochem. 61, 471-516. Review.

Puri, S., Bachert, C., Fimmel, C.J., and Linstedt, A.D. (2002). Cycling of early Golgi proteins via the cell surface and endosomes upon lumenal pH disruption. Traffic. 3, 641-653.

Qiu, Y., Xu, X., Wandinger-Ness, A., Dalke, D.P., and Pierce, S. (1994). Separation of subcellular compartments containing distinct functional forms of MHC class II. J. Cell Biol. 125, 595-605.

Ram, R.J., Li, B., and Kaiser, C.A. (2002). Identification of Sec36p, Sec37p, and Sec38p: components of yeast complex that contains Sec34p and Sec35p. Mol. Biol. Cell 13, 1484-1500.

Reilly, B.A., Kraynack, B.A., VanRheenen, S.M., and Waters, M.G. (2001). Golgi-to-endoplasmic reticulum (ER) retrograde traffic in yeast requires Dsl1p, a component of the ER target site that interacts with a COPI coat subunit. Mol. Biol. Cell 12, 3783–96.

Riederer, M.A., Soldati, T., Shapiro, A., Lin, J., and Pfeffer, S.R. (1994). Lysosome biogenesis requires rab9 function and receptor recycling from endosomes to the trans-Golgi network. J. Cell Biol. 125, 573-582.

Rizo, J., and Sudhof, T.C. (2002). Snares and Munc18 in synaptic vesicle fusion. Nat. Rev. Neurosci. 3, 641-653.

Roberg, K.J., Crotwell, M., Espenshade, P., Gimeno, R. and Kaiser, C.A. (1999). LST1 is a SEC24 homologue used for selective export of the plasma membrane ATPase from the endoplasmic reticulum. J. Cell Biol. 145, 659-672.

Rossi, G., Kolstad, K., Stone, S., Palluault, F., and Ferro-Novick, S. (1995). BET3 encodes a novel hydrophilic protein that acts in conjunction with yeast SNAREs. Mol. Biol. Cell 6, 1769-1780.

Rothman, J.E. (1994). Mechanisms of intracellular protein transport. Nature 372, 55-63. Review.

Rothman, J.E., and Orci, L. (1992). Molecular dissection of the secretory pathway. Nature 355, 409-415.

Rothman, J.E. and Warren, G. (1994). Implications of the SNARE hypothesis for intracellular membrane topology and dynamics. Curr. Biol. 4, 220-233. Review.

Rothman, J.E. and Wieland, F.T. (1996). Protein sorting by transport vesicles. Science 272, 227-234.

Sacher, M., and Ferro-Novick, S. (2001). Purification of TRAPP from Saccharomyces cerevisiae and identification of its mammalian counterpart. Methods Enzymol. 329, 234-241.

Sacher, M., Barrowman, J., Wang, W., Horecka, J., Zhang, Y., Pypaert, M., Ferro-Novick, S. (2001). TRAPP I implicated in the specificity of tethering in ER-to-Golgi transport. Mol. Cell. 7, 433-442.

Sacher, M., Barrowman, J., Schieltz, D., Yates, J.R.3rd and Ferro-Novick, S. (2000). Identification and characterization of five new subunits of TRAPP. Eur. J. Cell Biol. 79, 71-80.

Sacher, M., Jiang, Y., Barrowman, J., Scarpa, A., Burston, J., Zhang, L., Schieltz, D., Yates III, J.R., Abeliovich, H., and Ferro-Novick, S. (1998). TRAPP, a highly conserevd novel complex on the cis-Golgi that mediates vesicle docking and fusion. EMBO J. 17, 2494-2503.

Saito-Nakano, Y. and Nakano, A. (2000). Sed4p functions as a positive regulator of Sar1p probably through inhibition of the GTPase activation by Sec23p. Genes Cell 5, 1039-1048.

Sambrook, J., Fritsch, E.F., and Maniatis, T. (1989). Molecular Cloning: A Laboratory Manual, Cold Spring Harbor Laboratory, Cold Spring Harbor, NY

Sandoval, I.V. and Bakke, O. (1994). Targeting of membrane proteins to endosomes and lysosomes. Trends Cell Biol. 4, 292-297.

Sapperstein, S.K., Walter, D.M., Grosvenor, A.R., Heuser, J.E., and Waters, M.G. (1995). p115 is a general vesicular transport factor related to the yeast endoplasmic reticulum to Golgi transport factor Uso1p. Proc. Natl. Acad. Sci. USA 92, 522–526.

Sapperstein, S.K., Lupashin, V.V., Schmitt, H.D., and Waters, M.G. (1996). Assembly of the ER to Golgi SNARE complex requires Uso1p. J. Cell Biol. 132, 755–767.

Sato, T.K., Rehling, P., Peterson, M.R., and Emr, S.D. (2000). Class C Vps protein complex regulates vacuolar SNARE pairing and is required for vesicle docking/fusion. Mol. Cell 6, 661–671.

Schekman, R. and Orci, L. (1996). Coat proteins and vesicle budding. Science 271, 1526-1533.

Scheller, R.H. (1995). Membrane trafficking in the presynaptic nerve terminal. Neuron 14, 893-897. Review.

Schimmoller, F., Simon, I., and Pfeffer, S.R. (1998). Rab GTPases, directors of vesicle docking. J. Biol. Chem. 273, 22161-22164.

Seals, D.F., Eitzen, G., Margolis, N., Wickner, W.T., and Price, A. (2000). A Ypt/Rab effector complex containing the Sec1 homolog Vps33p is required for homotypic vacuole fusion. Proc. Natl. Acad. Sci. U. S. A. 97, 9402-9407.

Seet, L.-F., and Hong, W. (2001). Endofin, an endosomal FYVE domain protein J. Biol. Chem. 276, 42445–42454.

Segev, N. (1991). Mediation of the attachment or fusion step in vesicular transport by the GTP-binding Ypt1 protein. Science. 252(5012), 1553-1556.

Serafini, T., Orci, L., Amherdt, M., Brunner, M., Kahn, R.A., and Rothman, J.E. (1991). ADP-ribosylation factor is a subunit of the coat of Golgi-derived COP-coated vesicles: a novel role for a GTP-binding protein. Cell 67, 239-253.

Shimoni, Y., Kurihara, T., Ravazzola, M., Amherdt, M., Orci, L. and Schekman, R. (2000). Lst1p and Sec24p cooperate in sorting of the plasma membrane ATPase into COPII vesicles in Saccharomyces cerevisiae. J. Cell Biol. 151, 973-984.

Shisheva, A., Buxton, J., Czech, M.P. (1994). Differential intracellular localizations of GDP dissociation inhibitor isoforms. Insulin-dependent redistribution of GDP dissociation inhibitor-2 in 3T3-L1 adipocytes. J. Biol. Chem. 269, 23865-23868.

Shorter, J., Beard, M.B., Seemann, J., Dirac-Svejstrup, A.B., and Warren, G. (2002). Sequential tethering of Golgins and catalysis of SNAREpin assembly by the vesicle-tethering protein p115. J. Cell Biol. 157, 45–62.

Simonsen, A., Lippe, R., Christoforidis, S., Gaullier, J.M., Brech, A., Callaghan, J., Toh, B.H., Murphy, C., Zerial, M., and Stenmark, H. (1988). EEA1 links PI(3)K function to Rab5 regulation of endosome fusion. Nature 394, 494-498.

Siniossoglou, S., and Pelham, H.R. (2001). An effector of Ypt6p binds the SNARE Tlg1p and mediates selective fusion of vesicles with late Golgi membranes. EMBO J. 20, 5991–5998.

Siniossoglou, S., and Pelham, H.R. (2002). Vps51p links the VFT complex to the SNARE Tlg1p. J. Biol. Chem. 277, 48318-48324.

Söllner, T., Whiteheart, S.W., Brunner, M., Erdjument-Bromage, H., Geromanos, S., Tempst, P. and Rothman, J.E. (1993). SNAP receptors implicated in vesicle targeting and fusion. Nature 362, 318-324.

Sonnichsen, B., Lowe, M., Levine, T., Jamsa, E., Dirac-Svejstrup, B., and Warren, G. (1998). A role for giantin in docking COPI vesicles to Golgi membranes. J. Cell Biol. 140, 1013-1021.

Sorkin, A. and Carpenter, G. (1993). Interaction of activated EGF receptors with coated pit adaptins. Science 261(5121), 612-615.

Spelbrink, R.G., and Nothwehr, S.F. (1999). The yeast GRD20 gene is required for protein sorting in the trans-Golgi network/endosomal system and for polarization of the actin cytoskeleton. Mol. Biol. Cell 10, 4263–4281.

Spiess, M. and Lodish, H.F. (1985). An internal signal sequence: the asialoglycoprotein receptor membrane anchor. Cell 44, 177-185.

Steegmaier, M., Yang, B., Yoo, J.S., Huang, B., Shen, M., Yu, S., Luo, Y. and Scheller, R.H. (1998). Three novel proteins of the syntaxin/SNAP-25 family. J. Biol. Chem. 273, 34171-34179.

Stenmark, H., Vitale, G., Ullrich, O. and Zerial, M. (1995). Rabaptin-5 is a direct effector of the small GTPase Rab5 in endocytic membrane fusion. Cell 83, 423-432.

Steyer, J.A., Horstmann, H. and Almers, W. (1997). Transport, docking and exocytosis of single secretory granules in live chromaffin cells. Nature 388, 474-478.

Subramaniam, V.N., bin Mohd Yusoff, A.R., Wong, S.H., Lim, G.B., Chew, M. and Hong, W. (1992). Biochemical fractionation and characterization of proteins from Golgi-enriched membranes. J. Biol. Chem. 267, 12016-12021.

Subramaniam, V.N., Krijnse-Locker, J., Tang, B.L., Ericsson, M., Yusoff, A.R.b.M., Griffiths, G., and Hong, W. (1995). Monoclonal antibody HFD9 identifies a novel 28 kDa integral membrane protein on the cis-Golgi. J. Cell Sci. 108, 2405–2414.

Subramaniam, V.N., Loh, E. and Hong W. (1997). NSF and α-SNAP mediate dissociation of GS28-syntaxin 5 Golgi SNARE complex. J. Biol. Chem. 272, 25441-25444.

Subramaniam, V.N., Peter, F., Philip, R., Wong, S.H. and Hong W. (1996). GS28, a 28-kilodalton Golgi SNARE that participates in ER-Golgi transport. Science 272, 1161-1163.

Südhof, T.C. (1995). The synaptic vesicle cycle: a cacade of protein-protein interactions. Nature 375, 645-653.

Sugihara, K., Asano, S., Tanaka, K., Iwamatsu, A., Okawa, K., and Ohta, Y. (2002). The exocyst complex binds the small GTPase RalA to mediate filopodia formation. Nat. Cell Biol. 4, 73-78.

Sutton, R.B., Fasshauer, D., Jahn, R., and Brunger, A.T. (1998). Crystal structure of a SNARE complex involved in synaptic exocytosis at 2.4 A resolution. Nature 395, 347-353.

Suvorova, E.S., Duden, R., and Lupashin, V.V. (2002). The Sec34/Sec35p complex, a Ypt1p effector required for retrograde intra-Golgi trafficking, interacts with Golgi SNAREs and COPI vesicle coat proteins. J. Cell Biol. 157, 631-643.

Suvorova, E.S., Kurten, R.C., and Lupashin, V.V. (2001). Identification of a human orthologue of Sec34p as a component of the cis-Golgi vesicle tethering machinery. J. Biol. Chem. 276, 22810–22918.

Tang, B.L., Low, D.Y. and Hong, W. (1998c). Syntaxin 11: a member of the syntaxin family without a carboxyl terminal transmembrane domain. Biochem. Biophys. Res. Commun. 245, 627-632.

Tang, B.L., Low, D.Y., Lee, S.S., Tan, A.E. and Hong, W. (1998a). Molecular cloning and localization of human syntaxin 16, a member of the syntaxin family of SNARE proteins. Biochem. Biophys. Res. Commun. 242, 673-679.

Tang, B.L., Low, D.Y., Tan, A.E. and Hong, W. (1998b). Syntaxin 10: a member of the syntaxin family localized to the trans-Golgi network. Biochem. Biophys. Res. Commun. 242, 345-350.

Tang, B.L., Ong, Y.S., Huang, B., Wei, S., Wong, E.T., Qi, R., Horstmann, H., and Hong, W. (2001). A membrane protein enriched in endoplasmic reticulum exit sites interacts with COPII. J. Biol. Chem. 276, 40008–40017.

Tang, B.L., Tan, A.E., Lim, L.K., Lee, S.S., Low, D.Y. and Hong, W. (1998d). Syntaxin 12, a member of the syntaxin family localized to the endosome. J. Biol. Chem. 273, 6944-6950.

Tang, B.L., Zhang, T., Low, D.Y., Wong, E.T., Horstmann, H., and Hong, W. (2000). Mammalian homologues of yeast sec31p. An ubiquitously expressed form is localized to endoplasmic reticulum (ER) exit sites and is essential for ER-Golgi transport. J. Biol. Chem. 275, 13597–13604.

Teng, Y.H., Wang, Y. and Tang, B.L. (2001). The syntaxins. Genome Biology 2, reviews 3012.1-3012.7.

Terbush, D.R., Maurice, T., Roth, D., and Novick, P. (1996). The exocyst is a multiprotein complex required for exocytosis in Saccharomyces cerevisiae. EMBO J. 15, 6483–6494.

TerBush, D.R., and Novick, P. (1995). Sec6, Sec8, and Sec15 are components of a multisubunit complex which localizes to small bud tips in Saccharomyces cerevisiae. J. Cell Biol. 130, 299-312.

Thoreau, V., Berges, T., Callebaut, I., Guillier-Gencik, Z., Gressin, L., Bernheim, A., Karst, F., Mornon, J.P., Kitzis, A. and Chomel, J. (1999). Molecular cloning,

expression analysis, and chromosomal localization of human syntaxin 8 (STX8). Biochem. Biophys. Res. Commun. 257, 577-583.

Ting, A.E., Hazuka, C.D., Hsu, S.C., Kirk, M.D., Bean, A.J., and Scheller, R.H. (1995). rSec6 and rSec8, mammalian homologs of yeast proteins essential for secretion. Proc. Natl. Acad. Sci. 92, 9613-9617.

Tisdale, E.J., Bourne, J.R., Khosravi-Far, R., Der, C.J., and. Balch, W.E. (1992). GTP-binding mutants of rab1 and rab2 are potent inhibitors of vesicular transport from the endoplasmic reticulum to the Golgi complex. J. Cell Biol. 119, 749-761.

Tochio, H., Tsui, M.M., Banfield, D.K., and Zhang, M. (2001). An autoinhibitory mechanism for nonsyntaxin SNARE proteins revealed by the structure of Ykt6p Science 293, 698-702.

Ungar, D., Oka, T., Brittle, E.E., Vasile, E., Lupashin, V.V., Chatterton, J.E., Heuser, J.E., Krieger, M., and Waters, M.G. (2002). Characterization of a mammalian Golgi-localized protein complex, COG, that is required for normal Golgi morphology and function. J Cell Biol. 157, 405-415.

Valdez, A.C., Cabaniols, J.P., Brown, M.J., and Roche, P.A. (1999). Syntaxin 11 is associated with SNAP-23 on late endosomes and the trans-Golgi network. J. Cell Sci. 112, 845-854.

van Ijzendoorn, S.C., Tuvim, M.J., Weimbs, T., Dickey, B.F., and Mostov, K.E. (2002). Direct interaction between Rab3b and the polymeric immunoglobulin receptor controls ligand-stimulated transcytosis in epithelial cells. Dev. Cell 2, 219–228.

Van Rheenen, S.M., Cao, X., Sapperstein, S.K., Chiang, E.C., Lupashin, V.V., Barlowe, C., and Waters, M.G. (1999). Sec34p, a protein required for vesicle tethering to the yeast Golgi apparatus, is in a complex with Sec35p. J. Cell Biol. 147, 729–742.

VanRheenen, S.M., Cao, X., Lupashin, V.V., Barlowe, C., and Waters, M.G. (1988). Sec35p, a novel peripheral membrane protein, is required for ER to Golgi vesicle docking. J. Cell Biol. 141, 1107-1119.

von Mollard, G.F. and Stevens, T.H. (1999). The Saccharomyces cerevisiae v-SNARE Vti1p is required for multiple membrane transport pathways to the vacuole. Mol. Biol. Cell 10, 1719-1732.

von Mollard, G.F. and Stevens, T.H. (1998). A human homolog can functionally replace the yeast vesicle-associated SNARE Vti1p in two vesicle transport pathways. J. Biol. Chem. 273, 2624-2630.

von Mollard, G.F., Nothwehr, S.F., Stevens, T.H. (1997). The yeast v-SNARE Vti1p mediates two vesicle transport pathways through interactions with the t-SNAREs Sed5p and Pep12p. J. Cell Biol. 137, 1511-1524.

Walter, D.M., Paul, K.S., and Waters, M.G. (1998). Purification and characterization of a novel 13 S hetero-oligomeric protein complex that stimulates in vitro Golgi transport. J. Biol. Chem. 273, 29565–29576.

Wang, W., and Ferro-Novick, S. (2002). A Ypt32p exchange factor is a putative effector of Ypt1p. Mol. Biol. Cell 13, 3336–3343.

Wang, H., Frelin, L. and Pevsner, J. (1997). Human syntaxin 7: a Pep12p/Vps6p homologue implicated in vesicle trafficking to lysosomes. Gene 199, 39-48.

Waters, M.G., and Hughson, F.M. (2000). Membrane tethering and fusion in the secretory and endocytic pathways. Traffic 1, 588–597.

Waters, M.G., Serafini, T. and Rothman, J.E. (1991). 'Coatomer': a cytosolic protein complex containing subunits of non-clathrin-coated Golgi transport vesicles. Nature 349, 248-251,

Waters, M.G., and Pfeffer, S.R. (1999). Membrane tethering in intracellular transport. Curr. Opin. Cell Biol. 11, 453-459. Review.

Waters, M.G., Clary, D.O., and Rothman, J.E. (1992). A novel 115-kD peripheral membrane protein is required for intercisternal transport in the Golgi stack. J. Cell Biol. 118, 1015-1026.

Weimbs, T., Low, S.H., Chapin, S.J., Mostov, K.E., Bucher, P., and Hofmann, K. (1997). A conserved domain is present in different families of vesicular fusion proteins: a new superfamily. Proc. Natl. Acad. Sci. USA 94, 3046-3051.

Whiteheart, S.W., and Kubalek, E.W. (1995). SNAPs and NSF: general members of the fusion apparatus. Trends Cell Biol. 5, 64-69.

Whyte, J.R., and Munro, S. (2002). Vesicle tethering complexes in membrane traffic. J. Cell Sci. 115, 2627–2637.

Whyte, J.R., and Munro, S. (2001) The Sec34/35 Golgi transport complex is related to the exocyst, defining a family of complexes involved in multiple steps of membrane traffic. Dev. Cell 1, 527–537.

Wong, S.H., Xu, Y., Zhang, T., and Hong, W. (1998). Syntaxin 7, a novel syntaxin member associated with the early endosomal compartment. J. Biol. Chem. 273, 375-380.

Wong, S.H., Xu, Y., Zhang, T., Griffiths, G., Lowe, S.L., Subramaniam, V.N., Seow, K.T., and Hong, W. (1999). GS32, a novel golgi SNARE of 32 kDa, interacts preferentiall with syntaxin 6. Mol. Biol. Cell 10, 119-134.

Woodman, P.G., Rodriguez, L., and Stirling, C.J. (1996). Functional conservation of cytosolic proteins required for endosomal vesicle fusion. Yeast 12, 1251-1262.

Wu, X., Steet, R.A., Bohorov, O., Bakker, J., Newell, J., Krieger, M., Spaapen, L., Kornfeld, S., and Freeze, H.H. (2004). Mutation of the COG complex subunit gene COG7 causes a lethal congenital disorder. Nature Med. published online 25 April.

Wuestehube, L.J., Duden, R., Eun, A., Hamamoto, S., Korn, P., Ram, R., and Schekman, R. (1996). New mutants of Saccharomyces cerevisiae affected in the transport of proteins from the endoplasmic reticulum to the Golgi complex. Genetics 142, 393-406.

Xu, D., Joglekar, A.P., Williams, A.L., and Hay, J.C. (2000). Subunit structure of a mammalian ER/Golgi SNARE complex. J. Biol. Chem. 275, 39631–39639.

Xu, Y., Wong, S.H., Zhang, T and Hong, W. (1988). A 29-kilodalton Golgi SNARE (Vti1-rp2) implicated in protein trafficking in the secretory pathway. J. Biol. Chem. 273, 21783-21789.

Yang, B., Gonzalez, L. Jr, Prekeris, R. Steegmaier, M., Advani, R.J., and Scheller, R.H. (1999). SNARE interactions are not selective. Implications for membrane fusion specificity. J Biol Chem 274, 5649-5653.

Zaremba, S., and Keen, J.H. (1983). Assembly polypeptides from coated vesicles mediate reassembly of unique clathrin coats. J. Cell Biol. 97, 1339-1347.

Zerfaoui, M., Fukuda, M., Langlet, C., Mathieu, S., Suzuki, M., Lombardo, D., and El-Battari, A. (2002). The cytosolic and transmembrane domains of the beta 1,6 N-acetylglucosaminyltransferase (C2GnT) function as a cis to medial/Golgi-targeting determinant. Glycobiology 12, 15-24.

Zerial, M., and McBride, H. (2001). Rab proteins as membrane organizers. Nat. Rev. Mol. Cell Biol. 2, 107–117.

Zhang, C.J., Bowzard, J.B., Greene, M., Anido, A., Stearns, K., and Kahn, R.A. (2002). Genetic interactions link ARF1, YPT31/32 and TRS130. Yeast. 19, 1075-1086.

Zhang, T., and Hong, W. (2001). Ykt6 Forms a SNARE Complex with Syntaxin 5, GS28, and Bet1 and Participates in a Late Stage in Endoplasmic Reticulum-Golgi Transport. J. Biol. Chem. 276, 27480–27487.

Zhang, T., Wong, S.H., Tang, B.L., Xu, Y., Peter, F., Subramaniam, V.N., and Hong, W. (1997). The mammalian protein (rbet1) homologous to yeast Bet1p is primarily associated with the pre-Golgi intermediate compartment and is involved in vesicular transport from the endoplasmic reticulum to the Golgi apparatus. J. Cell Biol. 139, 1157-1168.

Zhang, X., Bi, E., Novick, P., Du, L., Kozminski, K.G., Lipschutz, J.H., and Guo, W. (2001). Cdc42 interacts with the exocyst and regulates polarized secretion J. Biol Chem. 276, 46745-46750.